AD_____

Award Number: W81XWH-09-1-0487

TITLE: Developing a Drosophila Model of Schwannomatosis

PRINCIPAL INVESTIGATOR: James A. Walker, Ph.D.

CONTRACTING ORGANIZATION: Massachusetts General Hospital
Boston, MA 02114-2696

REPORT DATE: August 2012

TYPE OF REPORT: Revised Annual

PREPARED FOR: U.S. Army Medical Research and Materiel Command
Fort Detrick, Maryland 21702-5012

REPORT DOCUMENTATION PAGE

Form Approved
OMB No. 0704-0188

1. REPORT DATE	2. REPORT TYPE	3. DATES COVERED
August 2012	Revised Annual	15 July 2011 – 14 July 2012

4. TITLE AND SUBTITLE

Developing a Drosophila Model of Schwannomatosis

5a. CONTRACT NUMBER

5b. GRANT NUMBER
W81XWH-09-1-0487

5c. PROGRAM ELEMENT NUMBER

6. AUTHOR(S)

James A. Walker

E-Mail: jwalker@helix.mgh.harvard.edu

5d. PROJECT NUMBER

5e. TASK NUMBER

5f. WORK UNIT NUMBER

7. PERFORMING ORGANIZATION NAME(S) AND ADDRESS(ES)

Massachusetts General Hospital
Boston, MA 02114-2696

8. PERFORMING ORGANIZATION REPORT NUMBER

9. SPONSORING / MONITORING AGENCY NAME(S) AND ADDRESS(ES)
U.S. Army Medical Research and Materiel Command
Fort Detrick, Maryland 21702-5012

10. SPONSOR/MONITOR'S ACRONYM(S)

11. SPONSOR/MONITOR'S REPORT NUMBER(S)

12. DISTRIBUTION / AVAILABILITY STATEMENT
Approved for Public Release; Distribution Unlimited

13. SUPPLEMENTARY NOTES

14. ABSTRACT

This project examines mutations found in familial cases of schwannomatosis in the tumor suppressor SMARCB1, a component of the SWI/SNF chromatin remodeling complex. Drosophila is being used to investigate the nature of the SMARCB1 mutations and the molecular consequences which give rise to schwannomas. Sensitized in vivo assays for SMARCB1 function using RNAi knockdown of Snr1 (fly ortholog of SMARCB1) reveal missense mutations from patients have varying degrees of residual function suggesting they are hypomorphic. Drosophila genetics has identified novel Snr1 interactions, including a potent interaction between Snr1 and the NF2/merlin tumor suppressor gene, which is also involved in schwannomatosis, as well as regulators of Cyclin E and the Hedgehog pathway. The consequences of SMARCB1/Snr1 knockdown on gene expression is being examined using microarrays. Purification of wild type and mutant SMARCB1 is being performed to examine altered protein interactions that may contribute to schwannomatosis.

15. SUBJECT TERMS
Scwhwannomatosis, chromatin remodeling, epigenetics, genetic interactions

16. SECURITY CLASSIFICATION OF:			17. LIMITATION OF ABSTRACT	18. NUMBER OF PAGES	19a. NAME OF RESPONSIBLE PERSON
a. REPORT	b. ABSTRACT	c. THIS PAGE			USAMRMC
U	U	U	UU	60	19b. TELEPHONE NUMBER *(include area code)*

Table of Contents

Introduction

Schwannomatosis is characterized by multiple spinal, peripheral, and cranial nerve schwannomas in the absence of vestibular nerve schwannomas. Molecular analyses have identified mutations in *NF2* being somatically acquired in schwannomas from patients with schwannomatosis, although linkage studies have excluded *NF2* as a germline transmissible schwannomatosis gene (MacCollin *et al.,* 2003). Recent genetic studies have revealed germline mutations in the tumor-suppressor gene *SMARCB1* in familial schwannomatosis (Hadfield *et al.*, 2008; Hulsebos *et al*., 2007; Boyd *et al*., 2008). A tumor suppressor role for *SMARCB1* was first suggested by frequent loss of function mutations in malignant atypical teratoid rhabdoid tumors (Biegel *et al*., 1999; Versteege *et al*., 1998). SMARCB1 is a component of the SWI/SNF chromatin remodeling complex which consists of 8-11 subunits. By interacting with DNA-binding transcription (co)-factors to recruit histone acetyltransferases and histone deacetylase complexes, the SWI/SNF complex functions to regulate gene expression, DNA replication and repair, and cell division (Euskirchen *et al*., 2012). Intriguingly, however, *SMARCB1* mutations appear to explain only a fraction of familial and sporadic schwannomatosis cases, suggesting the existence of yet another, apparently closely-linked, causative gene on chromosome 22.

We have developed a Drosophila model of schwannomatosis, to help elucidate the specific molecular events that give rise to this disease. Our main objective was to uncover new functions of SMARCB1 and its Drosophila ortholog, Snr1, to help answer the following two fundamental questions: How do germline mutations in *SMARCB1* give rise to two very different tumor predisposition syndromes, namely late-onset familial schwannomatosis and highly malignant pediatric rhabdoid tumors? Why is *SMARCB1* the only human SWI/SNF subunit thus far implicated as a potent tumor suppressor so far? We hypothesized that SMARCB1 may have an important role independent from that of being a core constituent of the SWI/SNF complex. Alternatively, if disease-

causing mutations in SMARCB1 affect the function of this complex, this would suggest that lesions (yet to be described) in genes encoding other SWI/SNF complex components could also contribute to schwannomatosis.

We are grateful that this award has been approved for a no cost extension for a further six months. This will enable us to complete the proposed studies and to prepare the results for publication. Consequently, this report will take the form of an Annual Report and concentrates on the findings detailed in the Statement of Work for months 25-36. A Final Report concluding these studies will be submitted in February 2013, as requested.

Body

Specific Aim 1. Generating transgenic lines for testing *SMARCB1* disease-causing mutations and for genetic screening.

The work in Specific Aim 1 was been completed and was detailed in the previous two annual reports. The findings are summarized here (Figure 1) since the results discussed in Specific Aim 2 make reference to them.

- Human SMARCB1 can compensate for loss of Drosophila Snr1
- SMARCB1 disease-causing mutations are unable to rescue the lethality of Snr1 mutants.
- Characterization of *Snr1* RNAi phenotypes (shown in Figure 1)
- Testing SMARCB1 mutants for ability to rescue Snr1 RNAi phenotypes

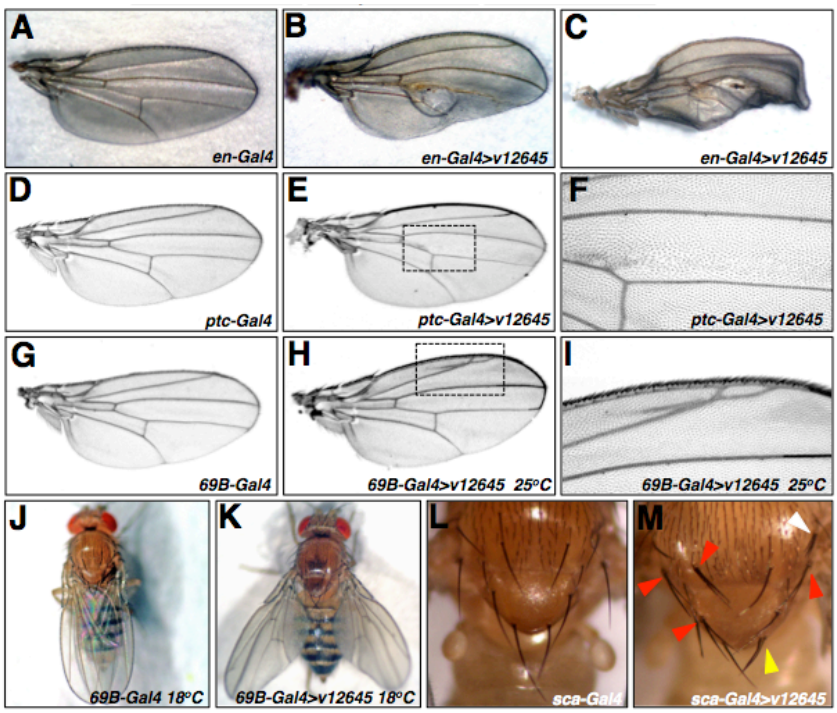

Figure 1. Snr1 RNAi phenotypes observed by driving *UAS-Snr1 RNAi* line using tissue-specific Gal4 drivers at the indicated temperatures. A-C *engrailed-Gal4* driving RNAi knock down in the posterior half of the wing results in blistering; D-F *ptc-Gal4* driving in a stripe in the middle of the wing causes planar cell polarity defects; G-I *69B-Gal4* driven *Snr1* RNAi results in ectopic vein formation in the anterior of the wings, as well as a held-out wing phenotype (J and K). *Scaborous-Gal4 >UAS-Snr1 RNAi* results in either the duplication or absence of bristles on the thorax. In each case control flies (Gal4 driver alone) is shown – A, D, G, J and L.

Specific Aim 2: **To identify dominant genetic modifiers of Snr1 function.**

• Months 15-30

Screen Exelixis Collection of transposons using *UAS-shRNA-Snr1*, *GMR-Gal4* or *UAS-shRNA Snr1*, *eng-Gal4*. Secondary screens will be conducted as soon as a modifier is identified. Confirm interaction with alleles from different sources.

• Months 31-36

Characterizing the function of modifiers either as constituents, or regulators, of Snr-containing complexes, or as targets of such complexes.

(a) A candidate genetic interaction: *Snr1* genetically interacts with *merlin* (*NF2*)

We devoted considerable time during Years 1 and 2 to investigating the genetic interaction that we identified between *Snr1* and the Drosophila *NF2* homolog *Merlin* (*Mer*, summarized in Figure 2). Since *SMARCB1* and *NF2* are both inactivated in at least some schwannomatosis tumors, which others have suggested constitute a unique four-hit mechanism (Sestini et al., 2008), the genetic interaction between *Snr1* and *Merlin* in Drosophila is a useful phenotype to probe the potential functional interaction between the SWI/SNF complex and NF2 signaling pathways. Since Merlin functions in the Salvador-Warts-Hippo (SWH) pathway (Oh and Irvine, 2010), we explored the hypothesis that Snr1, as part of the Brahma complex, may function to regulate this pathway at some level.

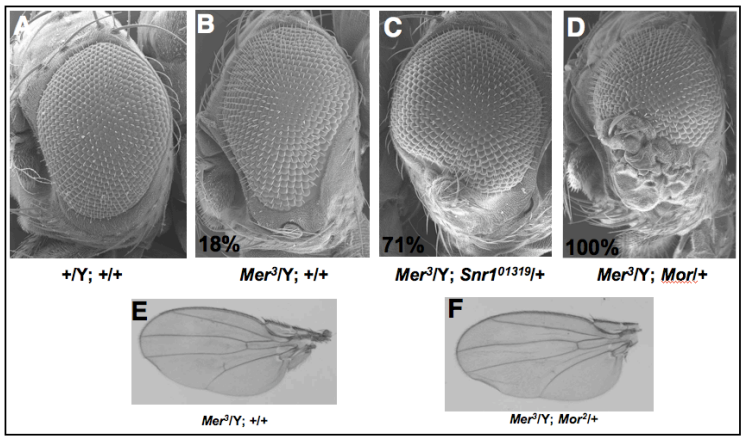

Figure 2. *Snr1* and *Mor* genetically interact with *Mer*. A-D Electron micrographs of respective genotypes. Loss of one copy of *Snr1* or *Mor* dominantly enhances Mer^3 ectopic vibrissae phenotype. % refers to the number of flies with at least one eye showing ectopic vibrissae. E. Mer^3 wing shows overgrowth and disruption of vein structure. F. Alleles of *mor* enhances overgrowth and causes increased interruption of the posterior cross vein.

We have now concluded these experiments and found no evidence that reduced levels *Snr1* affect the SWH pathway (described in previous report). We therefore hypothesized that *Snr1* affects signaling downstream of *Mer,* independent of the SWH pathway. Possible mechanisms for the *Snr1-Mer* interaction include the Brm complex regulating expression of *Mer* itself, or another protein that alters Mer function/signaling. Arguing against the former, we tested whether loss of Brm complex genes have a transcriptional affect on *Mer* using qRT-PCR. We found no significant difference in *Mer* mRNA levels in wing discs with either *Brm* or *Snr1* RNAi driven with the *en-Gal4* driver (Figure 3A).

Further, we used a transgene to express a dominant negative form of Merlin ($Mer^{\Delta BB}$) under the control of the *apterous-Gal4* (kindly provided by Dr. R. Fehon) that gives ectopic veins in the wing anterior. This transgenic $Mer^{\Delta BB}$ phenotype does not rely on the endogenous *Mer* promoter. Arguing that reductions in Brm complex components affect Merlin protein activity itself, reducing Snr1 levels by RNAi modified the wing phenotype in flies (Figure 3D). Additionally, an allele of Snr1 also enhanced the defects in *Ap-Gal4> $Mer^{\Delta BB}$* wings (Figure 3E).

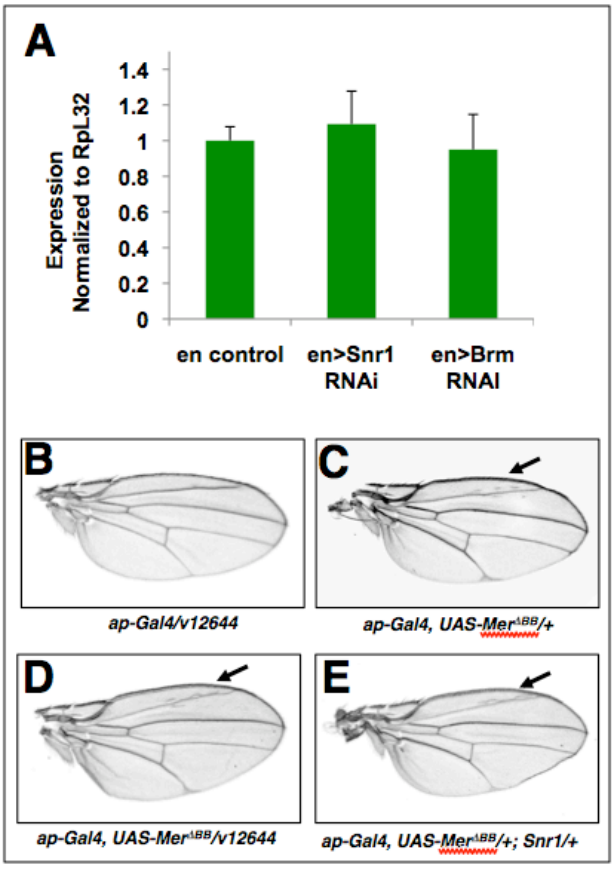

Figure 3 *Snr1* affects *Mer* protein function rather than transcription of *Mer* A. qRT-PCR of RNA from wing discs with knocked down levels of Snr1 and Brm (from *en-GAL4>Snr1 RNAi* and *en-GAL4>Brm RNAi* animals) to assess *Mer* mRNA levels. Results were normalized to *RpL32* expression. B. Snr1 RNAi using the weak *UAS-shRNAi* line v12644 and the *apterous-Gal4* driver gives no obvious defects. C-E Expressing a *UAS-$Mer^{\Delta BB}$* transgene under the control of *ap-Gal4* driver result in ectopic veins (arrows). This phenotype (C) is enhanced by addition of the *UAS-shRNAi* line v12644 targeting Snr1 (D) or dominantly using a Snr1 allele (E).

(b) Using *Snr1* transgenic RNAi to screen for novel Snr1/SMARCB1 interactors

Our proposed plan was to conduct a genome-wide screen to search for modifiers of *Snr1* RNAi phenotypes. A number of potential phenotypes were identified that are amenable to performing such screens (shown in Figure 1 and Figure 5A). For our initial screens we decided to use the strong *UAS-Snr1-shRNA* transgene (*v12645*) with the *ey-Gal4* driver (Figure 4A). This combination results in a highly penetrant roughened eye of reduced size. The *en-Gal4* and *ptc-Gal4* drivers were used for subsequent secondary tests to confirm any genetic modifier hits (Figure 1 B, C, E and F).

Flies were generated with the *UAS-Snr1-shRNA* transgene, and either *en-Gal4*, *ptc-Gal4* or *ey-Gal4* along with a *Gal80* balancer chromosome. *Gal80* represses *Gal4* function and therefore silences the *UAS-RNAi* transgene (Figure 4). In this way we were able to maintain healthy screening stocks, which when out-crossed to potential modifiers results in removal of *Gal80*, thereby activating the *Snr1* RNAi transgene.

Allele	*en-Gal4>Snr1 RNAi*	*ey-Gal4>Snr1 RNAi*
-	Blistered wings	Severely reduced eye
CycE	SUP	SUP
Cdc2c	SUP	SUP
Rpd3	ENH	ENH
Brm	ENH	ENH
Mor	ENH	ENH
Osa	ENH	ENH
dpp	ENH	ENH
ex	ENH	ENH

Table 1 Modification of Snr1 RNAi phenotypes in wing and eye using alleles of known genetic interactors (CycE, Cdc2c, Rpd3, Brm, Osa, Mor) and novel Snr1 interactors (ex and dpp).

Confirming the validity of our screening approach, alleles of genes encoding Brahma complex components *mor*, *osa* and *brm* enhanced *Snr1* RNAi phenotypes as expected (Table 1). Alleles of *expanded* (ex), *decapentaplegic* (*dpp*) and *cyclin E* also dominantly modified the phenotypes (Table 1). Interestingly, alleles of *expanded* (ex), *decapentaplegic* (*dpp*) and *cyclin E* have

also been shown to interact with *Mer*, the Drosophila *NF2* ortholog called *merlin* (McCartney et al., 2000; Hamaratoglu et al., 2006).

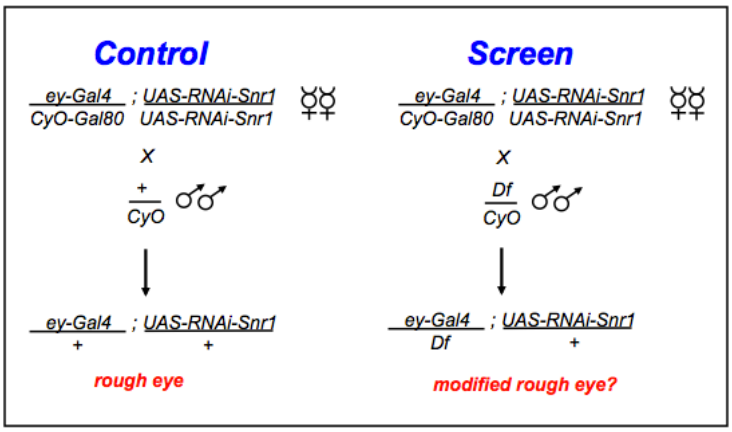

Figure 4. ***Designing a suitable genetic screen based on the Snr1 RNAi phenotype in the eye.*** Scheme shows the screening line, which was constructed with *ey-Gal4* being held in check by the presence of Gal80 inhibitor so that *Snr1* RNAi is not active. Once crossed out, the absence of Gal80 in progeny permits *ey-Gal4>UAS-Snr1 RNAi* resulting in a severe eye phenotype (control cross). In the screen crosses, the RNAi line is mated to flies containing molecularly defined deficiencies (Df). The effect of the deficiency is assessed by comparing the resulting eye phenotype with that generated by the control cross.

(c) Initial genetic screens using *Snr1* transgenic RNAi

In the 2nd Year Report we described that we started a systematic screen the TRiP collection of RNAi lines in an attempt to identify novel *Snr1* modifiers using our *ey-Gal4>UAS-Snr1-shRNA* line. We reported that initial testing of this approach using a number of expected modifiers such as *Osa* and *Brm* looked promising. However, on screening several hundred RNAi lines for novel interactions, we found that almost half of these RNAi lines gave potent effects when driven by *ey-Gal4* in the developing eye by themselves (i.e. in the absence of the *UAS-Snr1-shRNA* transgene). Since these effects would obscure any *bona fide* modification of the *Snr1* RNAi phenotype in an initial screen, we realized that secondary screens to eliminate their non-specific effect on the *Snr1* RNAi phenotype would be prohibitively labor intensive.

We also proposed to screen the Exelixis Collection of transposons housed at the Harvard Medical School (Months 15-30). A pilot screen of about 300 lines from this collection suggested that this would not be a fruitful approach. Many of the transposons are inserted in introns of genes and therefore do not constitute loss of function alleles. The pilot screen revealed no novel genetic modifications

that could be attributed to an inserted transposon. We subsequently discontinued both these approaches and reverted to a deficiency screen described below.

(d) Deficiency screen for modifiers of *Snr1* RNAi phenotypes identifies novel interactors

The *ey-Gal4>UAS-Snr1-shRNA* line was used in a screen with molecularly defined deficiencies from the Bloomington Stock Collection (including Exelixis, BSC and DrosDel deficiencies). The initial pilot screen that we described in the previous report (Year 2) was extended to include deficiencies spanning the second chromosome. We concentrated our efforts to the 2nd chromosome so far for technical reasons (the presence or absence of the CyO balancer is easy to score). However, our screening scheme (Figure 4) has also allowed us to start screening deficiencies on the X chromosome. Table 2 describes the number of deficiencies screened and the number of initial hits. In many cases, not only did the deficiency reduce the severity of the eye phenotype, but also increased the viability of *ey-Gal4>UAS-Snr1-shRNA* flies, resulting in greater than usual numbers of progeny obtained (compared to the control crosses). The modifying deficiencies represent genetic interactions between genes uncovered by the deletion with *Snr1*.

The deficiency hits from our modifier screen were analyzed in order to identify the responsible genes underlying the genetic interaction with *Snr1*. We focused on deficiencies that strongly suppress the eye phenotype, since these are most likely to represent the most specific and interesting interacting genes. We also concentrated on loci that were uncovered by multiple overlapping deficiencies that consistently modified the *Snr1* RNAi eye phenotype, but that failed to show an effect on either RNAi or the *UAS*/*Gal4* system by themselves in control experiments. The two most exciting hits from the screen are discussed below and are shown in Figure 5.

Chromosome	# deficiencies screened	Enhancers	Suppressors
2L	144	8	13
2R	103	5	7
X	26	2	1

Table 2 Results of deficiency screen using *ey-Gal4>Snr1 RNAi.* Table shows number of deficiencies screened on each chromosome arm and the number of enhancers and suppressors. These include modifiers that may be non-specific and have effects on the *UAS-Gal4* system or RNAi independently of *Snr1.*

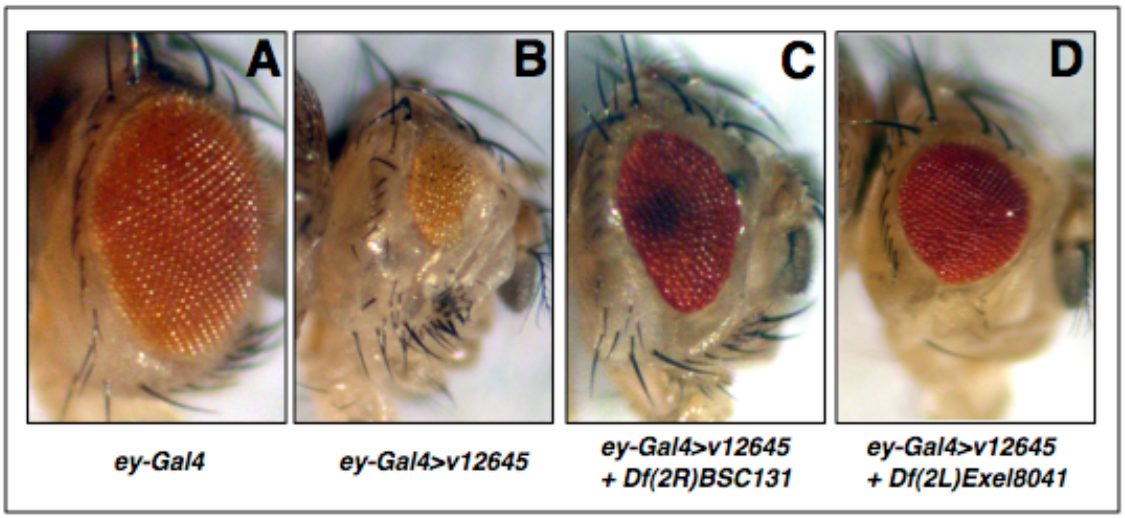

Figure 5. *Snr1* RNAi eye phenotypes. Driving the *UAS-Snr1-shRNA* transgene (v12645) with *ey-Gal4* results in a highly penetrant reduced eye phenotype (B). The control fly without the RNAi line has a wild type appearance (A). The effect of two suppressing deficiencies on the *Snr1* RNAi defect are shown (C and D) and are described in the text.

(i) The Cyclin E agonist *dacapo* genetically interacts with *Snr1*

Df(2R)BSC131 and Df(2R)BSC132 are partially overlapping deficiencies that both strongly suppress the eye phenotype of *ey-Gal4>UAS-Snr1-shRNA* (Figure 5C). Df(2R)BSC131 is the smaller of the two deletions and uncovers 18 protein-encoding genes. These include the Matrix metalloproteinase (*Mmp2*), spaghetti-squash activator (*sqa*), which is involved in regulation of the TOR pathway and *dacapo* (*dap*), an agonist of Cyclin E. Although these are all

interesting candidate interactors, we considered *dap* to be the most likely gene responsible. Mutations in the Brm complex genes have been isolated as dominant suppressors of S-phase defects associated with cyclin E (Brumby et al., 2002). Further, *Snr1* has been shown to interact genetically with a subset of genes involved in cell cycle control, including *cyclin E* (Zraly et al., 2004). Alleles of *dap* were obtained from various sources (Dap^{4} and Dap^{04454}) and tested with our screening lines. Both gave a suppression of the RNAi eye phenotype similar to that of the Df(2R)BSC131 deficiency, confirming that *dap* is a suppressor of *Snr1* (data not shown).

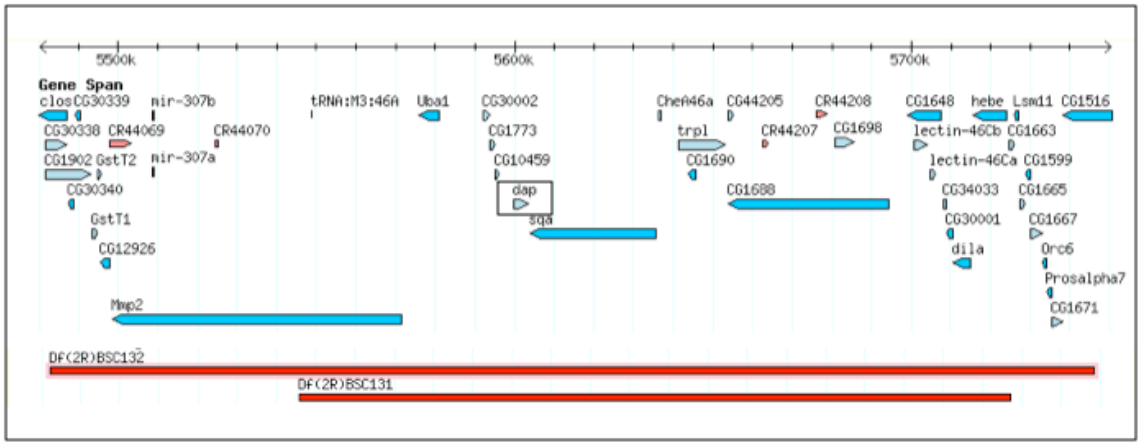

Figure 6. Region of chromosome 2R uncovered by suppressing deficiencies BSC131 and BSC132. The red bars represent the extent of the deficiencies. BSC131 is the smaller of the two and thus defines the minimal interacting locus, containing 18 protein-coding genes. The responsible gene identified, *dap*, is indicated by the boxed area.

(ii) A regulator of the Hedgehog pathway, *second wave mitotic* (*swm*), genetically interacts with *Snr1*

A second suppressing loci, represented by Df(2L)Exel8041 and Df(2L)BSC301 uncover 22 genes in common (Figure 7). The most attractive candidate amongst these genes is *second mitotic wave missing* (*swm*). We subsequently obtained alleles of *swm* (swm^{F14} and swm^{37Dh-1}) and when crossed to the *Snr1* RNAi line, they suppress the eye phenotype to a similar degree to the deficiencies (not shown). *swm* encodes a zinc finger protein that might be involved in protein-protein interactions or nucleic acid binding, an RNA-

recognition motif (RRM) and nuclear localization signals. It was initially identified in a genetic screen for *smoothened* (*smo*) interactors and has been shown to be involved in the negative regulation of the hedgehog (Hh) signaling pathway (Casso *et al*., 2008). Signaling by Hedgehog (Hh) proteins shapes most tissues and organs in both vertebrates and invertebrates, and its misregulation has been implicated in many human diseases, including tumorigenesis. Recently, the glioma-associated oncogene family zinc finger-1 (GLI1), a crucial effector of Hh signaling, was shown to interact physically with SMARCB1 (Jagani *et al.*, 2010). Further, SMARCB1 was shown to localize to Gli1-regulated promoters and loss of SMARCB1 was demonstrated to result in activation of the Hh-Gli pathway.

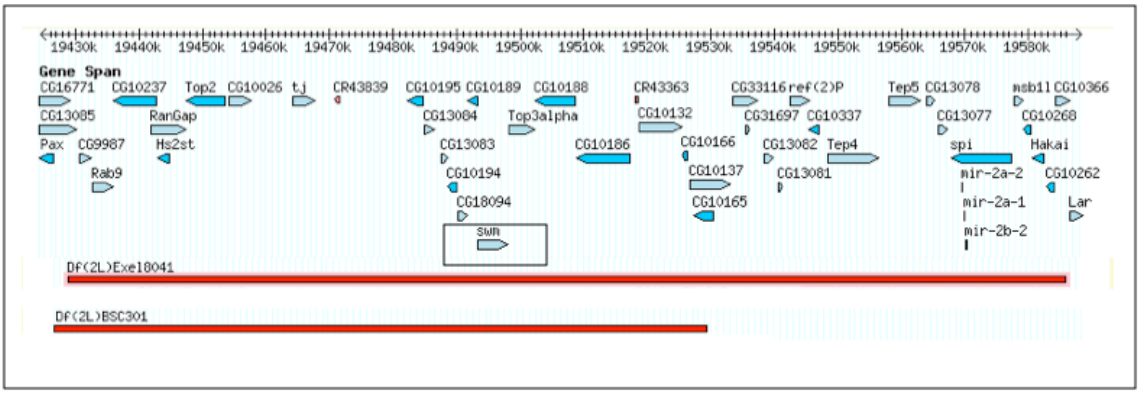

Figure 7. Region of chromosome 2L uncovered by suppressing deficiencies Exel8041 and BSC301. Red bars represent the extent of regions uncovered by the deficiencies. The minimal interacting locus, contains 22 protein-coding genes. The responsible gene identified, *swm*, is indicated by the boxed area.

Other experiments have implicated SMARCB1 as a key mediator of Hh signaling and that aberrant activation of GLI1 is a previously undescribed targetable mechanism contributing to the growth of malignant rhabdoid tumor cells. Our finding of a genetic interaction between *Snr1* and *swm* in *Drosophila* therefore demonstrates that the link between SMARCB1 (whether it be SWI/SNF dependent or not) and the Hh pathway is conserved between humans and flies and is therefore worthy of further investigation.

Spatially and temporally choreographed cell cycles accompany the differentiation of the *Drosophila* retina. Recent studies indicate that signaling

pathways with well-known roles in patterning also directly regulate cell proliferation. During the differentiation of the retina, Hh, Dpp, Notch and the EGF receptor regulate proliferation spatially through transcriptional regulation of *string*, *dacapo*, and as yet unidentified regulators of Retinoblastoma and Cyclin E/Cdk2 activities (reviewed in Baker, 2007). We hypothesize that when *Snr1* levels are reduced in the developing eye, these signaling pathways are disrupted.

(e) Functional relevance of *Snr1* interactors identifed

There are two human homologues of swm - RBM26 (chromosome 13) and RBM27 (chromosome 5) – so unfortunately neither represent the elusive potentially other causative schwannomatosis gene on chromosome 22. However, we will continue to examine whether other Hh pathway genes could be similarly implicated. As for *dacapo*, its human homologue is cyclin-dependent kinase inhibitor 1B (p27, Kip1) and is on chromsome 12.

We crossed the deficiencies that uncover *swm* and *dacapo*, as well as *swm* and *dacapo* alleles to the *en-Gal4* and *ptc-Gal4* lines driving *UAS-Snr1-shRNA* to examine whether they can modify wing phenotypes or whether these interactions are eye-specific. We found that both the deficiencies and alleles dominantly suppress the ectopic vein phenotypes at the posterior cross vein (Figure 8). Therefore *swm* and *dacapo* interact with *Snr1* in both the eye and the wing during development.

We are also using epistasis experiments to determine whether these genetic modifiers act upstream or downstream of *Snr1*. In addition, we are testing whether *dap* and/or *swm* modify *brm* and *mor* RNAi phenotypes in the eye or wing. In this way we will be able to assess whether these interactions are unique to *Snr1*. It is possible that Snr1 functions in a subset of complexes in different tissues or developmental times. By testing these modifiers with *brm* and *mor* knocked down in a variety of different tissues it is possible that we will find Snr1 functions independent from that of the Brm complex. In addition, we are preparing to investigate the possible role of the Hh pathway in the glial

phenotype that we identified using *Snr1* knockdown using the *repo-Gal4* driver that we described in the 2nd Year Report.

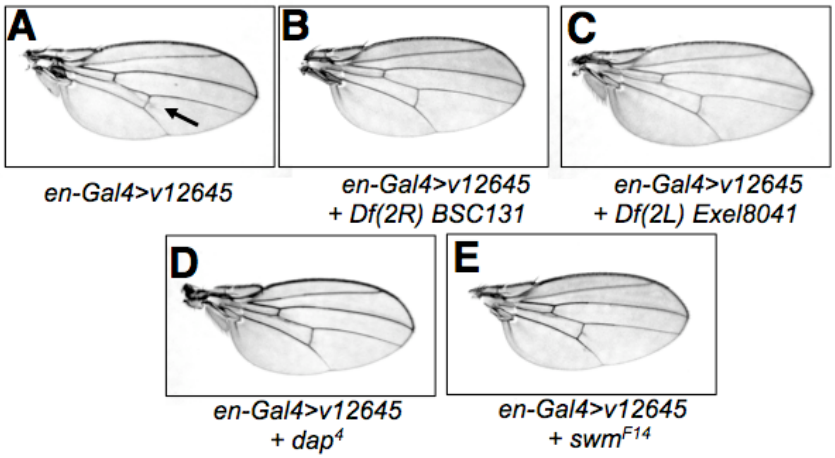

Figure 8. *swm* and *dap* interact with *Snr1* in the wing. Larvae with *Snr1* knockdown in the wing (e*n-Gal4>12645*) were reared at room temperature to reduce the blistering phenotype (seen in Figure 1 B and C). A. At RT the wing shows an ectopic vein at the posterior cross vein (PCV) – indicated by an arrow. Introduction of the deficiencies that uncover *dap* and *swm* respectively (B and C) or alleles (D and E) suppress the appearance of the ectopic veins.

We are also using epistasis experiments to determine whether these genetic modifiers act upstream or downstream of *Snr1*. In addition, we are testing whether *dap* and/or *swm* modify *brm* and *mor* RNAi phenotypes in the eye or wing. In this way we will be able to assess whether these interactions are unique to *Snr1*. It is possible that Snr1 functions in a subset of complexes in different tissues or developmental times. By testing these modifiers with *brm* and *mor* knocked down in a variety of different tissues it is possible that we will find Snr1 functions independent from that of the Brm complex. In addition, we are preparing to investigate the possible role of the Hh pathway in the glial phenotype that we identified using *Snr1* knockdown using the *repo-Gal4* driver that we described in the 2nd Year Report.

Specific Aim 3. To analyze genes which are aberrantly expressed in *Snr1* mutants.

- Months 19-22 Test hits from microarray screen for genetic interactions with *Snr1* and *brm*, *mor* etc.

- Months 23-36 Characterize mis-regulated genes from *Snr1* mutant tissues**.** Assess biological roles of selected candidate genes from microarray screens with standard Drosophila techniques.

(a) Snr1 knockdown in S2 cells: microarray analysis.

We reported previously on our complementary approach of developing a *Drosophila* tissue culture system to examine SMARCB1 function. We demonstrated that RNAi knockdown of *Snr1* in S2 cells results in a G2/M arrest of the cell cycle. Further, we tested whether SMARCB1 mutants can relieve cell cycle arrest by simultaneously knocking down *Snr1* and transfecting with constructs to express either wild type SMARCB1 or SMARCB1 with patient mutations in an add-back experiment. FACS analysis revealed that only wild type SMARCB1 could effectively rescue the cell cycle arrest of *Snr1* depleted S2 cells, demonstrating that the disease-causing missense mutations alter the function of SMARCB1 in this assay.

Subsequently we prepared RNA from S2 cells in which *Snr1* had been knocked down using dsRNA and performed microarray analysis. In concordance with a previous study (Zraly *et al*., 2006), we found the hormone-responsive ecdysone-induced genes (*Eig*) *Eig71Eh* and *Eig71Ei* were significantly up-regulated (~5-fold) when *Snr1* levels are reduced. We also found that *Cyclin G* (*CycG*) mRNA levels were significantly reduced (~4-fold) on *Snr1* RNAi. *Drosophila* CycG has recently been shown to negatively regulate cell growth and also has prominent effect on G1 and S phases (Faradji *et al.*, 2011). We speculate that the reduction of CycE levels upon *Snr1* RNAi could be responsible for the cell cycle arrest that we observed (discussed in 2nd Year Report) and/or the *Snr1* RNAi-induced cell size increase previously observed (Zraly *et al*., 2006). We are currently designing follow up experiments to investigate this hypothesis.

(b) Knock down the expression of Snr in developing fly tissues using RNAi to examine transcriptional targets

We hypothesize that examining the transcriptional targets of *Snr1* in developing tissues will be more physiologically relevant than in S2 cells. Previous microarray studies used RNA from the pupal stage and also identified ecdysone-regulated genes as being Brm complex targets (Zraly *et al*., 2006). Given our success with *Snr1* RNAi knockdown in the developing eye and wing imaginal discs in identifying novel genetic interactions, we are focusing our attention of using these tissues for microarray experiments. Driving the *UAS-Snr1 RNAi* line using ey-*Gal4* has profound effects on development of the eye, which undoubtedly are due to transcriptional defects. We will therefore examine any changes in gene expression in the developing eye in the context of our identification of regulators of CycE and the Hedgehog pathway as novel genetic interactors of *Snr1* in this tissue.

We have spent considerable time amplifying fly lines to generate sufficient material for dissection, RNA collection and subsequent microarray analysis. We intend to use the remaining time covered by the no cost extension to this award to complete the other parts of Specific Aim 3, which include bioinformatics to look for gene clustering, comparison with genetic modifier screens (including the other deficiency screen hits that have yet to be pursued) and testing hits from microarray screen for genetic interactions with *Snr1*, particularly in *Repo-Gal*-driven *Snr1* RNAi knockdown in glial cells.

Specific Aim 4. To identify and analyze the functional significance of proteins that associate with Snr1/SMARCB1.

- Months 18-36 Protein interaction studies to determine whether direct binding to Snr1/SMARCB1. Genetic experiments with selected physical inetractors from TAP-tag screens. Determine functional significance of Snr1/SMARCB1-associating proteins using standard techniques.

(a) Testing whether SMARCB1 mutants have altered interactions in the Brahma Complex

Previously we reported the generation of constructs for expression of SMARCB1 (both wild type and with patient mutations), in both Drosophila S2 cells and mammalian cells. Tagging of these proteins with N-terminal tandem FLAG and HA epitopes allowed us to purify them along with their associated proteins. We attempted to purify wild type SMARCB1 using the FLAG epitope. Using whole cell lysates from S2 cells 48 hours post-transfection we successfully purified FLAG-SMARCB1 and associated proteins. Mass spectrometry of precipitated protein complexes showed that known components of the Brm complex were purified along with SMARCB1, as expected. These included Brm, Mor, Osa and BAP60 (Table 3). We also found a large number of other proteins that were likely contaminants. Purification of the disease-causing mutant SMARCB1 proteins from total S2 cell lysates showed a similar complement of interacting proteins, with no significant differences from that of wild type SMARCB1 (Table 3). However, since the purifications did not detect all the known Brm complex members, we are unable to conclude that the SMARCB1 point mutations disrupt specific protein-protein interactions that we were unable to detect, even in the wild type control.

Protein	Mol. Mass (kDa)	SMARCB1-WT	SMARCB1-P14H	SMARCB1-R53L	SMARCB1-R374Q
Snr1	42	15	12	13	11
Brm	185	7	8	6	3
Osa	285	6	4	7	4
Mor	134	7	7	5	4
BAP60	58	2	2	1	2

Table 3 Results of protein interactors detected using FLAG-tagged SMARCB1 in S2 cells. Drosophila S2 cells were transfected with constructs expressing either wild–type or mutant SMARCB1 proteins. After purification using an anti-FLAG column, precipitated proteins were subjected to mass spectroscopy. The number of detected peptides for each protein is indicated. Only the known Brahma complex components that were detected are shown. An extensive list of other proteins was also detected, presumed to be contaminants.

To circumvent this we subsequently employed a protocol to purify nuclei from S2 cells, with the idea that nuclear lysates may help us reveal other interacting proteins. Unfortunately, despite repeated attempts to purify FLAG-SMARCB1 complexes from nuclear fractions and extensive trouble-shooting, we were unsuccessful with this approach.

(b) Purification of complexes with Snr1 in fly embryos

A similar approach of examining altered protein complexes *in vivo* is underway in flies, using the HA-tagged Snr1 and SMARCB1 transgenes used in Specific Aim 1. These transgenes are being driven ubiquitously with the *actin5C-Gal4* driver. We will prepare nuclear extracts from collected embryos (with the help of Dr. M. Korenjak) and then attempt to purify Snr1 complexes using the HA-tag. We will compare the results with the genetic hits identified in Specific Aim 2 since we anticipate that novel physical interactors may be uncovered by modifying deficiencies.

Key Research Accomplishments for Year 3

- Completed study examining differential ability of transgenic expression of human SMARCB1 to rescue *Snr1* RNAi phenotypes
- Identified novel phenotype caused by RNAi knockdown of *Snr1* in the eye using *ey-Gal4*
- *Snr1* and *Mer* genetically interact; however, Snr1 does not play a role in regulating the Hippo pathway. Loss of *Snr1* appears to affect Merlin function (not *Mer* transcriptional regulation)
- Completed 2nd chromosome deficiency screen to look for modifiers of the *Snr1* RNAi-induced phenotypes in the eye (*ey-Gal4>* and *en>UAS-Snr1 RNAi*). Secondary screens in wing (*en-Gal4>* and *ptc>UAS-Snr1 RNAi*)
- Identified *swm* and *dap* as *Snr1* genetic suppressors
- RNAi knockdown of *Snr1* in S2 cells results in gene expression changes similar to those seen in a previous study. RNA from *Snr1* RNAi knockdown in eye and wing imaginal discs prepared for subsequent microarray analysis.
- Purification of mutant SMARCB1 proteins (encoded by disease-cuaing mutations) from total S2 cell lysates showed a similar complement of interacting proteins, with no significant differences from that of wild type SMARCB1
- Refining purification of HA-SMARCB1 (wild type and mutants) from embryo nuclear lysates in order to determine whether mutants affect protein-protein interactions.

Reportable Outcomes for Year 3

- The research findings were presented at invited seminars at the following institutions:

  St. George's Medical School, University of London, UK 19th January 2012

University of Manchester, Nowgen Centre, UK 24th January 2012
Southampton University, Center for Biological Sciences, 26th January 2012
University of Cambridge, Dept. of Zoology, UK 10th May 2012

- Attended the Children's Tumor Foundation NF Conference in New Orleans (June 9th-12th 2012)

- Published review in *Disease Models and Mechanisms* on 'Modeling tumor Invasion and Metastasis in Drosophila'. *See Appendix 1.*

- Published paper in *PLoS Genetics* (Longworth *et al.,* 2012) in collaboration with Drs. M. Longworth and N. Dyson (MGH Cancer Center) During the this study we gained experience in microarray analysis and tissue sectioning, both of which were valuable during the current project. *See Appendix 2.*

- Our ongoing collaboration with Drs. Scott Plotkin and Miriam Smith (Mass General Hospital) investigating the expression of mutant SMARCB1 in schwannomatosis patients resulted in a paper in *Human Molecular Genetics* (Smith *et al.*, 2012). This work is directly related to the current award since it examines the same mutations that we are using in our Drosophila model. *See Appendix 3.*

Conclusion

We are examining mutations in the tumor suppressor gene SMARCB1 that are found in familial cases of schwannomatosis. *Drosophila* is being used to investigate the nature of the SMARCB1 mutations and their molecular consequences, which give rise to schwannomas. We have made good progress to address the questions in each of the four specific aims.

We have completed Specific Aim 1 - our examination of the differential ability of transgenic expression of human SMARCB1 to rescue phenotypes

caused by RNAi knockdown of Snr1, the fly ortholog of SMARCB1. These assays have revealed that SMARCB1 missense mutations from patients have varying degrees of residual function suggesting that, at least some of them, are hypomorphic in nature and so differ from SMARCB1 mutations that are found in the case of early onset AT/RT.

For Specific Aim 2 - we have completed the deficiency screen to look for modifiers of the *Snr1* RNAi-induced phenotypes in the eye (*ey-Gal4>UAS-Snr1 RNAi*). This has identified several potent *Snr1* interactors – the CycE regulator *dacapo* and *second wave mitotic* (*swm*), a negative regulator the Hedgehog pathway. These may represent important clues to the pathways that are misregulated when *Snr1* is lost in both the developing eye and wing. The recent finding by others of a physical interaction of SMARCB1 with GLI1, an effector of Hh signaling, suggests that our *Drosophila* model will be useful for gaining further insights into the interaction of the SWI/SNF complex with this important signaling pathway.

For Specific Aim 3 we have developed a *Drosophila* S2 tissue culture system in which we can knockdown *Snr1* using dsRNA. We have shown by add-back assays that SMARCB1 bearing disease-causing missense mutations is unable to effectively rescue the cell cycle arrest. We have used this system to examine the consequences of *Snr1* knockdown on gene expression using microarrays. The changes in gene expression were similar to those reported in a previous study. However, our finding that *CycG* expression is reduced suggests further experiments to investigate whether misregulation of this cell cycle regulator on *Snr1* knockdown could account for the observed differences in cell growth.

For Specific Aim 4 we have successfully developed a protocol to allow us to purify proteins complexed with FLAG-SMARCB1 transfected into S2 cells. By conducting the same procedure with SMARCB1 bearing mutations from schwannomatosis patients, we have so far been unable to identify any altered protein-protein interactions or complex formation.

We plan to write up the results from Specific Aims 1 and 2 for publication while we are completing experiments outlined in Specific Aims 3 and 4 during the no-cost extension. Together, these approaches in *Drosophila* will address the functional consequences of the disease-causing mutations in SMARCB1 from familial cases of schwannomatosis.

References

Baker, N.E. (2007) Patterning signals and proliferation in Drosophila imaginal discs. *Curr Opin Genet Dev.* 2007 Aug;17(4):287-93.

Biegel, J. A., Zhou, J. Y., Rorke, L. B., Stenstrom, C., Wainwright, L. M., and Fogelgren, B. (1999). Germ-line and acquired mutations of INI1 in atypical teratoid and rhabdoid tumors. *Cancer Res 59*, 74-79.

Boyd, C., Smith, M.J., Kluwe, L., Balogh, A., Maccollin, M., and Plotkin, S.R. (2008). Alterations in the SMARCB1 (INI1) tumor suppressor gene in familial schwannomatosis. *Clin Genet 74*, 358-366.

Brumby AM, Zraly CB, Horsfield JA, Secombe J, Saint R, Dingwall AK, Richardson H. (2002) Drosophila cyclin E interacts with components of the Brahma complex. *EMBO J.* 2002 Jul 1;21(13):3377-89.

Casso, D.J, Liu, S., Iwaki, D.D., Ogden, S.K and Kornberg, T.B. (2008) A screen for modifiers of hedgehog signaling in Drosophila melanogaster identifies swm and mts. *Genetics.* 178(3):1399-413.

Euskirchen G, Auerbach RK, Snyder M. (2012) SWI/SNF chromatin-remodeling factors: multiscale analyses and diverse functions. *J Biol Chem.* 287(37): 30897-905. doi: 10.1074/jbc.R111.309302. Epub 2012 Sep 5.

Faradji F, Bloyer S, Dardalhon-Cuménal D, Randsholt NB, Peronnet F. (2011) Drosophila melanogaster Cyclin G coordinates cell growth and cell proliferation. *Cell Cycle.* 10(5):805-18.

Hadfield, K. D., Newman, W. G., Bowers, N. L., Wallace, A., Bolger, C. M., Colley, A., McCann, E., Trump, D., Prescott, T., and Evans, G. (2008). Molecular characterisation of SMARCB1 and NF2 in familial and sporadic schwannomatosis. *J Med Genet.* 45, 332-339.

Hamaratoglu F, Willecke M, Kango-Singh M, Nolo R, Hyun E, Tao C, Jafar-Nejad H, Halder G. (2006) The Tumor suppressor genes NF2/Merlin and Expanded act through Hippo signaling to regulate cell proliferation and apoptosis. *Nat Cell Biol.* 8(1):27-36

Hulsebos, T.J., Plomp, A.S., Wolterman, R.A., Robanus-Maandag, E.C., Baas, F., and Wesseling, P. (2007). Germline mutation of INI1/SMARCB1 in familial schwannomatosis. *Am J Hum Genet 80*, 805-810.

Jagani Z, Mora-Blanco EL, Sansam CG, McKenna ES, Wilson B, Chen D, Klekota J, Tamayo P, Nguyen PT, Tolstorukov M, Park PJ, Cho YJ, Hsiao K, Buonamici S, Pomeroy SL, Mesirov JP, Ruffner H, Bouwmeester T, Luchansky

SJ, Murtie J, Kelleher JF, Warmuth M, Sellers WR, Roberts CW, Dorsch M. (2010) Loss of the tumor suppressor Snf5 leads to aberrant activation of the Hedgehog-Gli pathway. *Nat Med.*16(12):1429-33.

Longworth, M.S., Walker, J.A., Anderssen, E., Moon, N-S., Gladden, A., Heck, M.M., Ramaswamy, S. and Dyson, N.J. (2012) A shared role for RBF1 and dCAP-D3 in the regulation of transcription with consequences for innate immunity. *PLoS Genet.* 8(4):e1002618.

MacCollin, M., Willett, C., Heinrich, B., Jacoby, L. B., Acierno, J. S., Jr., Perry, A., and Louis, D. N. (2003). Familial schwannomatosis: exclusion of the NF2 locus as the germline event. *Neurology 60*, 1968-1974.

McCartney, B.M., Kulikauskas, R.M., LaJeunesse, D.R., and Fehon, R.G. (2000). The neurofibromatosis-2 homologue, Merlin, and the tumor suppressor expanded function together in Drosophila to regulate cell proliferation and differentiation. *Development 127*, 1315-1324.

Miles, W.O., Dyson, N.J. and Walker, J.A. (2011) Modeling tumor invasion and metastasis in Drosophila. *Dis. Model Mech.* 4(6): 753-761

Oh, H. and Irvine, K.D. (2010) Yorkie: the final destination of Hippo signaling. *Trends in Cell Biol.* 20(7), 410-417.

Sestini, R., Bacci, C., Provenzano, A., Genuardi, M., and Papi, L. (2008). Evidence of a four-hit mechanism involving SMARCB1 and NF2 in schwannomatosis-associated schwannomas. *Hum Mutat 29*, 227-231.

Smith, M.J., Walker, J.A., Shen, Y., Stemmer-Rachamimov, A., Gusella, J.F. and Plotkin, S.R. (2012) cDNA analysis of *SMARCB1 (INI1)* mutations in familial and sporadic schwannomatosis. *Hum. Mol. Genet.* 21 (24) 5239-5245 *doi: 10.1093/hmg/dds370*

Versteege, I., Sevenet, N., Lange, J., Rousseau-Merck, M. F., Ambros, P., Handgretinger, R., Aurias, A., and Delattre, O. (1998). Truncating mutations of hSNF5/INI1 in aggressive paediatric cancer. *Nature 394*, 203-206.

Zraly, C. B., Marenda, D. R., and Dingwall, A. K. (2004). SNR1 (INI1/SNF5) mediates important cell growth functions of the Drosophila Brahma (SWI/SNF) chromatin remodeling complex. *Genetics 168*, 199-214.

Zraly, C.B., Middleton, F.A and Dingwall, A.K. (2006) Hormone-response genes are direct in vivo regulatory targets of Brahma (SWI/SNF) complex function. *J Biol Chem.* 281(46):35305-15.

Disease Models & Mechanisms 4, 753-761 (2011) doi:10.1242/dmm.006908

Modeling tumor invasion and metastasis in *Drosophila*

Wayne O. Miles[1], Nicholas J. Dyson[1] and James A. Walker[1,2,*]

Conservation of major signaling pathways between humans and flies has made *Drosophila* a useful model organism for cancer research. Our understanding of the mechanisms regulating cell growth, differentiation and development has been considerably advanced by studies in *Drosophila*. Several recent high profile studies have examined the processes constraining the metastatic growth of tumor cells in fruit fly models. Cell invasion can be studied in the context of an in vivo setting in flies, enabling the genetic requirements of the microenvironment of tumor cells undergoing metastasis to be analyzed. This Perspective discusses the strengths and limitations of *Drosophila* models of cancer invasion and the unique tools that have enabled these studies. It also highlights several recent reports that together make a strong case for *Drosophila* as a system with the potential for both testing novel concepts in tumor progression and cell invasion, and for uncovering players in metastasis.

Introduction

Cancer is a leading cause of death worldwide and, according to the World Health Organization, was responsible for the death of 7.9 million people in 2007 (www.who.int). This disease is characterized by the uncontrolled malignant growth of cells; however, the vast majority of human fatalities arise from secondary metastatic tumors. These secondary tumors generally spread from the original site via the blood or lymphatic system and are highly invasive and aggressive. The metastatic process involves several discrete biological steps: loss of cellular adhesion, increased motility and invasiveness, entry and survival of tumor cells in the circulation, their exit into new tissue, and their eventual colonization of a distant site (Chambers et al., 2002; Gupta and Massague, 2006). Understanding the mechanisms that promote tumor invasion and the role of the microenvironment is important for developing therapeutic strategies to treat metastatic cancers (Yang and Weinberg, 2008; Nguyen et al., 2009; Hanahan and Weinberg, 2011).

Over the last decade, the fruit fly *Drosophila melanogaster* has become an important model system for cancer studies. Reduced redundancy in the *Drosophila* genome compared with that of humans, coupled with the ability to conduct large-scale genetic screens in this organism, has enabled its use to determine the molecular characterization of important signaling cascades, developmental processes and growth control. For example, our understanding of the Hippo, Notch, Dpp and JAK-STAT signaling pathways, all of which are involved in tumor formation, has been enhanced by research in *Drosophila* (for reviews, see Brumby and Richardson, 2005; Vidal and Cagan, 2006; Januschke and Gonzalez, 2008). *Drosophila* genetics has revealed many genes that, when mutated or dysregulated, result in or contribute to tumorigenesis. Hyperplastic tumor suppressors, including components of the Hippo pathway, promote increased proliferation or survival, but do not disrupt tissue structure or differentiation. By contrast, *Drosophila* neoplastic tumor suppressors, such as the apical-basal cell polarity regulators (e.g. Lgl), lead to loss of tissue architecture, defects in differentiation and failure to exit the cell cycle. Elegant genetic and cell biology techniques have enabled the effects of tumor suppressors and oncogenes to be examined in the context of the whole animal. The capacity to generate patches (clones) of mutant tissue for specified genes during fly development has facilitated investigations into the role of the microenvironment in tumor development. Similarly, studies using clonal analysis in *Drosophila* have begun to elucidate cell competition mechanisms, which could potentially confer malignant cells with a growth advantage over their neighbors.

In conjunction with studies using other model organisms, flies have contributed greatly to our understanding of the mechanisms involved in cancer initiation and progression, revealing previously unknown molecular components and concepts. In turn, these have served to guide researchers who use mammalian systems to study cancer. This Perspective focuses on recent developments using fly tumor models that have been generated by tumor suppressor mutations or oncogene overexpression to induce neoplastic tumors of neuronal and epithelial origin as a means to probe the mechanisms involved in cellular invasion and metastasis.

Insights from metastatic neuronal tumors in the developing larval brain

Single gene mutations in a unique subset of genes {*lethal (3) malignant brain tumor* [*l(3)mbt*], *brain tumor* (*brat*), *discs large*

[1]Massachusetts General Hospital Center for Cancer Research and Harvard Medical School, 149, 13th Street, Charlestown, MA 02129, USA
[2]Center for Human Genetic Research, Massachusetts General Hospital, Boston, MA 02114, USA
*Author for correspondence (jwalker@helix.mgh.harvard.edu)

(*dlg*), *scribble* (*scrib*), *lethal giant larvae* (*lgl*), *miranda* (*mira*), *prospero* (*pros*), *partner of inscuteable* (*pins*) (for reviews see Januschke and Gonzalez, 2008; Froldi et al., 2008)} cause malignant neoplastic tumors in the *Drosophila* larval brain. These genes have crucial roles in regulating proliferation and development [*l(3)mbt*] (Gateff et al., 1993) and apical-basal cell polarity (*dlg* and *scrib*) (Woods et al., 1989; Bilder et al., 2000).

The human homologs of Dlg, Scrib and Lgl are important regulators of cell polarity, and mutations or splice variants have been linked to poor prognosis for colorectal (Schimanski et al., 2005) and hepatocarcinoma (Lu et al., 2009) patients. Importantly, all three complex components are targets for E6 papillomavirus-mediated degradation (Nakagawa and Huibregtse, 2000; Humbert et al., 2003; Handa et al., 2007). L(3)mbt has also been linked to various myeloid haemopoietic disorders (Boccuni et al., 2003) and is important for DNA replication and genomic stability (Gurvich et al., 2010).

Of these fly neoplastic tumor suppressors, *lgl* and *brat* are the best characterized. Lgl is localized to the cellular cortex, and functions in the same genetic pathway as *dlg* and *scrib* to maintain cellular polarity. Neuroblasts from *lgl* mutant larvae undergo aberrant symmetrical cell divisions, rather than the normal asymmetric divisions that are required for neuroblast and ganglion mother cell production (Mechler et al., 1985). Brat regulates ribosomal RNA (rRNA) synthesis and is a translational repressor. Brat is also asymmetrically localized to the ganglion mother cell after neuroblast division and is necessary for neuronal differentiation and proliferation control (Arama et al., 2000). Malignant tumors resulting from mutations in these fly neoplastic tumor suppressors cause late larval lethality but can be propagated and will metastasize when allografted into a recipient adult host (Gateff, 1978; Januschke and Gonzalez, 2008).

Metastasis of *lgl* and *brat* tumors

The Shearn group has utilized allograft experiments to investigate the metastatic behavior of *lgl* and *brat* mutant cells (Fig. 1A). Neoplastic brain tumors labeled with β-galactosidase (encoded by *lacZ*) from mutant larvae were dissected and allografted into the abdomens of wild-type adult flies. These tumors grew rapidly and resulted in host lethality within 12 days. Ovaries from allograft recipients were dissected and assayed for cells expressing *lacZ*. Because the ovary is contained in a non-porous epithelial sheet and muscle layers surround the ovarioles, only cells that are capable of metastasizing can invade into this organ (Fig. 1A). *lacZ*-positive cells were detected in recipient ovarioles from *lgl* and *brat* mutant tumors but not from control brains. These *lacZ*-positive cells in the ovary were shown to retain their neuronal and glial cell markers. This work provided the first evidence that *Drosophila* cells can metastasize through epithelial tissue and colonize new sites distant from the initial tumor (Beaucher et al., 2007a).

To understand the processes regulating this metastasis, a candidate approach was used to identify genes that are required for invasion by *lgl* and *brat* cells. Matrix metalloproteases (MMPs) have long been linked to metastasis in human cancer and were therefore excellent candidates. The *Drosophila* genome encodes two MMPs (MMP1 and MMP2). MMP1 expression is strongly upregulated in *lgl* mutant cells and is necessary for their metastatic behavior (Beaucher et al., 2007b). By contrast, MMP1 expression is not required in *brat* mutant cells but is required in the host tissue, suggesting that MMP1 co-operates non-cell-autonomously with *brat* mutant cells to enable their metastasis.

Molecular profiling of *l(3)mbt* neuronal tumors

Recent studies from the Gonzalez group have taken a fresh approach to identifying genes required for *l(3)mbt* tumor growth (Janic et al., 2010). *l(3)mbt* is a substoichiometric member of the *Drosophila* dREAM-Myb complex, which is required for gene silencing, and functions in establishing and maintaining differentiation states (Lewis et al., 2004). Similar to *lgl* and *brat* tumors, those arising from *l(3)mbt* mutations result in larval lethality and can be allografted (Fig. 1B).

By conducting extensive expression arrays on larval neuronal and allograft cultured tumors, gene expression profiles were identified for tumors that result from single gene mutations [in *l(3)mbt*, *brat*, *lgl*, *mira*, *pros* and *pins*] (Janic et al., 2010). By comparing profiles, Janic and colleagues characterized an *l(3)mbt*-specific tumor signature. The concatenate sequencing of Piwi-interacting RNAs (piRNAs) and microRNAs from these tumors identified small RNA changes that are characteristic of the *l(3)mbt* tumors. Together with immunohistochemical analyses, these approaches provide a basis for understanding the gene expression changes that are specific to *l(3)mbt* tumors. The *l(3)mbt* tumor signature surprisingly contains a disproportionately high number of germline-specific genes and microRNAs. This result suggests that a germline fate is associated with *l(3)mbt* tumor growth, and is in agreement with studies from *Caenorhabditis elegans* that linked soma-to-germline transition with increased fitness and longevity (Curran et al., 2009; Wang et al., 2005).

Genetic studies then tested the capacity of mutations in upregulated germline-specific genes to modify *l(3)mbt* tumor formation and allograft metastasis (Janic et al., 2010). Interestingly, only mutations in a subset of germline-specific genes (*piwi*, *vasa*, *aub* and *nos*) could suppress *l(3)mbt* tumor formation. By contrast, other upregulated germline-specific transcripts (*zpg*, *Pxt* and *AGO*) were unable to prevent tumor formation or metastatic growth. This result suggests that only a limited number of germline-specific genes are capable of restricting tumor growth. These findings provide a detailed understanding of the gene expression and small RNA changes in *l(3)mbt* neoplastic tumors, and highlight the possibility that a soma-to-germline transition accompanies metastasis. However, this approach has not yet identified genes that are specifically required for invasion, because all metastatic suppressors also prevented *l(3)mbt* tumor growth. Further analysis of the *l(3)mbt* tumor signature will hopefully identify other metastasis-promoting factors.

Using mutations to generate neoplastic tumors has significant advantages. First, only a single mutational event is required to initiate tumor growth in an isogenic background. Second, the *l(3)mbt* alleles are particularly advantageous because they are temperature sensitive, permitting gene expression arrays to be conducted from a single stock at both permissive and restrictive temperatures. Finally, these tumors develop rapidly and metastasize when allografted. These experiments permit expansion of the tumor mass for biochemical analysis and metastasis modeling.

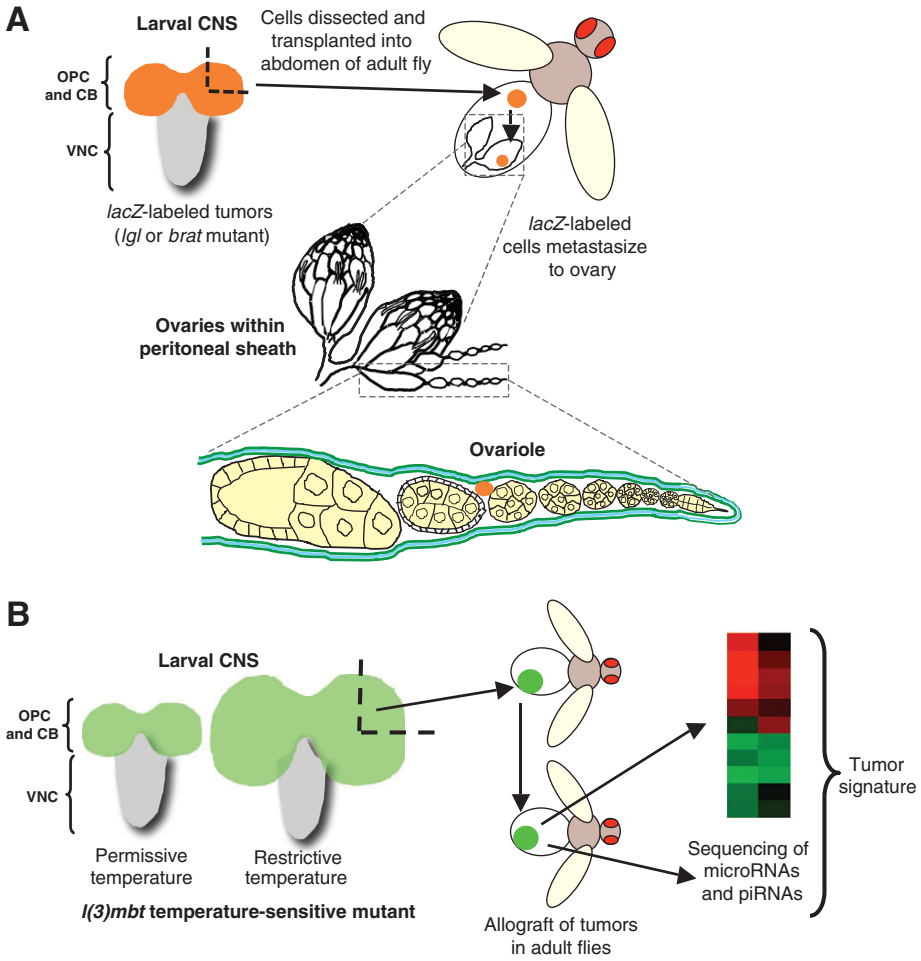

Fig. 1. *Drosophila* models of tumor metastasis caused by loss-of-function mutations in *lgl or brat* and *l(3)mbt*. The *Drosophila* larval brain is composed of two hemispheres and the ventral nerve cord (VNC). Mutant tumorous tissue in these models is restricted to the outer proliferative center (OPC) and central brain (CB) regions. (A) Neoplastic brain tumors caused by mutations in either *lgl* or *brat* can be engineered to express a reporter gene (*lacZ*; orange). Larval brains from these *lgl* or *brat* mutant animals are quartered and transplanted into the abdomens of adult female flies. The transplanted tissue continues to proliferate in the abdomen and, after several days, the ovaries of the host can be dissected and examined by immunofluorescence to detect labeled tumor cells that have metastasized. *Drosophila* ovaries are encased within a peritoneal sheath. Each ovary consists of 15-20 ovarioles, which are surrounded by an epithelial sheath of cells in addition to a muscle layer (blue) between two layers of extracellular matrix (green). Any *lacZ*-expressing cells found within the ovarioles must have traversed these layers and are therefore considered to have undergone metastasis. (B) Modeling metastasis using tumors caused by loss-of-function mutations in *l(3)mbt*. Temperature-sensitive mutations in *l(3)mbt* result in tissue overgrowth in the developing larval CNS when grown at restrictive temperatures (29°C). Tumor tissue (engineered to express GFP) can be dissected and transplanted into the abdomens of wild-type adult flies (allografts). These can be maintained and multiple rounds of allografts can be performed by transplantation into other flies, thereby generating sufficient material for biochemical analysis (e.g. microarray analysis, sequencing and western blotting). Comparison of the expression profiles of *l(3)mbt* and *brat* mutant tumors enabled an *l(3)mbt*-specific tumor expression signature to be obtained (Janic et al., 2010).

Insights from neuronal metastatic tumors induced by oncogene overexpression

Modeling *Ras*^{V12} tumors in the larval eye neural epithelium

Overexpression of oncogenic Ras protein (Ras^{V12}) causes benign tumor growth in *Drosophila*. This model has been used to identify pathways that are required for tumor development and metastasis. The mosaic analysis with a repressible cell marker (MARCM) technique can be used to generate clones expressing activated Ras^{V12} by FLP-FRT-mediated mitotic recombination; clones are concomitantly labeled with a visible marker (*UAS-GFP*) (Theodosiou and Xu, 1998; Lee and Luo, 2001; Elliott and Brand, 2008). Using an eye-specific flippase (*ey-FLP*) to convert an inactive *GAL4* driver (*Act>y+>GAL4*) to an active conformation (*Act>GAL4*) enables the ectopic expression of *UAS* transgenes to be stimulated in the larval neural tissue, in an otherwise wild-type animal (Pagliarini and Xu, 2003). Expression of activated Ras (*UAS-Ras*^{V12}) causes benign tumor growth in the larval midbrain, which can be visualized through imaging living larvae or pupae directly. These benign tumors can then be used to identify genetic modifiers that are required for either initial tumor development and/or metastasis (Fig. 2A).

This system identified the cell polarity genes *scrib*, *lgl* and *dlg* as being crucial for constraining metastatic growth (Pagliarini and Xu,

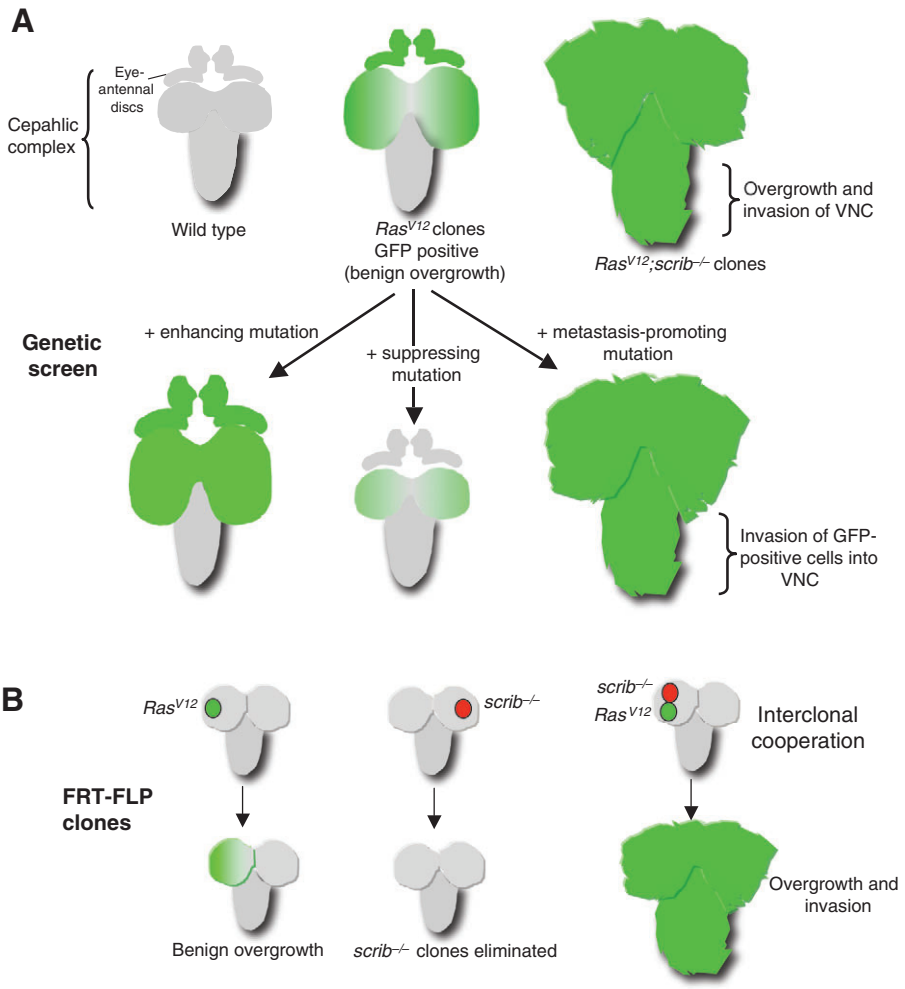

Fig. 2. Modeling tumor invasion and metastasis in the *Drosophila* larval brain. (A) Ras^{V12} overexpression clones generated by the MARCM system in eye-antennal discs. These clones (marked with GFP, and shown in green) produce a benign overgrowth throughout the cephalic complex. When *Ras^{V12}* clones are also mutant for *scrib*, they become tumorigenic and metastasize, as shown by invasion of GFP-labeled cells into the ventral nerve cord (VNC). Genetic screens have identified modifiers of the *Ras^{V12}* phenotype [suppressor, JNK; enhancer, *large giant lethal* (*lgl*); metastatic enhancer, *deep orange* (*dor*)] (Chi et al., 2010; Wu et al., 2010). (B) Interclonal cooperation of *Ras^{V12}* and *scrib$^{-/-}$* clones. As described in A, Ras^{V12} overexpression produces benign overgrowth. *scrib$^{-/-}$* clones grow at a reduced rate and are excluded via cell competition. Adjacent *Ras^{V12}* and *scrib$^{-/-}$* clones cooperate to overproliferate and undergo metastasis. The large tumor and metastatic growth consists almost exclusively of *Ras^{V12}* cells, suggesting that *scrib$^{-/-}$* cells actively cooperate with *Ras^{V12}* cells during the early stages of tumor growth and metastasis (Wu et al., 2010).

2003). All three of them genetically interact and cause overgrowth of *Ras^{V12}* tissue when mutated. These studies also identified *bazooka*, *stardust* and *cdc42* as factors that do not induce overgrowth when mutated singly but can strongly stimulate oncogenic Ras-mediated tumor growth and metastasis (Pagliarini and Xu, 2003). Each of these genes can also regulate cell polarity and E-cadherin expression. Crucially, although downregulation of E-cadherin is necessary for *Ras^{V12};scrib$^{-/-}$*-induced metastasis, it is not sufficient, implicating other contributing factors in metastatic growth.

The relationship between oncogenic Ras and JNK signaling

Several *Drosophila* laboratories have highlighted the importance of the oncogenic cooperation between Ras and JNK signaling. Constitutive activation of the Ras signaling pathway prevents fly cells from undergoing JNK-mediated apoptosis in response to cellular stresses (Brumby and Richardson, 2003; Brumby and Richardson, 2005). The Xu group has linked JNK upregulation to cell polarity and changes in E-cadherin expression in *Ras^{V12};scrib$^{-/-}$* clones (Igaki et al., 2006). They also demonstrated that overexpression of negative regulators of the JNK pathway [using a transgene to express a dominant-negative form of *Drosophila* JNK (encoded by the *bsk* gene)] prevents tumor formation and metastasis (Igaki et al., 2006). The Bohmann laboratory has shown that the invasion potential of *Ras^{V12};scrib$^{-/-}$* clones is dependent on the Fos-mediated transcriptional activation of *mmp1* downstream of JNK (Uhlirova and Bohmann, 2006). Expression of the MMP inhibitor, TIMP, or *mmp1* RNA interference (RNAi) knockdown, was able to suppress cell invasiveness (Uhlirova and Bohmann, 2006).

Recent studies of the *sds22* gene in *Drosophila* have strengthened the idea that epithelial integrity and JNK signaling cooperate to drive the metastatic growth of *Ras^{V12};scrib$^{-/-}$* clones (Jiang et al., 2011). Sds22 is a conserved regulatory subunit of protein phosphatase 1 (PP1), and acts as a regulator of epithelial polarity and as a neoplastic tumor suppressor in *Drosophila* (Grusche et al., 2009). Loss of *sds22* in *Ras^{V12}* clones results in reduced epithelial integrity, and the clones become invasive. Overexpression of Sds22 in *Ras^{V12};scrib$^{-/-}$* cells largely suppresses their tumorigenic growth, and mechanistic studies suggest that Sds22-PP1 inhibits non-muscle myosin II and JNK activity (Jiang et al., 2011). The authors of this study also showed that human *SDS22* is deleted or downregulated in multiple types of carcinoma.

A recent study by the Richardson group identified key regulators of the actin cytoskeleton and cell morphology, including Rho1-

family GTPases and RhoGEFs, as Ras-cooperating proteins (Brumby et al., 2011). The hyperplastic eye phenotype produced by driving *UAS-Ras^{V12}* with *ey-GAL4* was screened for modifiers using a collection of P-element enhancer insertion lines bearing *UAS* promoter sequences. These lines result in overexpression of the gene adjacent to the insertion element in *Ras^{V12}* cells. JNK pathway activation is crucial for the cooperation of these actin cytoskeletal regulators with Ras^{V12}. The relevance to human cancer of the collaboration between oncogenic Ras and JNK was demonstrated in this study by correlating JNK signaling with the upregulation of Ras in breast cancers (Brumby et al., 2011).

The role of JNK signaling in promoting metastatic behavior seems to be context specific. In contrast to the promotion of Ras-induced metastasis by JNK, analysis of *lgl$^{-/-}$* clones suggests that the activity of Diap1 (a caspase inhibitor) and JNK loss are essential for invasion of mutant cells out of the clone (Grzeschik et al., 2010a; Grzeschik et al., 2010b). Although Diap1 expression is sufficient to inhibit widespread apoptosis, cells at the boundary of *lgl$^{-/-}$* clones undergo cell death in a JNK-dependent manner. By blocking the JNK signaling cascade, apoptosis of these cells is specifically inhibited, stimulating de-differentiation and cellular invasion.

Lysosome dysfunction in *Ras^{V12}* tumor growth and invasion

Recent studies from the Xu laboratory have used genetic screens to identify mutations that promote *Ras^{V12}* cell metastasis (Fig. 2A). The authors tested 3119 ethyl-methanesulfonate-mutagenized lines (on the X chromosome) for their capacity to modify *Ras^{V12}* larval tumors. This screen identified 516 suppressors and 351 enhancers of tumor growth, of which 23 enhanced tumor growth as well as metastasis (Chi et al., 2010). Two of these metastasis-promoting mutations occurred within the class C vacuolar protein sorting (VPS) complex member *deep orange* (*dor*). By testing mutations in genes encoding other components of this lysosome complex, namely *carnation* and *vps16A*, they confirmed that loss of lysosome activity stimulates metastatic growth of the *Ras^{V12}* tissue (Chi et al., 2010). Characterization of other modifiers from this screen might provide a clearer understanding of the mechanisms underlying Ras-mediated tumor growth in *Drosophila*. This study also confirmed their genetic findings: feeding chemical inhibitors of lysosomal function to larvae with *Ras^{V12}* overgrowths promoted tumor development and metastasis. This work illustrates the potential of *Drosophila* to screen for therapeutic cancer drugs in vivo, a system that might one day provide a cheap and rapid means for drug discovery.

Interclonal cooperation between *Ras^{V12}* and *scrib* mutant cells

Exciting recent work using the *Ras^{V12}-scrib$^{-/-}$* system has demonstrated a non-cell-autonomous effect between neighboring clones (called interclonal cooperation; Fig. 2B). Adjacent *Ras^{V12}* clones and *scrib$^{-/-}$* clones actively cooperate to form tumors and can metastasize (Wu et al., 2010). Interclonal tumors and metastatic growths are smaller than those produced from a single *Ras^{V12};scrib$^{-/-}$* clone but still represent a significant tumor burden to the hosts (Fig. 2B). During later stages of tumor development, these interclonal tumors are made up almost exclusively of Ras^{V12}-expressing cells, suggesting that the *scrib$^{-/-}$* mutant cells are only required for the initial stages of tumor formation and metastasis (Wu et al., 2010). These studies also identified the JAK-STAT signaling pathway as being a crucial downstream target of JNK activity, implicating JNK and JAK-STAT as important oncogenic drivers for *Ras*-mediated tumor growth (Wu et al., 2010). In agreement with these findings, the authors went on to demonstrate that JNK activation after wounding is also able to promote the overgrowth of *Ras^{V12}* cells. This study potentially forges a link between tissue damage and Ras-stimulated JNK activity – a situation resembling the chronic inflammation that has been reported to contribute to tumorigenesis in humans (Mantovani, 2010). Other recent *Drosophila* studies have also highlighted the role of the immune response in tumor growth (Box 1).

Screening for regulators of invasive growth caused by activation of the Notch pathway

The Notch signaling cascade was originally identified as an important regulator of proliferation and differentiation in flies. Extensive genetic and biochemical studies have identified and characterized the components and regulators of this pathway (Artavanis-Tsakonas and Muskavitch, 2010). *Drosophila* studies have revealed that, similar to oncogenic Ras, Notch signaling cooperates with JNK to promote dysregulation of epithelial integrity (Brumby and Richardson, 2003; Leong et al., 2009). Aberrant Notch signaling is associated with several human cancers, including skin, breast, lung and ovarian cancer (for a review, see Allenspach et al., 2002). Tumors containing amplifications of genes encoding Notch signaling components (e.g. Notch and Jagged) tend to be highly aggressive and metastatic.

Overexpression of the Notch activator Delta (Dl) using the *eyeless-GAL4* driver (*ey-GAL4>UAS-Dl*) stimulates a non-metastatic overproliferation of eye tissue. Flies treated with a γ-secretase inhibitor to prevent Notch receptor proteolysis showed complete rescue of the *ey-GAL4>UAS-Dl* phenotype (Palomero et al., 2007). This model has been employed by the Dominguez group to screen for modifiers of this phenotype using a library of P-element UAS insertion lines that result in gene overexpression

Box 1. The role of the immune system in tumor growth in *Drosophila*

Several recent reports suggest that the immune system plays a crucial role in *Drosophila* tumor models, as is the case in mammalian tumors. Circulating blood cells, known in *Drosophila* as hemocytes, are part of the fly immune system and have been found to associate with *Ras^{V12};scrib$^{-/-}$* tumors and to reduce tumor growth in *scrib$^{-/-}$* animals (Pastor-Pareja et al., 2008). The *Drosophila* genome encodes a single member of the tumor necrosis factor (TNF) family, named Eiger (Egr). Egr has been shown to be required for the JNK-dependent cell death of *scrib* or *dlg* clonal tissue (Igaki et al., 2009). In the absence of *egr*, these mutant clones grow aggressively and develop into tumors (Igaki et al., 2009). By contrast, another study showed that loss of *egr* in *Ras^{V12};scrib$^{-/-}$* tumors prevented invasive overgrowth, which was correlated with reduced JNK activation and a failure to express MMP1 (Cordero et al., 2010). Therefore, in the presence of oncogenic Ras, Egr seems to play a role as a tumor promoter. This study also revealed that Egr is produced in the hemocytes associated with *Ras^{V12};scrib$^{-/-}$* tumors (Cordero et al., 2010). Together, these *Drosophila* models might provide an excellent parallel to mammalian tumors, in which TNF is produced in both tumor cells and associated immune cells, where it has been shown to have both oncogenic and tumor-suppressive roles (Balkwill, 2009).

(Ferres-Marco et al., 2006). One of these lines, *eyeful*, strongly promoted the metastatic growth of *ey-GAL4>UAS-Dl* eye tissue, resulting in secondary eye growths throughout the body. Using various tissue-specific *GAL4* drivers, the authors demonstrated that co-expression of *Dl* and *eyeful* could stimulate massive overgrowth and metastatic invasion in multiple tissue settings. The *eyeful* construct was mapped within the divergently transcribed genes of *longitudinals lacking* (*lola*) and *pipsqueak* (*psq*), which produce a myriad of alternatively spliced BTB (BR-C, ttk and bab) proteins, which are required for the recruitment of histone deacetylases and Polycomb complexes to promoter regions. Further biochemical studies demonstrated that silencing of Retinoblastoma (Rbf) expression via promoter hypermethylation strongly contributed to the metastatic phenotype (Ferres-Marco et al., 2006).

This screen also identified the P-element insertion GS1D233C as an enhancer of the *ey-GAL4>UAS-Dl* phenotype. This insertion was mapped to the *Akt1* locus, which encodes an important serine/tyrosine kinase linked to phosphatase and tensin homolog (PTEN) and Notch signaling (Palomero et al., 2007). These results suggest that flies will provide a useful system to test new pharmacological reagents targeted against the Notch pathway.

The Hassan group used the *ey-GAL4>UAS-Dl/eyeful* phenotype to screen for mutations that could further enhance metastatic growth (Bossuyt et al., 2009). This screen identified *atonal* (*ato*), a transcription factor required for retinal terminal differentiation, as a crucial tumor suppressor. Mutations affecting *ato* dramatically enhanced tumor burden and metastasis rates, and tumors displayed elevated levels of proliferation markers (such as phosphorylated histone H3). Conversely, overexpression of *atonal* upregulated both Decapo (also known as p21 cell-cycle inhibitor) and phosphorylated-JNK levels, inhibiting proliferation and inducing apoptosis. Furthermore, overexpressing dominant-negative JNK (*bsk*) partially mimics *ato* downregulation in the *eyeful* (*ey-GAL4>UAS-Dl/eyeful*) model, indicating that JNK signaling is downstream of *atonal* and that *atonal* requires active JNK signaling to inhibit overgrowth (Bossuyt et al., 2009).

Modeling glioma in *Drosophila*

Developing *Drosophila* models of specific human tumor types is limited in many cases owing to the lack of directly homologous organs (e.g. pancreas, liver and lung). However, recent studies have capitalized on the similarity of mammalian and *Drosophila* glial cells to model glioblastoma in flies (Read et al., 2009; Witte et al., 2009). Glioblastomas are the most common tumors of the central nervous system (CNS), and their rapid proliferation and malignancy result in poor patient prognosis.

Mutation or amplification of the gene encoding epidermal growth factor receptor (EGFR) tyrosine kinase, loss of PTEN [which antagonizes the growth promoting effects of phosphoinositide 3-kinase (PI3K) signaling] or activating mutations in PI3K (Furnari et al., 2007) are genetic lesions that are commonly associated with gliomas. Consequently, the glial-specific *Repo-GAL4* driver (incorporating the promoter *reversed polarity*) was used to simultaneously express transgenes encoding constitutively active EGFR and PI3K in larval glia. Co-activation of EGFR (or Ras) and PI3K in larval glia results in neoplasia, neurological defects and lethality (Read et al., 2009; Witte et al., 2009). The overproliferation and neoplastic transformation seems to be specific for glia, because overexpression of EGFR and PI3K in neurons, neuroblasts or other glial cells (such as oligodendrocyte-like neuropil glia and astrocyte-like cortex glia) failed to transform them.

The neoplastic glia induced in this *Drosophila* model mimic the highly proliferative anaplastic glia from high-grade human gliomas. They ectopically express Cyclin-B (CycB), Cyclin-E (CycE) and MMP1, promoting cell cycle entry and invasive growth. These studies demonstrated that glia expressing activated EGFR or Ras and PI3K invade into inappropriate areas of the brain, such as along Bolwig nerves, which are not normally accompanied by glial cells (Read et al., 2009; Witte et al., 2009).

Genetic experiments have revealed that the malignant neoplastic transformation of larval glia induced by EGFR and PI3K occurs via a complex network of genetic factors that are commonly mutated or activated in human gliomas. These downstream effectors include Tor, Myc, G1 cyclin-Cdk complexes (such as those including Cyclin B or E) and the Rb-E2F pathway. Interestingly, pharmacological inhibitors, including compounds that are used to treat patients, rescued these phenotypes in larvae. An EGFR inhibitor (gefitinib) partially reduced the migration of EGFR- and PI3K-transformed glia, whereas a PI3K inhibitor (wortmannin) and an Akt inhibitor (triciribine) completely prevented invasion (Witte et al., 2009). Together, these studies suggest that this *Drosophila* model is useful for deciphering the signaling cascades underlying the abnormal behavior of glioma cells, including their metastatic potential.

Modeling tumor invasion in the epithelia of the *Drosophila* wing disc

Roles for both receptor and non-receptor tyrosine kinases in cell transformation and progression towards malignant phenotypes are well established (Blume-Jensen and Hunter, 2001). The SRC family kinases (SFKs) are membrane-linked non-receptor tyrosine kinases that are required for regulating adhesion and cytoskeleton reorganization, cell cycle progression, and migration (Guarino, 2010; Thomas and Brugge, 1997). Elevated SRC levels have been reported in a wide variety of human cancers, including those of the colon, liver, lung, breast and pancreas (Ishizawar and Parsons, 2004; Summy and Gallick, 2003). SFK activity is inhibited by the C-terminal SRC kinase (CSK) family of tyrosine kinases [CSK and CSK homologous kinase (CHK)] (Chong et al., 2005); both CSK and CHK phosphorylate and inactivate SFKs, and mutations disrupting this activity have been implicated in a plethora of cancers. Elevated SRC levels (either by amplification of SRC or loss of CSK function) promote anchorage-independent cell growth, tumor cell invasion and metastasis (Guarino, 2010). Although SRC is a crucial regulator of epithelial-mesenchymal transition (EMT), the exact mechanism of how SRC promotes metastatic growth remains elusive.

Recent studies from the Cagan group have utilized the pseudostratified epithelia of the *Drosophila* larval wing imaginal disc to model invasive cell growth (Vidal et al., 2006). Global depletion of the sole *Drosophila* CSK/CHK ortholog, Csk, using either RNAi or *Csk* mutations, elevates active levels of Src, leading to significant overgrowth in developing larvae. By contrast, targeting *Csk* depletion to a discrete stripe along the anterior-posterior (A-P) boundary of the larval wing disc using a *patched-GAL4* driver (*ptc-GAL4*) to express a *Csk* RNAi transgene (*UAS-Csk-RNAi*) produces a metastatic phenotype (Vidal et al., 2006).

Src-transformed cells lose their apical profile and are excluded from the epithelium. These cells invasively migrate through the basal extracellular matrix, and eventually apoptose (Fig. 3). This invasive migration has been used to model tumor metastasis. Invasion occurs only at the boundaries between *Csk* mutant cells and the adjacent wild-type cells, suggesting that the microenvironment is crucial in determining the outcome of the Src-activated cells (Vidal et al., 2006).

By utilizing this model of metastasis, Vidal and co-authors examined the capacity of GFP-labeled *Csk-RNAi* cells to invasively migrate in different mutant backgrounds. These studies implicate JNK signaling in the apoptotic response of *Csk-RNAi* cells. Mutations in *puckered* (*puc*), a *Drosophila* JNK-specific phosphatase, cause an upregulation in JNK signaling and enhance both the apoptotic and the invasion phenotype of *ptc>Csk-RNAi* cells. Conversely, *puc* overexpression (*UAS-puc*) using *ptc-GAL4* prevents apoptosis within the stripe. Similar experiments revealed that the small GTPase Rho1 is a positive mediator of the JNK signal in *Csk-RNAi* boundary cells, similar to that seen in activated Ras^{V12} tumors in the eye epithelia (discussed above) (Brumby et al., 2011).

Cadherin-containing complexes are required for maintaining adherens junctions, which are important for cell adhesion and tissue structure. Src modulates the integrity of these adhesion sites: E-cadherin-dependent adhesion is reduced in *ptc>Csk-RNAi* tissue. These results implicated E-cadherin in the recognition and elimination of *Csk-RNAi* cells. Depletion of E-cadherin suppresses both the migratory and apoptotic phenotypes of *ptc>Csk-RNAi* boundary cells. Using candidate approaches, p120-catenin and both MMPs (MMP1 and MMP2) were found to be important for the *Csk-RNAi* invasive phenotype (Vidal et al., 2006; Vidal et al., 2010).

mmp1 transcript levels were specifically upregulated at the leading edge of *Csk-RNAi* migrating cells (Singh et al., 2010; Vidal et al., 2010), suggesting that rearrangement of the extracellular matrix is crucial for this invasive growth.

In a separate study, the capacity of Src to contribute to Ras^{V12}-induced tumor growth was tested (Vidal et al., 2007), and malignant overgrowth of Ras^{V12} tumors was found to correlate with elevated Src levels. These studies suggest a progressive role for Src, whereby low levels promote proliferation during early tumorigenesis and high levels are required for the later stages of invasive migration and metastasis (Vidal et al., 2007).

Invasive migration phenotypes similar to those of *ptc>Csk-RNAi* cells are produced by the overexpression of the oncogene *Abl* in the A-P boundary of the wing disc (Singh et al., 2010). Co-expression of *ptc>Csk-RNAi* and *UAS-Abl* results in synergistic enhancement of the invasive phenotype. Conversely, the migration phenotype induced by *UAS-Csk-RNAi* is suppressed by reducing Abl function using RNAi. Together, these findings suggest that Abl functions downstream of Csk and Src to mediate cell invasion. In addition to activating JNK (required for cell invasion and apoptosis), Abl overexpression also stimulates ERK signaling, further promoting cellular proliferation. Interestingly, the authors of this study defined a positive feedback loop whereby Abl increases the activity of Src, resulting in signal amplification (Singh et al., 2010).

This system provides an excellent model in which to study the function of genes in cell proliferation, survival and invasive behavior in the context of cell polarity. Although these reports only tested candidate genes for their ability to modify the invasion phenotype induced by *Csk* RNAi, the system should prove amenable to genetic screening using *UAS-RNAi* fly lines to identify genes involved in

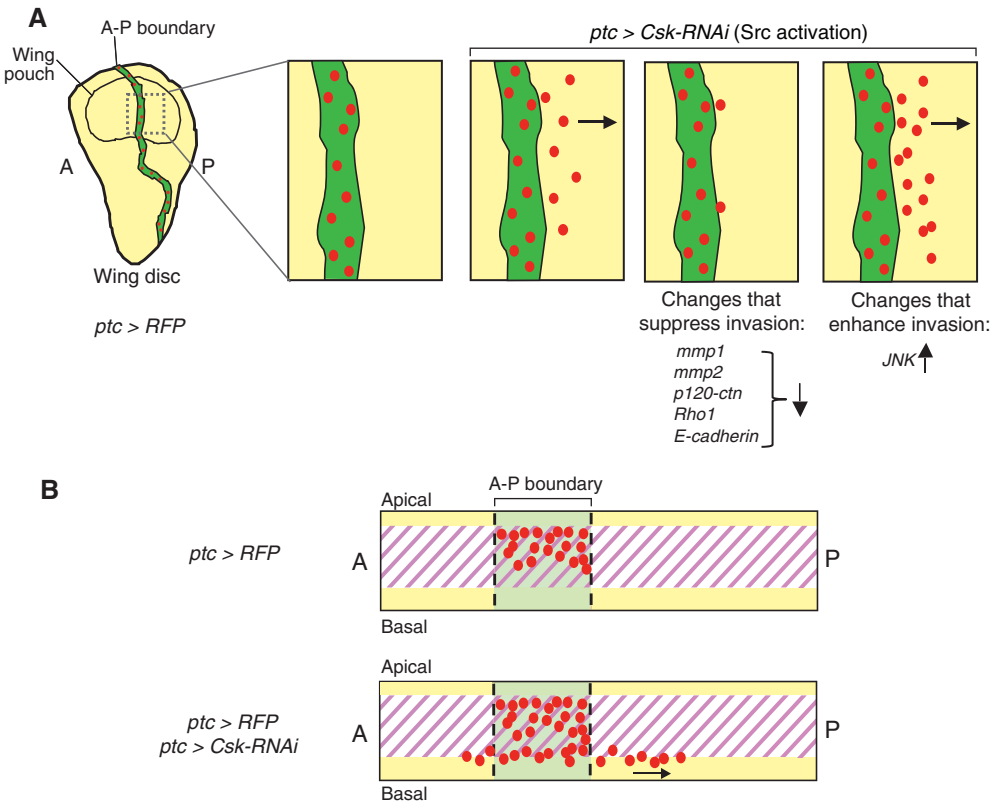

Fig. 3. Modeling tumor invasion in the *Drosophila* larval wing disc. (A) The larval wing disc consists of a sheet of epithelial cells (yellow). A *ptc-GAL4* driver is used to knock down Csk, a negative regulator of Src, specifically in a stripe along the A-P boundary, using an RNAi transgene (*UAS-Csk-RNAi*). The Src-transformed cells are labeled with red fluorescent protein (RFP). The *ptc* domain is shown in green. The *Csk-RNAi* cells at the boundary of the *ptc* domain have the potential to invade into the surrounding tissue. Activation of the JNK pathway or knockdown of regulators of the cytoskeleton (*mmp1*, *mmp2*, *p120-ctn*, *Rho1* and *E-cadherin*) using transgenic overexpression, different genetic backgrounds or RNAi, can either enhance or suppress the invasion of the *Csk-RNAi* cells, highlighting the importance of the tumor microenvironment (Vidal et al., 2006). (B) Horizontal cross-section of the boxed area of the wing disc shown in A. On silencing of Csk, labeled cells (red) are basally excluded and migrate from the boundary through the extracellular matrix (purple hatch).

metastasis. In addition, the identification of the factors that collaborate to control cell migration suggests possible approaches for dual therapeutic targeting in combating metastasis in various cancers.

Conclusions, limitations and perspectives

This review has highlighted the many advantages of *Drosophila* as a model for studying tumor progression. A streamlined genome, coupled with powerful genetic tools, provides a unique system in which to explore the mechanisms regulating the metastatic growth of tumor cells. However, as with any model organism, it has several limitations that should be considered. In mammals, malignant cells undergoing metastasis enter a local blood or lymph vessel before colonizing a distant tissue and forming secondary tumors. This is difficult to model in *Drosophila* because flies have rudimentary hematopoietic systems and a dramatically different lymphatic system compared with mammals. In addition, the metastatic potential of tumors induced in *Drosophila* is greatly reduced compared with their mammalian counterparts; tumor cells tend to invade the local surrounding tissue distally (e.g. in the cephalic complex in the case of Ras^{V12} overexpression).

Tumor formation is generally stimulated by a single mutation or activated oncogene expression in *Drosophila*. However, as the examples outlined here demonstrate, *Drosophila* has also proved to be a powerful experimental system for examining 'two-hit' models of tumor overgrowth and invasion. Although the *Drosophila* models discussed here are largely limited to tumors that develop in the larval stage, adult flies can be employed to examine the metastatic potential of these tumors using allografts, providing an ideal way to propagate tumors for extended studies.

The systems of modeling tumor development in *Drosophila* capitalize on the unique advantages of this model organism coupled with recent innovative technologies (see Box 2). Undoubtedly, the major strength of *Drosophila* is the ease of conducting large-scale genetic screens, which can now make use of the large publicly available collections of isogenic deficiencies and RNAi lines that cover the entire genome (Dietzl et al., 2007; Parks et al., 2004). Elegant targeting techniques – including the UAS/GAL4 system, FLP-FRT-mediated recombination and MARCM clonal analysis – enable gene knockdown in specific tissues or patches of cells, bypassing issues of organism lethality. Because these cancer models involve an in vivo setting, they are also ideally suited for studies that examine the role of the microenvironment. In addition, *Drosophila* offers the potential for drug screening. Together, these approaches make *Drosophila* an excellent model organism to elucidate the basic mechanisms governing tumorigenesis and tumor progression. Validation of this research in mammalian cancer models and human cancer cell lines could lead to new insights into tumor invasion. Metastasis modeling in *Drosophila* is in its infancy but, as better tools and models of specific tumor types are developed, it offers the potential to probe the basic mechanisms regulating cancer cell invasion.

Box 2. Advantages of *Drosophila* for modeling tumor invasion and metastasis

- The signaling pathways controlling growth, differentiation and development that are involved in tumorigenesis and tumor progression are largely conserved between *Drosophila* and humans.
- Models of tumor formation and cell invasion have been created in *Drosophila* using a wide variety of gene targeting strategies, such as loss-of-function mutations and tissue-specific RNAi knockdown, as well as transgenic overexpression of activated oncogenes found in human cancers.
- The ability to generate clones that are mutant for specific genes juxtaposed with wild-type cells using the FLP-FRT and MARCM systems allows the genetics of the tumor microenvironment required for invasion and metastasis to be examined.
- Genome-wide screens using either de novo mutagenesis or tissue-specific knockdown by RNAi in *Drosophila* can identify genes with previously unidentified roles in cancer progression.
- *Drosophila* tumor models can be used for pharmacological screening.

FUNDING

Work in the authors' laboratories is supported by the National Institutes of Health (NIH) [R01GM53202] to N.J.D.; and the Department of Defense (DOD) [W81XWH-09-1-0487] to J.A.W.

COMPETING INTERESTS

The authors declare that they do not have any competing or financial interests.

REFERENCES

Allenspach, E. J., Maillard, I., Aster, J. C. and Pear, W. S. (2002). Notch signaling in cancer. *Cancer Biol. Ther.* **1**, 466-476.

Arama, E., Dickman, D., Kimchie, Z., Shearn, A. and Lev, Z. (2000). Mutations in the beta-propeller domain of the *Drosophila* brain tumor (brat) protein induce neoplasm in the larval brain. *Oncogene* **19**, 3706-3716.

Artavanis-Tsakonas, S. and Muskavitch, M. A. (2010). Notch: the past, the present, and the future. *Curr. Top. Dev. Biol.* **92**, 1-29.

Balkwill, F. (2009). Tumour necrosis factor and cancer. *Nat. Rev. Cancer* **9**, 361-371.

Beaucher, M., Goodliffe, J., Hersperger, E., Trunova, S., Frydman, H. and Shearn, A. (2007a). *Drosophila* brain tumor metastases express both neuronal and glial cell type markers. *Dev. Biol.* **301**, 287-297.

Beaucher, M., Hersperger, E., Page-McCaw, A. and Shearn, A. (2007b). Metastatic ability of *Drosophila* tumors depends on MMP activity. *Dev. Biol.* **303**, 625-634.

Bilder, D., Li, M. and Perrimon, N. (2000). Cooperative regulation of cell polarity and growth by *Drosophila* tumor suppressors. *Science* **289**, 113-116.

Blume-Jensen, P. and Hunter, T. (2001). Oncogenic kinase signalling. *Nature* **411**, 355-365.

Boccuni, P., MacGrogan, D., Scandura, J. M. and Nimer, S. D. (2003). The human L(3)MBT polycomb group protein is a transcriptional repressor and interacts physically and functionally with TEL (ETV6). *J. Biol. Chem.* **278**, 5412-5420.

Bossuyt, W., De Geest, N., Aerts, S., Leenaerts, I., Marynen, P. and Hassan, B. A. (2009). The atonal proneural transcription factor links differentiation and tumor formation in *Drosophila*. *PLoS Biol.* **7**, e40.

Brumby, A. M. and Richardson, H. E. (2003). scribble mutants cooperate with oncogenic Ras or Notch to cause neoplastic overgrowth in *Drosophila*. *EMBO J.* **22**, 5769-5779.

Brumby, A. M. and Richardson, H. E. (2005). Using *Drosophila melanogaster* to map human cancer pathways. *Nat. Rev. Cancer* **5**, 626-639.

Brumby, A. M., Goulding, K. R., Schlosser, T., Loi, S., Galea, R., Khoo, P., Bolden, J. E., Aigaki, T., Humbert, P. O. and Richardson, H. E. (2011). Identification of novel ras-cooperating oncogenes in *Drosophila melanogaster*: a RhoGEF/Rho-family/JNK pathway is a central driver of tumorigenesis. *Genetics* **188**, 105-125.

Chambers, A. F., Groom, A. C. and MacDonald, I. C. (2002). Dissemination and growth of cancer cells in metastatic sites. *Nat. Rev. Cancer* **2**, 563-572.

Chi, C., Zhu, H., Han, M., Zhuang, Y., Wu, X. and Xu, T. (2010). Disruption of lysosome function promotes tumor growth and metastasis in *Drosophila*. *J. Biol. Chem.* **285**, 21817-21823.

Chong, Y. P., Mulhern, T. D. and Cheng, H. C. (2005). C-terminal Src kinase (CSK) and CSK-homologous kinase (CHK)-endogenous negative regulators of Src-family protein kinases. *Growth Factors* **23**, 233-244.

Cordero, J. B., Macagno, J. P., Stefanatos, R. K., Strathdee, K. E., Cagan, R. L. and Vidal, M. (2010). Oncogenic Ras diverts a host TNF tumor suppressor activity into tumor promoter. *Dev. Cell* **18**, 999-1011.

Curran, S. P., Wu, X., Riedel, C. G. and Ruvkun, G. (2009). A soma-to-germline transformation in long-lived *Caenorhabditis elegans* mutants. *Nature* **459**, 1079-1084.

Dietzl, G., Chen, D., Schnorrer, F., Su, K. C., Barinova, Y., Fellner, M., Gasser, B., Kinsey, K., Oppel, S., Scheiblauer, S. et al. (2007). A genome-wide transgenic RNAi library for conditional gene inactivation in *Drosophila*. *Nature* **448**, 151-156.

Elliott, D. A. and Brand, A. H. (2008). The GAL4 system: a versatile system for the expression of genes. *Methods Mol. Biol.* **420**, 79-95.

Ferres-Marco, D., Gutierrez-Garcia, I., Vallejo, D. M., Bolivar, J., Gutierrez-Avino, F. J. and Dominguez, M. (2006). Epigenetic silencers and Notch collaborate to promote malignant tumours by Rb silencing. *Nature* **439**, 430-436.

Froldi, F., Ziosi, M., Tomba, G., Parisi, F., Garoia, F., Pession, A. and Grifoni, D. (2008). *Drosophila* lethal giant larvae neoplastic mutant as a genetic tool for cancer modeling. *Curr. Genomics* **9**, 147-154.

Furnari, F. B., Fenton, T., Bachoo, R. M., Mukasa, A., Stommel, J. M., Stegh, A., Hahn, W. C., Ligon, K. L., Louis, D. N., Brennan, C. et al. (2007). Malignant astrocytic glioma: genetics, biology, and paths to treatment. *Genes Dev.* **21**, 2683-2710.

Gateff, E. (1978). Malignant neoplasms of genetic origin in *Drosophila melanogaster*. *Science* **200**, 1448-1459.

Gateff, E., Loffler, T. and Wismar, J. (1993). A temperature-sensitive brain tumor suppressor mutation of *Drosophila melanogaster*: developmental studies and molecular localization of the gene. *Mech. Dev.* **41**, 15-31.

Grusche, F. A., Hidalgo, C., Fletcher, G., Sung, H. H., Sahai, E. and Thompson, B. J. (2009). Sds22, a PP1 phosphatase regulatory subunit, regulates epithelial cell polarity and shape [Sds22 in epithelial morphology]. *BMC Dev. Biol.* **9**, 14.

Grzeschik, N. A., Parsons, L. M., Allott, M. L., Harvey, K. F. and Richardson, H. E. (2010a). Lgl, aPKC, and Crumbs regulate the Salvador/Warts/Hippo pathway through two distinct mechanisms. *Curr. Biol.* **20**, 573-581.

Grzeschik, N. A., Parsons, L. M. and Richardson, H. E. (2010b). Lgl, the SWH pathway and tumorigenesis: it's a matter of context & competition! *Cell Cycle* **9**, 3202-3212.

Guarino, M. (2010). Src signaling in cancer invasion. *J. Cell. Physiol.* **223**, 14-26.

Gupta, G. P. and Massague, J. (2006). Cancer metastasis: building a framework. *Cell* **127**, 679-695.

Gurvich, N., Perna, F., Farina, A., Voza, F., Menendez, S., Hurwitz, J. and Nimer, S. D. (2010). L3MBTL1 polycomb protein, a candidate tumor suppressor in del(20q12) myeloid disorders, is essential for genome stability. *Proc. Natl. Acad. Sci. USA* **107**, 22552-22557.

Hanahan, D. and Weinberg, R. A. (2011). Hallmarks of cancer: the next generation. *Cell* **144**, 646-674.

Handa, K., Yugawa, T., Narisawa-Saito, M., Ohno, S., Fujita, M. and Kiyono, T. (2007). E6AP-dependent degradation of DLG4/PSD95 by high-risk human papillomavirus type 18 E6 protein. *J. Virol.* **81**, 1379-1389.

Humbert, P., Russell, S. and Richardson, H. (2003). Dlg, Scribble and Lgl in cell polarity, cell proliferation and cancer. *BioEssays* **25**, 542-553.

Igaki, T., Pagliarini, R. A. and Xu, T. (2006). Loss of cell polarity drives tumor growth and invasion through JNK activation in *Drosophila*. *Curr. Biol.* **16**, 1139-1146.

Igaki, T., Pastor-Pareja, J. C., Aonuma, H., Miura, M. and Xu, T. (2009). Intrinsic tumor suppression and epithelial maintenance by endocytic activation of Eiger/TNF signaling in *Drosophila*. *Dev. Cell* **16**, 458-465.

Ishizawar, R. and Parsons, S. J. (2004). c-Src and cooperating partners in human cancer. *Cancer Cell* **6**, 209-214.

Janic, A., Mendizabal, L., Llamazares, S., Rossell, D. and Gonzalez, C. (2010). Ectopic expression of germline genes drives malignant brain tumor growth in *Drosophila*. *Science* **330**, 1824-1827.

Januschke, J. and Gonzalez, C. (2008). *Drosophila* asymmetric division, polarity and cancer. *Oncogene* **27**, 6994-7002.

Jiang, Y., Scott, K. L., Kwak, S. J., Chen, R. and Mardon, G. (2011). Sds22/PP1 links epithelial integrity and tumor suppression via regulation of myosin II and JNK signaling. *Oncogene* **30**, 3248-3260.

Lee, T. and Luo, L. (2001). Mosaic analysis with a repressible cell marker (MARCM) for *Drosophila* neural development. *Trends Neurosci.* **24**, 251-254.

Leong, G. R., Goulding, K. R., Amin, N., Richardson, H. E. and Brumby, A. M. (2009). Scribble mutants promote aPKC and JNK-dependent epithelial neoplasia independently of Crumbs. *BMC Biol.* **7**, 62.

Lewis, P. W., Beall, E. L., Fleischer, T. C., Georlette, D., Link, A. J. and Botchan, M. R. (2004). Identification of a *Drosophila* Myb-E2F2/RBF transcriptional repressor complex. *Genes Dev.* **18**, 2929-2940.

Lu, X., Feng, X., Man, X., Yang, G., Tang, L., Du, D., Zhang, F., Yuan, H., Huang, Q., Zhang, Z. et al. (2009). Aberrant splicing of Hugl-1 is associated with hepatocellular carcinoma progression. *Clin. Cancer Res.* **15**, 3287-3296.

Mantovani, A. (2010). Molecular pathways linking inflammation and cancer. *Curr. Mol. Med.* **10**, 369-373.

Mechler, B. M., McGinnis, W. and Gehring, W. J. (1985). Molecular cloning of lethal(2)giant larvae, a recessive oncogene of *Drosophila melanogaster*. *EMBO J.* **4**, 1551-1557.

Nakagawa, S. and Huibregtse, J. M. (2000). Human scribble (Vartul) is targeted for ubiquitin-mediated degradation by the high-risk papillomavirus E6 proteins and the E6AP ubiquitin-protein ligase. *Mol. Cell. Biol.* **20**, 8244-8253.

Nguyen, D. X., Bos, P. D. and Massague, J. (2009). Metastasis: from dissemination to organ-specific colonization. *Nat. Rev. Cancer* **9**, 274-284.

Pagliarini, R. A. and Xu, T. (2003). A genetic screen in *Drosophila* for metastatic behavior. *Science* **302**, 1227-1231.

Palomero, T., Sulis, M. L., Cortina, M., Real, P. J., Barnes, K., Ciofani, M., Caparros, E., Buteau, J., Brown, K., Perkins, S. L. et al. (2007). Mutational loss of PTEN induces resistance to NOTCH1 inhibition in T-cell leukemia. *Nat. Med.* **13**, 1203-1210.

Parks, A. L., Cook, K. R., Belvin, M., Dompe, N. A., Fawcett, R., Huppert, K., Tan, L. R., Winter, C. G., Bogart, K. P., Deal, J. E. et al. (2004). Systematic generation of high-resolution deletion coverage of the *Drosophila melanogaster* genome. *Nat. Genet.* **36**, 288-292.

Pastor-Pareja, J. C., Wu, M. and Xu. T. (2008). An innate immune response of blood cells to tumors and tissue damage in Drosophila. *Dis. Model Mech.* **1**, 144-154.

Read, R. D., Cavenee, W. K., Furnari, F. B. and Thomas, J. B. (2009). A *Drosophila* model for EGFR-Ras and PI3K-dependent human glioma. *PLoS Genet.* **5**, e1000374.

Schimanski, C. C., Schmitz, G., Kashyap, A., Bosserhoff, A. K., Bataille, F., Schafer, S. C., Lehr, H. A., Berger, M. R., Galle, P. R., Strand, S. et al. (2005). Reduced expression of Hugl-1, the human homologue of *Drosophila* tumour suppressor gene lgl, contributes to progression of colorectal cancer. *Oncogene* **24**, 3100-3109.

Singh, J., Aaronson, S. A. and Mlodzik, M. (2010). *Drosophila* Abelson kinase mediates cell invasion and proliferation through two distinct MAPK pathways. *Oncogene* **29**, 4033-4045.

Summy, J. M. and Gallick, G. E. (2003). Src family kinases in tumor progression and metastasis. *Cancer Metastasis Rev.* **22**, 337-358.

Theodosiou, N. A. and Xu, T. (1998). Use of FLP/FRT system to study *Drosophila* development. *Methods* **14**, 355-365.

Thomas, S. M. and Brugge, J. S. (1997). Cellular functions regulated by Src family kinases. *Annu. Rev. Cell Dev. Biol.* **13**, 513-609.

Uhlirova, M. and Bohmann, D. (2006). JNK- and Fos-regulated Mmp1 expression cooperates with Ras to induce invasive tumors in *Drosophila*. *EMBO J.* **25**, 5294-5304.

Vidal, M. and Cagan, R. L. (2006). *Drosophila* models for cancer research. *Curr. Opin. Genet. Dev.* **16**, 10-16.

Vidal, M., Larson, D. E. and Cagan, R. L. (2006). Csk-deficient boundary cells are eliminated from normal *Drosophila* epithelia by exclusion, migration, and apoptosis. *Dev. Cell* **10**, 33-44.

Vidal, M., Warner, S., Read, R. and Cagan, R. L. (2007). Differing Src signaling levels have distinct outcomes in *Drosophila*. *Cancer Res.* **67**, 10278-10285.

Vidal, M., Salavaggione, L., Ylagan, L., Wilkins, M., Watson, M., Weilbaecher, K. and Cagan, R. (2010). A role for the epithelial microenvironment at tumor boundaries: evidence from *Drosophila* and human squamous cell carcinomas. *Am. J. Pathol.* **176**, 3007-3014.

Wang, D., Kennedy, S., Conte, D., Jr, Kim, J. K., Gabel, H. W., Kamath, R. S., Mello, C. C. and Ruvkun, G. (2005). Somatic misexpression of germline P granules and enhanced RNA interference in retinoblastoma pathway mutants. *Nature* **436**, 593-597.

Witte, H. T., Jeibmann, A., Klambt, C. and Paulus, W. (2009). Modeling glioma growth and invasion in *Drosophila melanogaster*. *Neoplasia* **11**, 882-888.

Woods, D. F. and Bryant, P. J. (1989). Molecular cloning of the lethal(1)discs large-1 oncogene of *Drosophila*. *Dev. Biol.* **134**, 222-235.

Wu, M., Pastor-Pareja, J. C. and Xu, T. (2010). Interaction between Ras(V12) and scribbled clones induces tumour growth and invasion. *Nature* **463**, 545-548.

Yang, J. and Weinberg, R. A. (2008). Epithelial-mesenchymal transition: at the crossroads of development and tumor metastasis. *Dev. Cell* **14**, 818-829.

OPEN ACCESS Freely available online

PLoS GENETICS

A Shared Role for RBF1 and dCAP-D3 in the Regulation of Transcription with Consequences for Innate Immunity

Michelle S. Longworth[1]*, James A. Walker[2,3], Endre Anderssen[2], Nam-Sung Moon[4], Andrew Gladden[5], Margarete M. S. Heck[6], Sridhar Ramaswamy[2], Nicholas J. Dyson[2]

1 Department of Molecular Genetics, The Lerner Research Institute, Cleveland Clinic, Cleveland, Ohio, United States of America, **2** Massachusetts General Hospital Cancer Center and Harvard Medical School, Charlestown, Massachusetts, United States of America, **3** Center for Human Genetic Research, Massachusetts General Hospital, Boston, Massachusetts, United States of America, **4** Department of Biology, Developmental Biology Research Initiative, McGill University, Montreal, Canada, **5** Department of Genetics, The University of Texas MD Anderson Cancer Center, Houston, Texas, United States of America, **6** Centre for Cardiovascular Science, Queen's Medical Research Institute, University of Edinburgh, Edinburgh, United Kingdom

Abstract

Previously, we discovered a conserved interaction between RB proteins and the Condensin II protein CAP-D3 that is important for ensuring uniform chromatin condensation during mitotic prophase. The *Drosophila melanogaster* homologs RBF1 and dCAP-D3 co-localize on non-dividing polytene chromatin, suggesting the existence of a shared, non-mitotic role for these two proteins. Here, we show that the absence of RBF1 and dCAP-D3 alters the expression of many of the same genes in larvae and adult flies. Strikingly, most of the genes affected by the loss of RBF1 and dCAP-D3 are not classic cell cycle genes but are developmentally regulated genes with tissue-specific functions and these genes tend to be located in gene clusters. Our data reveal that RBF1 and dCAP-D3 are needed in fat body cells to activate transcription of clusters of antimicrobial peptide (AMP) genes. AMPs are important for innate immunity, and loss of either dCAP-D3 or RBF1 regulation results in a decrease in the ability to clear bacteria. Interestingly, in the adult fat body, RBF1 and dCAP-D3 bind to regions flanking an AMP gene cluster both prior to and following bacterial infection. These results describe a novel, non-mitotic role for the RBF1 and dCAP-D3 proteins in activation of the *Drosophila* immune system and suggest dCAP-D3 has an important role at specific subsets of RBF1-dependent genes.

Citation: Longworth MS, Walker JA, Anderssen E, Moon N-S, Gladden A, et al. (2012) A Shared Role for RBF1 and dCAP-D3 in the Regulation of Transcription with Consequences for Innate Immunity. PLoS Genet 8(4): e1002618. doi:10.1371/journal.pgen.1002618

Editor: Giovanni Bosco, Univeristy of Arizona, United States of America

Received May 10, 2011; **Accepted** February 8, 2012; **Published** April 5, 2012

Funding: MSL was supported by a Leukemia and Lymphoma Society Career Development Fellowship Award, by a Charles King Trust Fellowship Award, and by Cleveland Clinic Foundation Seed funds. JAW was supported by a grant from the DOD (W81XWH-09-1-04871). NJD is the Saltonstall Scholar of the Massachusetts General Hospital Cancer Center. This study was supported by NIH grants GM53203 and CA64402 (to NJD) and CIHR grant MOP-93666 (to N-SM). The funders had no role in study design, data collection and analysis, decision to publish, or preparation of the manuscript.

Competing Interests: The authors have declared that no competing interests exist.

* E-mail: longwom@ccf.org

Introduction

The RB family proteins (pRB, p130 and p107 in humans; RBF1 and RBF2 in *Drosophila*) co-ordinate changes in gene expression. Understanding the types of programs that these proteins regulate is important because of the unequivocal link between the inactivation of RB proteins and human cancer. Mutation of the retinoblastoma tumor susceptibility gene (*RB1*) is the rate-limiting step in the genesis of retinoblastoma and over 90% of human tumors exhibit reduced pRB function [1,2].

RB family members are best-known for their roles in the regulation of E2F-dependent transcription. E2F-controlled genes are needed for cell proliferation and RB proteins suppress the expression of these targets during G0 and G1 of the cell cycle [3]. In addition, RB proteins are also important for the regulation of genes that are not involved in cell cycle progression. For example, osteoblast differentiation is modulated by pRB through its interaction with Runx2 [4]; in muscle cells, pRB promotes the expression of muscle-specific differentiation markers, enabling these cells to irreversibly exit the cell cycle [5–7]; in *Drosophila*, RBF1 cooperates with the Hippo pathway to maintain photoreceptor differentiation, independent of dE2F1 activity [8]. Such E2F-independent functions may help to explain why the inactivation of RB proteins can have very different consequences in different cellular contexts. However, many of the E2F-independent activities of RB proteins are not well-understood. At present, it is unclear if pRB has different activities in different cell types, or whether there is a yet-to-be discovered, general process that allows RB proteins to activate or repress the expression of variable sets of genes in different cell types.

Recent studies have suggested that pRB family members may impact the organization of higher-order chromatin structures, in addition to their local effects on the promoters of individual genes [9]. Mutation of pRB causes defects in pericentric heterochromatin [10] and RBF1 is necessary for uniform chromatin condensation in proliferating tissues of *Drosophila* larvae [11]. Part of the explanation for these defects is that RBF1 and pRB promote the localization of the Condensin II complex protein, CAP-D3 to DNA both in *Drosophila* and human cells [11]. Depletion of pRB from human cells strongly reduces the level of CAP-D3 associated with centromeres during mitosis and causes centromere dysfunction [12].

Condensin complexes are necessary for the stable and uniform condensation of chromatin in early mitosis [13–16]. They are

Author Summary

The retinoblastoma protein (pRB) is a tumor suppressor protein known for its ability to repress transcription of E2F-dependent genes and induce cell cycle arrest. We have previously shown that RB proteins in *Drosophila* and human cells interact with the Condensin II subunit, CAP-D3, in an E2F-independent manner. Condensins promote condensation of chomosomes in mitosis. Our previous studies suggested that the *Drosophila* pRB and CAP-D3 homologs, RBF1 and dCAP-D3, co-localize on DNA and may share a function in cells that never undergo mitosis. In this study, we show that one non-mitotic function shared between RBF1 and dCAP-D3 is the regulation of many non-cell-cycle-related, clustered, and cell-type-specific transcripts including a conserved family of genes that are important for the immune response in the fly. In fact, results show that normal levels of dCAP-D3 and RBF1 expression are necessary for the ability of the fly to clear infection with human bacterial pathogens. This work demonstrates that dCAP-D3 proteins can regulate a unique subset of RBF1-dependent transcripts *in vivo* and identifies a novel role for both RBF1 and dCAP-D3 protein in activation of innate immune genes, which may be conserved in human cells.

conserved from bacteria to humans with at least two types of Condensin complexes (Condensin I and II) present in higher eukaryotes. Both Condensin I and II complexes contain heterodimers of SMC4 and SMC2 proteins that form an ATPase which acts to constrain positive supercoils [17,18]. Each type of Condensin also contains three specific non-SMC proteins that, upon phosphorylation, stabilize the complex and promote ATPase activity [14,19,20]. The kleisin CAPH and two HEAT repeat containing subunits, CAP-G and CAP-D2 are components of Condensin I, while the kleisin CAP-H2 and two HEAT repeat containing subunits, CAP-G2 and CAP-D3, are constituents of Condensin II.

Given the well-established functions of Condensins during mitosis, and of RBF1 in G1 regulation, the convergence of these two proteins was unexpected. Nevertheless, mutant alleles in the non-SMC components of Condensin II suppress RBF1-induced phenotypes, and immunostaining experiments revealed that RBF1 displays an extensive co-localization with dCAP-D3 (but not with dCAP-D2) on the polytene chromatin of *Drosophila* salivary glands [11]. This co-localization occurs in cells that will never divide, suggesting that Condensin II subunits and RBF1 co-operate in an unidentified process in non-mitotic cells. In various model organisms, the mutation of non-SMC Condensin subunits has been associated with changes in gene expression [21–24] raising the possibility that dCAP-D3 may affect some aspect of transcriptional regulation by RBF1. However, the types of RBF1-regulated genes that might be affected by dCAP-D3, the contexts in which this regulation becomes important, and the consequences of losing this regulation are all unknown.

Here we identify sets of genes that are dependent on both *rbf1* and *dCap-D3*. The majority of genes that show altered expression in both *rbf1* and *dCap-D3* mutants (larvae or adults) are not genes involved in the cell cycle, DNA repair, proliferation, but are genes with cell type-specific functions and many are spaced within 10 kb of one another in "gene clusters". To better understand this mode of regulation we have investigated the effects of RBF1 and dCAP-D3 on one of the most highly misregulated clusters which includes genes coding for antimicrobial peptides (AMPs). AMPs are produced in many organs, and one of the major sites of production is in the fat body. Following production in the fat body, AMPs are subsequently dumped into the hemolymph where they act to destroy pathogens [25]. RBF1 and dCAP-D3 are required for the transcriptional activation of many AMPs in the adult fly. Analysis of one such gene cluster shows that RBF1 and dCAP-D3 bind directly to this region and that they bind, in the fat body, to sites flanking the locus. RBF1 and dCAP-D3 are both necessary in the fat body for maximal and sustained induction of AMPs following bacterial infection, and RBF1 and dCAP-D3 deficient flies have an impaired ability to respond efficiently to bacterial infection. These results identify dCAP-D3 as an important transcriptional regulator in the fly. Together, the findings suggest that RBF1 and dCAP-D3 regulate the expression of clusters of genes in post-mitotic cells, and this regulation has important consequences for the health of the organism.

Results

RBF1 and dCAP-D3 regulate many of the same genes during the later stages of the *D. melanogaster* life cycle

Our previous data demonstrated that RBF1 co-localizes extensively with dCAP-D3 on polytene chromatin of non-dividing cells, leading us to hypothesize that the two proteins may co-operate to regulate transcription. To begin to test this idea, we first identified the stages of fly development where RBF1 and dCAP-D3 were most highly expressed. qRT-PCR using primers for *dCap-D3* and *rbf1* was performed on cDNA generated from various stages of the *Drosophila* life cycle (Figure 1A). The results demonstrate that both genes are transcribed at the highest levels in late third instar larval and adult stages. Concordantly, immunostaining for dCAP-D3 and RBF1 in cryosections of the abdomens of wild type flies confirmed that both proteins are highly expressed in the adult and that they are both present in the nuclei of many cells in normal adult tissues (Figure 1B).

Preliminary experiments showed that dCAP-D3 levels could influence the expression of very few of the previously identified RBF1-dependent transcripts. To gain a more complete understanding of the abundance and characteristics of RBF1/dCAP-D3 shared transcriptional targets, we carried out a microarray analysis of the entire *Drosophila melanogaster* genome and compared gene expression profiles of wild type, *dCap-D3* and *rbf1* mutant flies, at both the third instar larval and adult stages (Table S1). Since the null mutants are lethal, females expressing a transheterozygous combination of null and hypomorphic alleles were used for these experiments. The mutant flies used for microarray analysis expressed about 15% of wild type levels of each gene as judged by qRT-PCR and western blot (Figure S1). The microarray results revealed an extensive and highly significant overlap between RBF1 and dCAP-D3 regulated gene sets in both adults and larvae (Figure 2A and 2B). Shared target genes were evident in both upregulated and downregulated gene sets. Although some genes were mis-expressed in both larvae and adults, the majority of transcriptional changes were stage specific. The most highly significant p values for shared target gene sets were seen in upregulated larval genes (genes repressed by RBF1 and dCAP-D3 in the larvae, $p \leq 6.34E\text{-}130$) and downregulated adult genes (genes activated by RBF1 and dCAP-D3 in the adult, $p \leq 9.88E\text{-}95$) (Figure 2B). This suggests that RBF1 and dCAP-D3 may cooperate to repress specific programs during one stage of development and activate other programs in a later, more differentiated stage. Interestingly, at both stages, the genes dependent on both RBF1 and dCAP-D3 represented 15–17% of the total number of genes dependent on RBF1 in a given

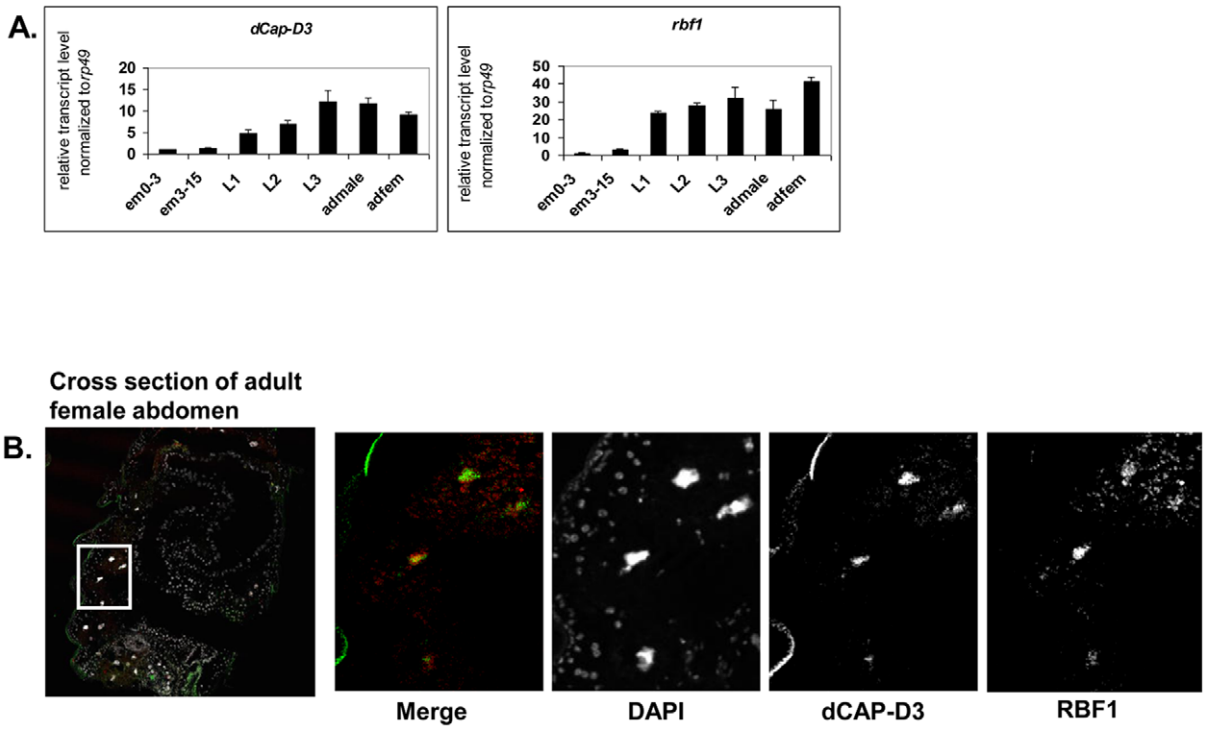

Figure 1. RBF1 and dCAP-D3 are highly expressed at later stages of development and co-localize in adult tissues. A) qRT-PCR for *rbf1* transcript levels and *dCap-D3* transcript levels in wild type *Drosophila* embryos aged for 0–3 hours (em0–3), embryos aged for 3–15 hours (em3–15), first instar larvae (L1), second instar larvae (L2), third instar larvae (L3), adult males (admale) or adult females (adfem) demonstrate high expression levels in the later life cycle stages. B) Immunostaining for RBF1 and dCAP-D3 in cryosections of adult female flies indicates co-localization in large nuclei of cells present underneath the cuticle. Images presented are a magnification of the area highlighted by the white box in the first image.
doi:10.1371/journal.pgen.1002618.g001

developmental stage and 47–55% of the total number of genes dependent on dCAP-D3 in a given developmental stage. Thus RBF1 appears to be important at close to half of the transcriptional targets of dCAP-D3.

Characteristics of RBF1/dCAP-D3 shared target genes

We noticed that the lists of RBF1/dCAP-D3 shared target genes had two general properties. First, these genes are almost completely different from the lists of E2F-regulated genes that have been reported previously [26]. As expected, many of the targets that were upregulated in *rbf1* mutant larvae could be categorized as E2F target genes involved in DNA repair, DNA replication and continuation of the cell cycle (comparison to microarray data from [26] and GO analyses of rbf1 mutant larvae-data not shown). However, few if any, of these cell cycle/proliferation related genes were altered in the *dCap-D3* mutant flies (Figure 2C) suggesting that *dCap-D3* regulates a different subset of RBF1 dependent targets. In fact, less than 6% of dCAP-D3/RBF1 shared target genes in larvae were found to be bound by dE2F1 in dE2F1 ChIP-chip experiments (Korenjak et. al., unpublished data). Unexpectedly, many of the known E2F target genes did not show a significant increase in expression in *rbf1* mutant adults (Figure 2C). This may reflect cell-type specific differences in the requirement for RBF1. In support of this idea, qRT-PCR analysis of dissected tissues showed that few E2F-regulated genes were upregulated in ovaries of *rbf1* mutants, but many did show a significant increase in the rest of the carcass (Figure S2). However, even in the tissues where these E2F-regulated proliferation genes did increase in expression levels in *rbf1* mutant adults, these transcripts were not upregulated in tissues from *dCap-D3* mutant flies (Figure S2). We infer that dCAP-D3 is not a key factor at most of the well-characterized E2F regulated genes in either larvae or adults. While unlikely, it is a formal possibility that the remaining amounts of dCAP-D3 protein present in the hypomorphic mutant flies might be sufficient for the regulation of E2F targets, but not for other target genes.

Second, we noted that genes that are similarly dependent on RBF1 and dCAP-D3 tend to be clustered on the genome and are often positioned within 10 kb of one another (Table 1). To determine whether this was an unusual feature, we compared the frequency of RBF1/dCAP-D3shared target genes positioned within 10 kb of one another to hundreds of simulations of randomly chosen *Drosophila* genes (Table 1). The results showed that genes exhibiting increased expression in *rbf1* and *dCap-D3* mutant adults (ie. genes that are apparently repressed both by RBF1 and dCAP-D3 are 25 times more likely to be clustered. Genes that were downregulated in *rbf1* and *dCap-D3* mutant adults (i.e. genes apparently activated by both RBF1 and dCAP-D3) are 15 times more likely to be clustered. Clustering of shared target genes was also seen in the larvae, although the fold difference was greatly diminished (5 fold) for the activated genes. Overall, the clustering effect was 3–7 fold more prevalent in dCAP-D3 regulated genes than in RBF-regulated genes. By way of comparison, RBF1/dCAP-D3 shared target genes in the larvae exhibited a much greater degree of clustering than the larval genes regulated by Hop or Nurf301, two other well-known chromatin remodeling proteins shown to regulate clusters of genes [27]. A list of the actual groupings of clustered genes is presented in Table S2.

Although proliferation-related genes were missing, gene ontology (GO) classification of the RBF1/dCAP-D3 shared target genes

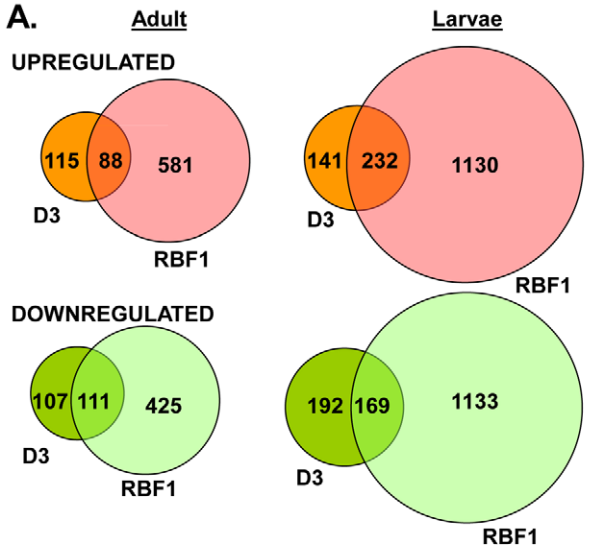

C.

	Wild Type	St Dev	dCAP-D3 mutant	St Dev	RBF1 mutant	St Dev
dnk	1.01	0.16	1.04	0.25	1.29	0.40
mus209	1.01	0.17	1.27	0.30	0.80	0.44
dup	1.01	0.22	1.12	0.24	1.22	0.04
dnapol alpha 50	1.01	0.13	1.10	0.22	1.58	0.42
dnapol delta	1.01	0.20	1.12	0.23	1.49	0.68
orc1	1.01	0.15	1.14	0.26	1.36	0.23
RnrS	1.00	0.07	1.45	0.25	1.65	0.47
Mcm7	1.00	0.04	1.38	0.16	1.59	0.75
Mcm3	1.01	0.14	1.06	0.16	1.25	0.16
Mcm2	1.01	0.15	1.33	0.19	1.07	0.40
Mcm5	1.00	0.05	1.43	0.22	1.55	0.54
CG5250	1.10	0.52	199.66	111.00	88.40	36.79

D.

UPREGULATED- larvae only	
GO:0003824	catalytic activity
GO:0008527	taste receptor activity

DOWNREGULATED-adults only	
GO:0050830	defense response to Gram-positive bacterium
GO:0001708	cell fate specification
GO:0007219	Notch signaling pathway
GO:0004252	serine-type endopeptidase activity
GO:0048513	organ development
GO:0000902	cell morphogenesis
GO:0035264	multicellular organism growth
GO:0051252	regulation of RNA metabolic process
GO:0007365	periodic partitioning
GO:0017171	serine hydrolase activity

B.

Upregulated shared target genes

	D3adult-WTadult	RBF1adult-WTadult	D3larvae-WTlarvae	RBF1larvae-WTlarvae
D3adult-WTadult		2.71E-58	7.25E-58	2.18E-23
RBF1adult-WTadult	9.88E-95		9.84E-27	5.58E-27
D3larvae-WTlarvae	1.58E-30	2.17E-15		6.34E-130
RBF1larvae-WTlarvae	4.27E-19	2.47E-37	6.98E-71	

Downregulated shared target genes

Figure 2. RBF1 and dCAP-D3 regulate many of the same transcripts in the fly. RNA was isolated from *rbf1* mutant and *dCap-D3* mutant female third instar larvae and adult flies. cDNA was hybridized to Nimblegen 385 k whole genome arrays. A) Venn diagrams show the numbers of RBF1, dCAP-D3 or RBF1/dCAP-D3 shared target genes which exhibited at least a 2 fold log change in expression with a p value of ≤0.15. Genes significantly upregulated in the mutant flies are shown in red while genes significantly downregulated are shown in green. B) P values for shared RBF1 and dCAP-D3 target genes indicate that RBF1 and dCAP-D3 regulate a significant number of the same genes in both adults and larvae. The numbers above the diagonal represent p-values for upregulated shared subsets and are colored red while the numbers below the diagonal represent p-values for downregulated shared genes and are colored green. C) qRT-PCR analyses of 12 E2F targets shows that the majority of RBF1/dCAP-D3 shared targets are not E2F targets. The one target that was significantly upregulated in dCAP-D3 and RBF1 mutant flies, *CG5250*, is highlighted in red. Results are the average of three independent experiments involving 10 female flies per genotype. D) Significant (p≤0.05) Gene Ontology (GO) groupings for shared target genes include defense response genes in the adult fly. The top box lists GO categories for upregulated shared genes in mutant larvae only, and the bottom box lists selected GO categories for downregulated shared genes in adults only. There were no significant GO groupings for upregulated shared target genes in adults or for downregulated shared target genes in the larvae.
doi:10.1371/journal.pgen.1002618.g002

revealed many significant categories in the lists of up- and downregulated genes in the adult, and for shared, repressed target genes in the larvae (Figure 2D, complete list for downregulated adult genes in Table S3). One of the most interesting GO categories represented in the adults were the defense response genes (GO:0050830). The fly relies on an innate immune system to defend against invading pathogens. This immune system is comprised of three major mechanisms: 1) phagocytosis, 2) induction of coagulation and melanization, and 3) production of Antimicrobial Peptides or AMPs.

Phagocytosis is a conserved mechanism that is often the primary cellular defense used by many organisms to engulf and destroy pathogens. In *Drosophila*, circulating blood cells called hemocytes phagocytose bacteria, fungi, and parasitic wasp eggs [28]. RBF1 and dCAP-D3 mutant adult microarray data was analyzed for changes in levels of 19 different genes reported to be involved in phagocytosis in *Drosophila* (Table S4). Of these 19 genes, 2 genes demonstrated significant changes in transcript levels in adults. *NimC1*, a gene expressed in plasmatocytes which make up 95% of *Drosophila* hemocytes, has been shown to be necessary for phagocytosis of bacteria [29], and was significantly upregulated in RBF1 and dCAP-D3 mutant adults. Embryonic and larval hematopoiesis depends on a number of transcription factors including Gcm [30,31]. *Gcm* transcripts were demonstrated to be downregulated in both RBF1 and dCAP-D3 adults (Table S4). While adult hemocytes do display phagocytic properties, they do not differentiate into specialized cells upon immune challenge [32,33], and it is therefore unlikely that misregulation of *gcm* in adults would affect phagocyte numbers.

In response to septic injury, proteolytic cascades are triggered which lead to coagulation and melanization. Reactive oxygen species formed during these processes, as well as the actual deposition of melanin, are thought to be toxic to microorganisms [34]. After scanning the literature for genes involved in coagulation and melanization, and then analyzing RBF1 and

Table 1. RBF1 and dCAP-D3 tend to regulate clusters of genes.

Gene Set	*Ratio for upregulated*^*	*Ratio for downregulated*^*
Whole adult dCAP-D3 mut	12.42	11.68
Whole adult RBF1 mut	3.93	4.41
Whole adult shared targets	25.00	15.87
Whole larvae dCAP-D3 mut	14.2	11.59
Whole larvae RBF1 mut	2.60	2.03
Whole larvae shared targets	22.58	3.68
Whole larvae Hop mut**	1.91	1.30
Whole larvae Nurf301 mut**	1.55	1.30

*The ratio of observed clustering to expected clustering for the lists of differentially expressed genes between mutant and wild -type organisms (fdr<0.15, log2 fc>0.1) shows that RBF1 and dCAP-D3 shared target genes are 6–10 fold more likely to be present in clusters. Chromosomal clustering is calculated as the number of pairs of genes within 10,000 bp among the differentially expressed genes. The expected number is the average clustering of 500 random gene lists of the same length as the corresponding list of differentially expressed genes.

**Raw data for Hop and Nurf301 mutant larvae was obtained from supplemental data files found in [27].

^False Discovery Rates for all ratios presented were <0.05.

doi:10.1371/journal.pgen.1002618.t001

dCAP-D3 mutant adult microarray data for changes in transcript levels of these genes, it was determined that only one of the reported genes, *CG8193* was significantly increased in both RBF1 and dCAP-D3 mutant adults (Table S5). CG8193/PPO2 is thought to encode a phenol-oxidase constitutively expressed in crystal cells, a type of hemocyte cell involved in melanization [35].

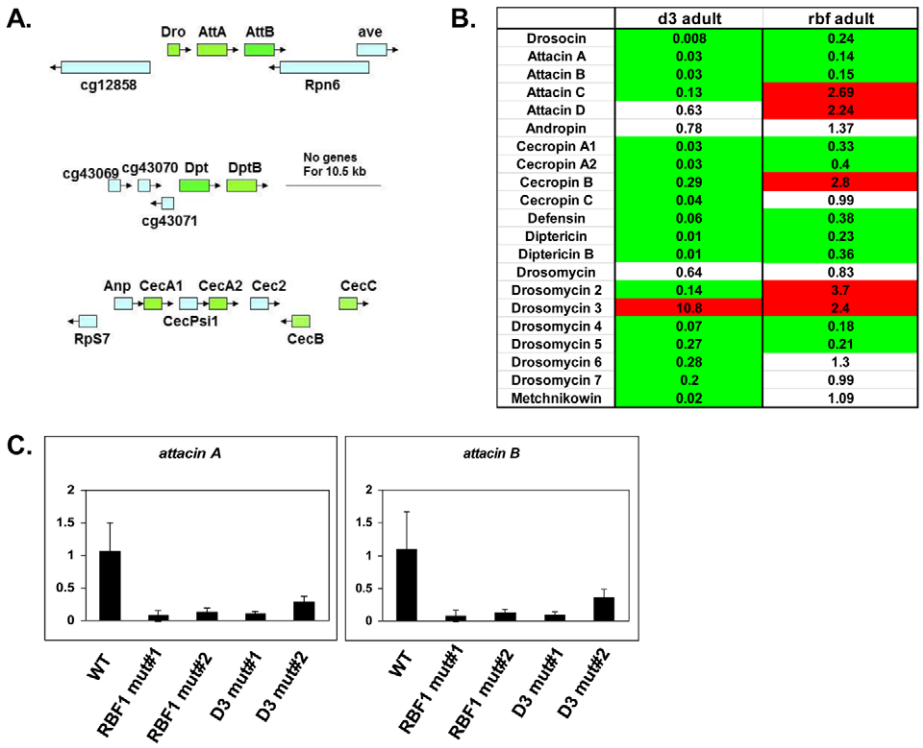

	d3 adult	rbf adult
Drosocin	0.008	0.24
Attacin A	0.03	0.14
Attacin B	0.03	0.15
Attacin C	0.13	2.69
Attacin D	0.63	2.24
Andropin	0.78	1.37
Cecropin A1	0.03	0.33
Cecropin A2	0.03	0.4
Cecropin B	0.29	2.8
Cecropin C	0.04	0.99
Defensin	0.06	0.38
Diptericin	0.01	0.23
Diptericin B	0.01	0.36
Drosomycin	0.64	0.83
Drosomycin 2	0.14	3.7
Drosomycin 3	10.8	2.4
Drosomycin 4	0.07	0.18
Drosomycin 5	0.27	0.21
Drosomycin 6	0.28	1.3
Drosomycin 7	0.2	0.99
Metchnikowin	0.02	1.09

Figure 3. RBF1 and dCAP-D3 activate basal transcript levels of genes coding for Antimicrobial Peptides (AMPs). A) Graphic depictions of three separate AMP loci. The *Attacin* and *Diptericin* loci are located on Chromosome 2R at 51C1 and 55F8, respectively. The *Cecropin* locus is located on Chromosome 3R at 99E2. Genes within each locus are drawn in correct orientation to one another but are not drawn to scale. Genes colored in green are downregulated in dCAP-D3 mutant adult carcasses dissected of ovaries and most are also downregulated RBF1 mutants. Genes colored in blue remain unchanged in dCAP-D3 and RBF1 mutants. B) qRT-PCR analyses of transcript levels for 21 AMPs in female adult bodies (N = 10) with ovaries dissected shows that dCAP-D3 and RBF1 each regulate a much larger number of AMPs than originally indicated by the microarray results. Genes significantly upregulated in the mutants are highlighted in red and genes significantly downregulated in the mutants are highlighted in green. Transcript levels were normalized to tubulin 84B. All results had false discovery rates ≤0.05. C) qRT-PCR analysis of cDNA from wild type (WT/w^{1118}), *rbf1* mutant #1 ($rbf1^{120a}/rbf1^{\Delta 14}$), *rbf1* mutant #2 ($rbf1^{120a}/rbf1^{120a}$), *dCap-D3* mutant #1 ($dCap\text{-}D3^{c07081}/dCap\text{-}D3^{\Delta 25}$) and *dCap-D3* mutant #2 ($dCap\text{-}D3^{c07081}/dCap\text{-}D3^{c07081}$) female adult whole flies confirms that two AMP target genes are regulated by both RBF1 and dCAP-D3, regardless of mutant genotype. Transcript levels were normalized to *tubulin 84B* mRNA levels.

doi:10.1371/journal.pgen.1002618.g003

However, overexpression of CG8193/PPO2 in cell lines or in flies does not induce constituitive melanization [36], nor did we see any evidence of melanotic lesions in RBF1 or dCAP-D3 mutant adults.

Several of the genes in the adult, downregulated GO category of "defense response to Gram positive bacteria" (Figure 2D and Table S3) fall into a family of proteins known as Antimicrobial Peptides or AMPs. In fact, two of these genes, *AttA* and *AttB*, represented some of the most highly deregulated targets in the mutant adults. Upon closer inspection of the microarray data, it was revealed that many other AMP genes were also deregulated in dCAP-D3 and/or RBF1 mutant adults, however their p-values were just below the confidence level. In addition, many of the AMP genes are present in clusters and located immediately next to one another in the genome (Figure 3A), making them an enticing group of genes for further study.

AMPs are shared targets of RBF1 and dCAP-D3 in the adult fat body

To confirm that the transcription of AMPs was indeed dependent on both RBF1 and dCAP-D3, qRT-PCR analysis was performed using cDNA generated from *dCap-D3* or *rbf1* transheterozygotes (using whole female mutant flies whose ovaries had been dissected) (Figure 3B). Results showed that 17 of the 21 AMPs tested were downregulated in the *Cap-D3* mutants and 10 of those genes were similarly dependent on RBF1. qRT-PCR for AMPs performed on different allelic combinations of *rbf1* and *Cap-D3* mutants gave similar results (Figure 3C).

AMPs constitute one of the major defense mechanisms against bacterial and/or fungal infection in the fly [25,37,38]. They are produced in various adult tissues but one of the main organs responsible for their production is the fat body. Once produced in the fat body, AMPs are secreted into the hemolymph where they destroy or inhibit growth of pathogens [39].

We set out to test the hypothesis that RBF1 and dCAP-D3 regulate AMP genes in the adult fat body. First, we examined whether RBF1 and dCAP-D3 are expressed in this cell type. The *yolk-GAL4* driver was used to express GFP in adult fat body cells, effectively marking this cell type in green. Combined immunostaining for RBF1 and dCAP-D3 localization in cryosections of adult wild type abdomens revealed a strong staining for both RBF1 and dCAP-D3 in the nuclei of adult fat body cells (Figure 4A, yellow arrows). *yolk-GAL4* has been characterized to drive expression in *Drosophila* at approximately 2–5 days post eclosure [40], making it possible to drive expression of transgenes after the majority of fly development has occurred. The staining for RBF1 and dCAP-D3 in the adult abdomens was specific, as *yolk-GAL4* driven expression of dsRNAs directed against RBF1 and dCAP-D3 specifically abrogated staining of their respective targets in fat body cells, without dramatically altering gross tissue morphology (Figure S3).

Next, we measured the changes in expression of AMPs in animals where *yolk-GAL4* driven expression of dsRNAs had reduced the expression of either RBF1 or dCAP-D3 in the fat body. qRT-PCR of cDNA from whole adult females showed a significant decrease in the expression of multiple AMP genes including *diptericin*, *diptericin B* and *Cecropin A2* (Figure 4B) in the knockdown flies. Interestingly, the fold change in transcript levels for *diptericin* was comparable to the changes seen in *dCap-D3* and *rbf1* mutant animals. These results suggest that the yolk-GAL4-expressing cells are a primary site of constitutive *diptericin* expression in adult flies and that in these cells, RBF1 and dCAP-D3 are both needed to drive the basal expression levels of specific AMPs.

Regulation of an AMP cluster by RBF1 and dCAP-D3 is direct and dynamically changes over the course of bacterial infection

AMP genes can be regulated by multiple transcription factors [41–44]. We sought to determine, therefore, whether transcriptional regulation of these genes by RBF1 and dCAP-D3 was direct. For our ChIP analysis we focused on *diptericin* and *diptericin B*; two AMP genes that are situated within 1200 bp of one another (Figure 5B), that have well characterized promoters [45–47], and whose basal expression was dependent on both RBF1 and dCAP-D3 in the fat body (Figure 3B and Figure 4B). In addition, the basal transcript levels of at least one other gene in the region, *CG43070*, was found to be significantly activated by both RBF1 and dCAP-D3 (Figure S4).

To study the binding of RBF1 and dCAP-D3 at the *diptericin* locus *in vivo*, transgenic fly lines were created which expressed N-terminally FLAG-HA tagged dCAP-D3 or N-terminally FLAG-HA tagged RBF1 under the control of the UAS promoter. These lines were then crossed to *yolk-GAL4/FM7* lines to create progeny in which the tagged protein was specifically expressed in the adult fat body. ChIP using FLAG antibody in FLAG-HA-dCAP-D3 expressing flies demonstrated that dCAP-D3 binds to two separate regions located approximately 3 kb upstream and 900 bp downstream of the *diptericin* locus (Figure 5A and red bars in Figure 5B). Since *diptericin* is strongly induced in response to bacterial infection, we examined the effect of infection with *S. aureus* on the binding of dCAP-D3 to the *diptericin* locus. Strikingly, dCAP-D3 binding to the upstream site significantly increased after *S. aureus* infection (compare red bars to yellow bars, Figure 5B).

ChIP for FLAG in FLAG-HA-RBF1 expressing flies indicated that RBF1 binds to the identical upstream and downstream regions of the *diptericin* locus as dCAP-D3 (red bars in Figure 5C). This binding was detected both before and after infection with *S. aureus* (blue and yellow bars in Figure 5C), but unlike the results for dCAP-D3 binding, RBF1 binding was most significant prior to infection. ChIP for FLAG protein in flies expressing the FLAG-HA construct alone showed almost no signal at any of the primer sets used in these experiments (Figure 5D). Taken together, ChIP results show that 1) RBF1 and dCAP-D3 can bind directly to an AMP gene cluster at identical binding sites, 2) that the binding sites flank the *diptericin* and *diptericin B* genes, and 3) dCAP-D3 binding increases when gene expression is induced in response to bacterial infection.

For comparison, we also performed ChIP for dCAP-D3 on the *CG5250* locus. *CG5250* was the one previously identified direct target of RBF1 [26] that we found to be repressed by RBF1 and dCAP-D3 and to be consistently upregulated in all tissues of *rbf1* and *dCap-D3* mutant animals (Figures S2 and S5A). ChIP using FLAG antibody in FLAG-HA-dCAP-D3 expressing flies demonstrated a small amount of binding in the open reading frame of *CG5250* (Figure S5B and S5C). This binding pattern obtained with the FLAG antibody closely resembled the ChIP signal found when a dCAP-D3 antibody was used to immunoprecipiate the endogenous dCAP-D3 protein expressed everywhere in the adult fly (Figure S5D).

The ability of RBF1 and dCAP-D3 to regulate basal levels of AMP transcription prompted the question of whether these proteins were also necessary for the regulation of AMP transcription in response to bacterial infection. cDNA was generated from female adult flies expressing dCAP-D3 or RBF1 dsRNAs specifically in the fat body, at various time-points post-infection with *Staphylococcus aureus* (Figure 6). dsRNAs have been used successfully in the past to decrease *in vivo* expression levels of

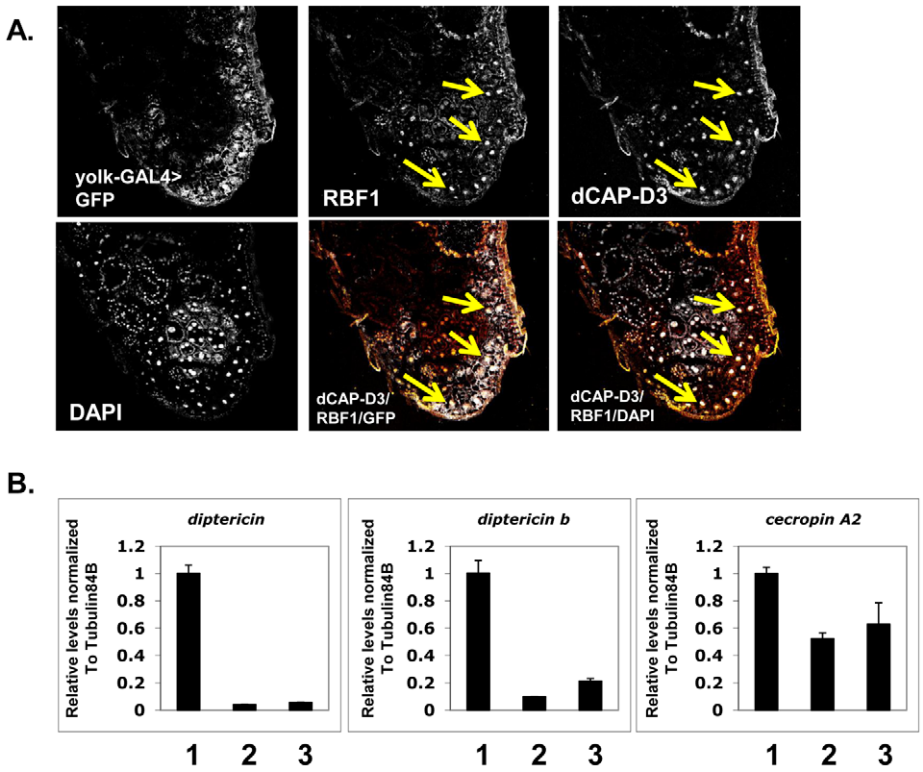

Figure 4. Basal AMP transcript levels are activated by RBF1 and dCAP-D3 specifically in the fat body. A) Immunofluorescence analysis of RBF1 and dCAP-D3 performed on cryosections of adult female flies expressing GFP under the control of the fat body specific *yolk-GAL4* driver indicates that RBF1 and dCAP-D3 co-localize in the nuclei of fat body cells. Yellow arrows highlight fat body cells. B) qRT-PCR analysis of cDNA from 1) flies expressing driver alone (*yolk-GAL4/+;+;+*), 2) flies expressing *rbf1 dsRNA (yolk-GAL4;+;UAS-rbf1 dsRNA)* in the fat body cells and 3) flies expressing *dCAP-D3 dsRNA (yolk-GAL4;+;UAS-dCAP-D3 dsRNA)* in the fat body cells shows significant decreases in AMP levels. For each genotype, N = 10.
doi:10.1371/journal.pgen.1002618.g004

proteins involved in innate immunity and to study their effects on responses to bacterial infection [48].

qRT-PCR for AMPs indicated two types of transcriptional defects in the RBF1 and dCAP-D3 deficient flies. In agreement with our earlier results, basal transcript levels of *diptericin* were reduced as a result of deficiency for either protein (Figure 6B, inset boxes). Following infection, *diptericin* transcripts remained very low in the dCAP-D3 deficient tissue and induction was minimal and severely delayed in comparison to GFP dsRNA expressing "wild type" control flies. RBF1 deficiency, however, allowed normal induction of *diptericin* transcripts. *Drosomycin* is an AMP gene downstream of the Toll pathway, and it is strongly induced following infection with Gram positive bacteria or fungi [49]. qRT-PCR for levels of *Drosomycin* revealed a much different defect in expression. Neither dCAP-D3 nor RBF1 deficiency in the fat body had any effect on basal levels of *Drosomycin*, a result consistent with our microarray data from whole flies. However, both dCAP-D3 and RBF1 deficiency caused significant decreases in the maximal expression levels of *drosomycin* at 24 hours post-infection (Figure 6A).

The biological response to bacterial infection in the fly requires dCAP-D3 and RBF1

Next, we tested whether the inefficient transcription of AMPs that results from decreased expression of RBF1 or dCAP-D3 has a significant effect on the ability of the fly to recover from exposure to pathogenic bacteria. Survival rates after infection with the Gram positive bacterium, *Staphylococcus aureus* (Figure 7A, Figure 8A) or with the Gram negative bacterium, *Pseudomonas aeruginosa* (Figure 7B, Figure 8B) were measured in five different genotypes: females expressing GFP dsRNAs under the control of the yolk-GAL4 driver ("wild-type controls", *yolk-GAL4* driving expression of dCAP-D3 dsRNA in the fat body, *yolk-GAL4* driving expression of RBF1 dsRNA in the fat body, and positive control females which were either mutant for the Eater protein or expressing dsRNAs against the IMD protein. IMD is a major mediator of innate immune signaling in *Drosophila* [50]. Eater is a known phagocytic receptor necessary for the response to infection with Gram positive bacteria [51]. We did not include data on flies expressing Eater dsRNAs under the control of yolk-GAL4, since Kocks et al [51] reported that Eater is not expressed in the fat body. In agreement with this, expression of Eater dsRNA in the fat body exhibited no changes in the ability of the fly to clear bacteria, while the Eater mutants described above showed a striking inability to phagocytize bacteria 5 hours following infection (data not shown and Figure 7). Following infection with *S. aureus*, both dCAP-D3 and RBF1 deficient flies were more susceptible to infection in comparison to flies expressing GFP dsRNAs (Figure 7A and Figure 8A). dCAP-D3 deficient flies were also more susceptible to infection with Gram negative bacteria, but this was not the case for RBF1 deficient flies, as their survival rates were not significantly decreased (Figure 7B and Figure 8B). These data demonstrate that acute knockdown of dCAP-D3 or RBF1 in the fat body of adult flies renders them more susceptible to bacterial infection, most likely due to inefficient transcription of AMP genes.

Recently, a number of reports have identified genes whose mutation can reduce the ability of the fly to survive bacterial

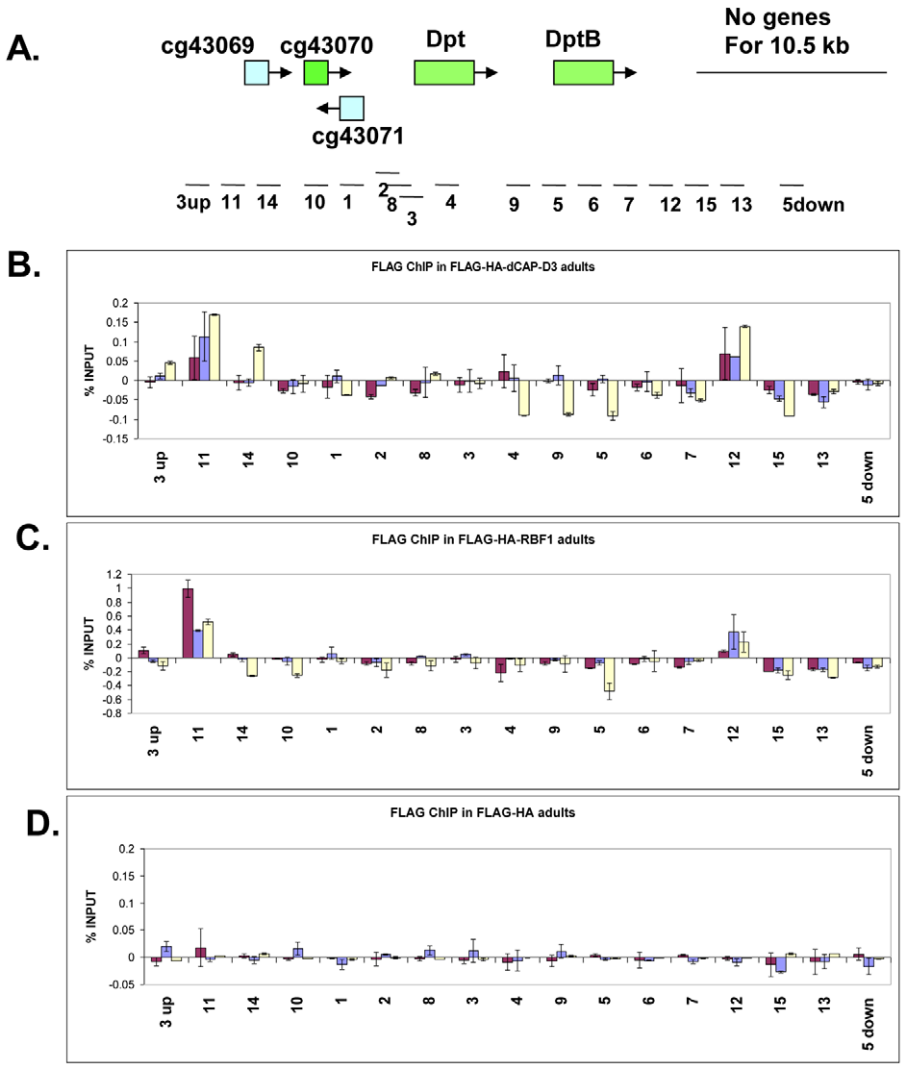

Figure 5. RBF1 and dCAP-D3 bind to an AMP locus *in vivo*. A) Graphic representation of the locus on which Chromatin Immunoprecipitation (ChIP) for RBF1 and dCAP-D3 in the adult fat body was performed. Genes highlighted in green are activated by both RBF1 and dCAP-D3 in the fat body. Positions of primer sets used are listed under the diagram of the locus. B) Chromatin immunoprecipitation for FLAG protein in female adult flies expressing FLAG-HA-dCAP-D3 in the fat body (*yolk-GAL4/+; +; UAS-FLAG-HA-dCap-D3/+*) demonstrates that the *diptericin* locus is a direct target of dCAP-D3. ChIP signal corresponding to FLAG-HA-dCAP-D3 binding in the absence of *Staphylococcus aureus* infection is colored in burgundy. ChIP signal corresponding to FLAG-HA-dCAP-D3 binding two and four hours after *S. aureus* infection is colored in blue and yellow, respectively. C) Chromatin immunoprecipitation for FLAG protein in female adult flies expressing FLAG-HA-RBF1 in the fat body (*yolk-GAL4/+; +; UAS-FLAG-HA-rbf1/+*) demonstrates that the locus is also a direct target of RBF1. Depiction of signal is as described in B. D) Chromatin immunoprecipitation for FLAG protein in female adult flies expressing FLAG-HA in the fat body (*yolk-GAL4/+; +; UAS-FLAG-HA/+*) demonstrates minimal non-specific binding of tag alone at the locus. Depiction of signal is as described in B.
doi:10.1371/journal.pgen.1002618.g005

infection, without influencing the ability of the fly to clear bacteria [52–54]. These genes have been described as having affects not on the resistance mechanisms which exist in the fly, but on the tolerance mechanisms of the fly. Tolerance mechanisms limit the damage caused to the host by the infection, but do not actually limit the pathogen burden [55]. To determine whether loss of dCAP-D3 and/or RBF1 expression in the fat body did indeed result in diminished capacity of the fly to clear bacteria, we performed bacterial clearance assays and measured the number of bacteria present in the fly from 0–20 hours post-infection (Figure 9). Results showed that flies deficient for RBF1 or dCAP-D3 behave more like positive control flies deficient for IMD or Eater proteins, and exhibit significant increases in bacterial numbers at 15 hours post-infection with *S. aureus*. This suggests that RBF1 and dCAP-D3 most likely affect the resistance mechanisms (i.e. AMP transcription), and not the tolerance mechanisms of the fly.

A second RBF family member, RBF2, regulates basal AMP transcription levels, but not induced levels, following infection

Since the observed defects in survival rates and AMP induction were not as severe for RBF1 deficient flies in comparison to dCAP-D3 deficient flies, we wondered whether the other *Drosophila* RBF member, RBF2, might compensate for loss of RBF1 activity. RBF2 has been shown to be upregulated upon depletion of RBF1, and co-regulates many genes with RBF1 as a part of the dREAM complex [26,56,57]. To address this question, we tested survival

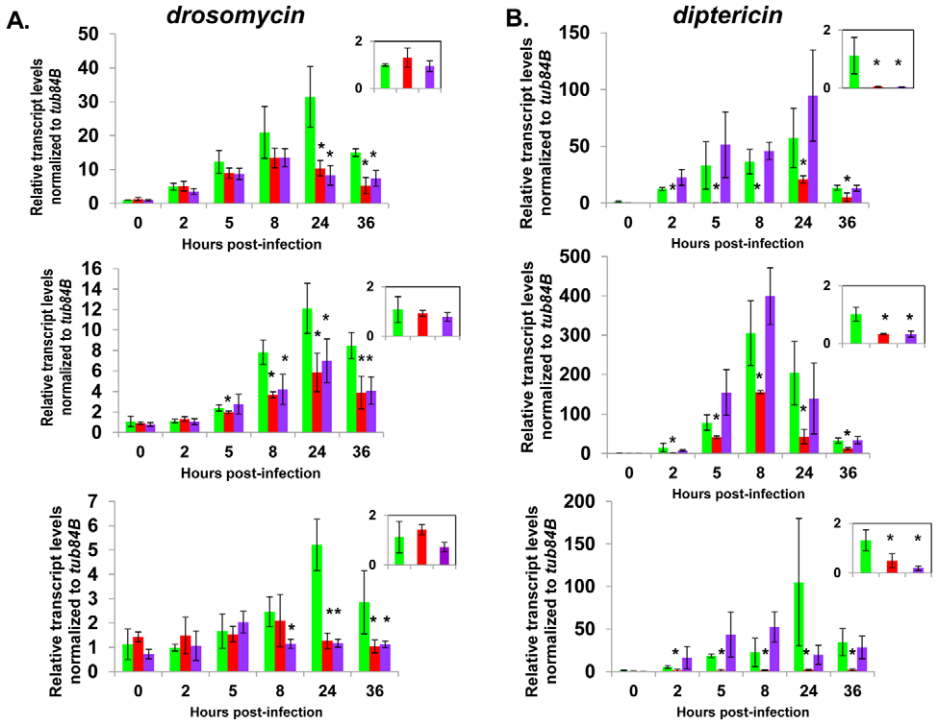

Figure 6. Complete AMP induction following bacterial infection depends on dCAP-D3 and RBF1. Adult female flies expressing RBF1 (purple) or dCAP-D3 (red) dsRNAs under the control of *yolk-GAL4* were infected with the Gram positive bacteria, *Staphylococcus aureus*. A) qRT-PCR analyses for transcript levels of the *Drosomycin* AMP gene in these flies show that while flies expressing GFP dsRNAs under the control of *yolk-GAL4* (green) undergo a large induction of AMPs at 8–24 hours post-infection, flies expressing dCAP-D3 or RBF1 dsRNA in the fat body fail to exhibit maximal, sustained induction. B) qRT-PCR analyses for transcript levels of the *Diptericin* AMP gene in these flies show that while flies expressing GFP or RBF1 dsRNAs under the control of *yolk-GAL4* (green) undergo a large induction of AMPs at 8–24 hours post-infection, flies expressing dCAP-D3 dsRNA in the fat body fail to exhibit maximal, sustained induction. The inset boxes in the upper right corner of each graph are a larger representation of the 0 hour timepoint and depict basal transcription levels. Asterisks emphasize statistical significance ($p \leq 0.05$) as determined by a students paired t-test. Three independent experiments are shown and results for each experiment are the average of three sets of five infected adults per genotype, per timepoint.
doi:10.1371/journal.pgen.1002618.g006

times and AMP induction in flies deficient for RBF2 in the fat body (yolk-GAL4<UAS-RBF2-dsRNA) or a combination of both RBF1 and RBF2 in the fat body (yolk-GAL4<UAS-RBF1 dsRNA, UAS-RBF2 dsRNA). The specific deficiencies in these flies were confirmed by qRT-PCR (Figure S6). qRT-PCR revealed that similar to the loss of RBF1 or dCAP-D3, loss of RBF2 or RBF1/RBF2 resulted in decreased basal transcript levels of *diptericin* but not *drosomycin* (Figure S7A and S7B, inset boxes). However, following infection with *S. aureus*, loss of RBF2 or RBF1/RBF2 did not cause decreased induction of either AMP transcript. In some cases, loss of both RBF1 and RBF2 actually resulted in an increase in *diptericin* transcription levels at 8 hours post infection. In response to infection with Gram positive bacteria (Figure S8A) or Gram negative bacteria (Figure S8B), RBF2 deficient or RBF1/RBF2 deficient flies did not exhibit any changes in survival rates that were significantly different from wild type control flies. These results demonstrate that RBF2 does regulate basal AMP transcript levels, but does not compensate for RBF1 in induction of AMP transcription in *Drosophila* following infection.

The shared regulation of innate immune gene clusters by RBF1 and dCAP-D3 may be conserved in human cells

AMPs are conserved in many metazoans and play a very important role in fighting pathogens in barrier epithelial cells at mucosal surfaces [58]. pRB and CAP-D3 have been previously shown to interact physically and functionally in human cells [11]. Remarkably, and perhaps unexpectedly, the regulation of AMP genes by RB and CAP-D3 proteins may also be conserved in human cells. To determine whether pRB and CAP-D3 could regulate genes in human cells and, more specifically, whether the co-regulation of AMPs was conserved, siRNAs were used to decrease pRB and CAP-D3 expression in human Retinal Pigment Epithelial (RPE-1) cells and in premonocytic U937 cells. (Figure S9A and data not shown). qRT-PCR analyses of the levels of five different AMPs revealed that two AMPs (DEFB-3 and DEFA-1) were expressed in RPE-1 cells and both genes were significantly downregulated following the depletion of either pRB or CAP-D3 (Figure S9B). Interestingly, these genes are also located in a very large gene cluster, the *Defensin* locus, encompassing over 20 different AMPs. These data raise the possibility that the regulation of AMPs by CAP-D3 and pRB, and the ability of these proteins to regulate gene clusters, are properties that may be conserved in human cells.

Discussion

In *Drosophila*, RB-family proteins are best known as transcriptional repressors of cell cycle and proliferation genes. Here we describe a different aspect of RB function and show that, together with the Condensin II protein dCAP-D3, RBF1 functions to regulate the expression of a large number of genes during *Drosophila* development. A surprising characteristic of RBF1/

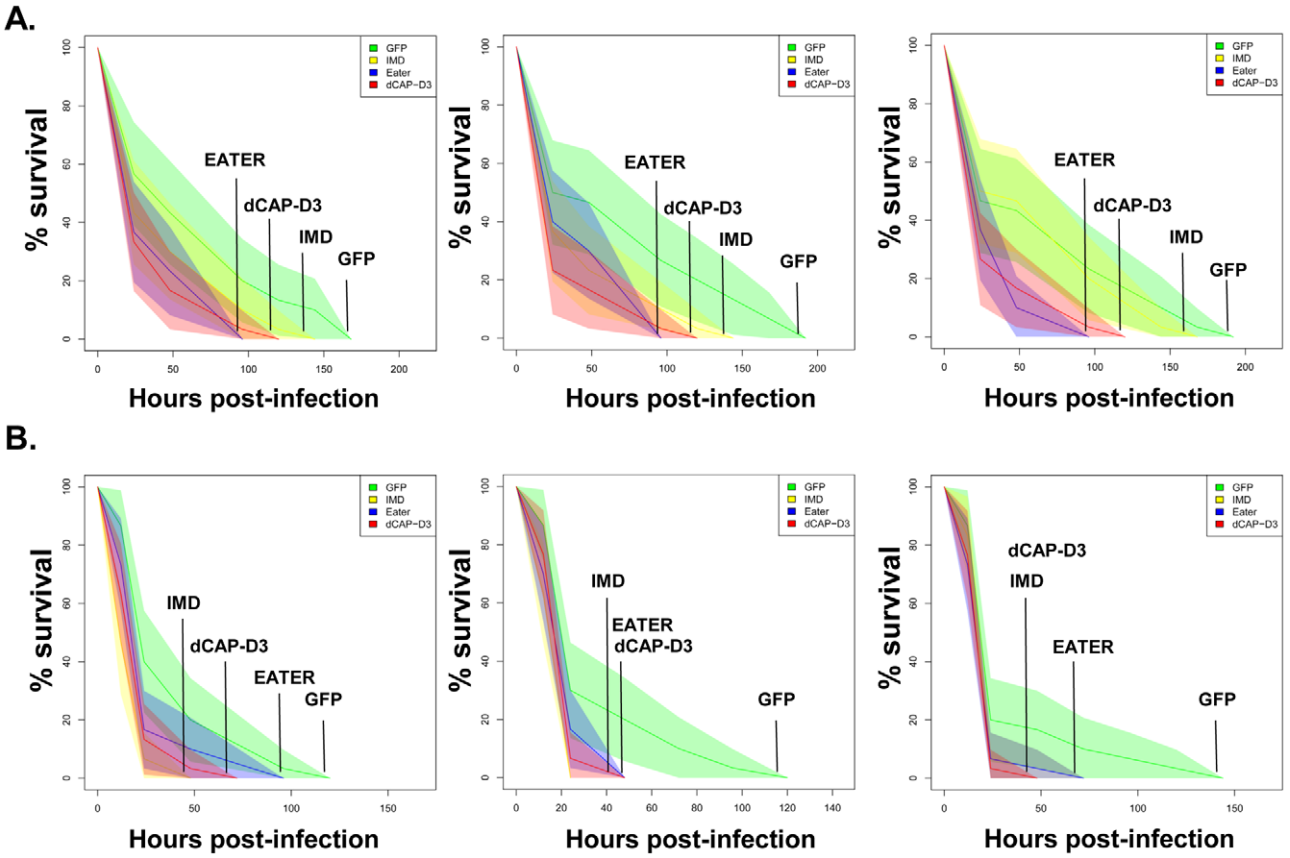

Figure 7. dCAP-D3 is necessary for a proper immune response to bacterial infection. Adult female flies expressing dCAP-D3 (red) dsRNAs under the control of *yolk-GAL4* were infected with the Gram positive bacterium, *Staphylococcus aureus* (A) or the Gram negative bacterium, *Pseudomonas aeruginosa* (B). Flies expressing GFP dsRNAs under the control of *yolk-GAL4* (green) were used as "wild-type" controls. Eater mutants which are defective in phagocytosis (blue) or flies expressing IMD dsRNAs which are compromised in a major innate immune signaling pathway (yellow) were used as positive controls. Results demonstrate that flies expressing reduced levels of dCAP-D3 in the fat body cells are more susceptible to either type of infection than wild type controls. Three independent experiments are depicted with results of each experiment shown as the average of three sets of 10 infected adults per genotype. These experiments were also performed using a sterile needle dipped in PBS to rule out death as a result of wounding and survival curves matched those of yolk-GAL4 expressing flies (data not shown). Results are presented as cox regression models with statistical significance ($p \leq 0.05$) represented as shaded areas above and below the curves.
doi:10.1371/journal.pgen.1002618.g007

dCAP-D3 regulated genes is that they do not seem to be the classically repressed genes with functions in cell cycle progression, DNA damage and DNA replication. Instead, many RBF1/dCAP-D3-dependent genes are classified as being involved in cell-type specific functions and include genes that are involved in enzymatic cascades, organ development and cell fate commitment.

The idea that dCAP-D3 and RBF1 could cooperate to promote tissue development and differentiation is supported by the fact that both proteins are most highly expressed in the late stages of the fly life cycle, and accumulate at high levels in the nuclei of specific cell types in adult tissues. As an illustration of the cell-type specific nature of RBF1/dCAP-D3-regulation we show that dCAP-D3 and RBF1 are both required for the constituitive expression of a large set of AMP genes in fat body cells. The loss of this regulation compromises pathogen-induction of gene expression and has functional consequences for innate immunity. Interestingly, different sets of RBF1/dCAP-D3-dependent genes were evident in the gene expression profiles of mutant larvae and adults. Given this, and the fact that the gene ontology classification revealed multiple groups of genes, we suggest that the targets of RBF1/dCAP-D3-regulation do not represent a single transcriptional program, but diverse sets of cell-type specific programs that need to be activated (or repressed) in specific developmental contexts.

The changes in gene expression seen in the mutant flies suggest that RBF1 has a significant impact on the expression of nearly half of the dCAP-D3-dependent genes. This fraction is consistent with our previous data showing partial overlap between RBF1 and dCAP-D3 banding patterns on polytene chromatin, and the finding that chromatin-association by dCAP-D3 is reduced, but not eliminated, in *rbf1* mutant animals and RBF1-depeleted cells. Although we have previously shown that RBF1 and dCAP-D3 physically associate with one another [11], and our current studies illustrate the fact that they each bind to similar sites at a direct target, the molecular events that mediate the co-operation between RBF1 and dCAP-D3 remain unknown.

These results represent the first published ChIP data for the CAP-D3 protein in any organism. Although we have only examined a small number of targets it is interesting to note that the dCAP-D3 binding patterns are different for activated and repressed genes (compare Figure 5 and Figure S5). More specifically, dCAP-D3 binds to an area within the open reading frame of a gene which it represses (Figure S5C and S5D). However, dCAP-D3 binds to regions which flank a cluster of genes that it activates (Figure 5). Whether or not this difference in binding is true for all dCAP-D3 regulated genes will require a more global analysis.

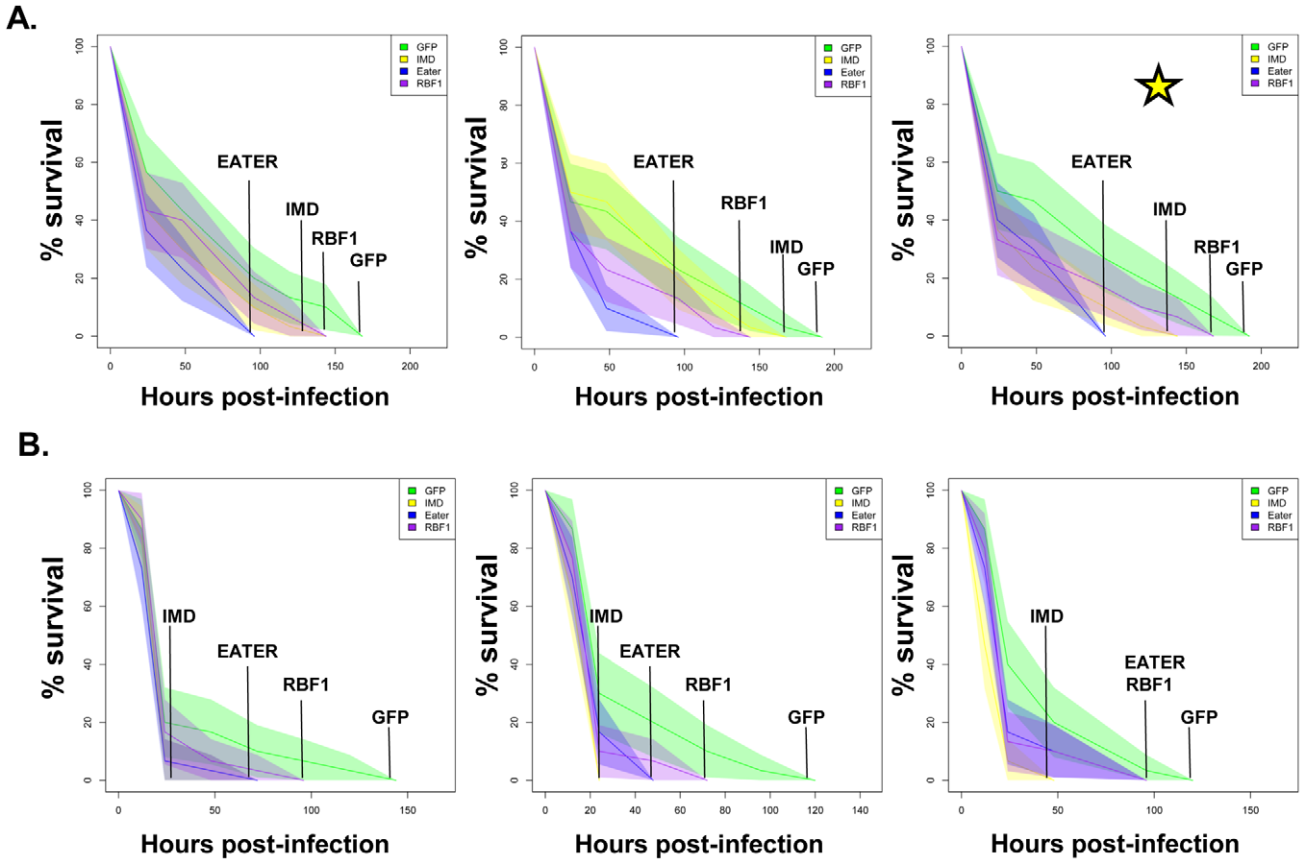

Figure 8. RBF1 is necessary for a proper immune response to Gram positive bacterial infection. Adult female flies expressing RBF1 (purple) dsRNAs under the control of *yolk-GAL4* were infected with the Gram positive bacterium, *Staphylococcus aureus* (A) or the Gram negative bacterium, *Pseudomonas aeruginosa* (B). Flies expressing GFP dsRNAs under the control of *yolk-GAL4* (green) were used as "wild-type" controls. Eater mutants which are defective in phagocytosis (blue) or flies expressing IMD dsRNAs which are compromised in a major innate immune signaling pathway (yellow) were used as positive controls. Results demonstrate that flies expressing reduced levels of RBF1 in the fat body cells are more susceptible to infection with Gram positive bacteria (A) than wild type controls. Three independent experiments are depicted with results of each experiment shown as the average of three sets of 10 infected adults per genotype. Results are presented as cox regression models with statistical significance ($p \leq 0.05$) represented as shaded areas above and below the curves. In the third experiment in (A), which is highlighted by a star, the survival endpoint becomes significant when the confidence level is changed to 90% ($p \leq 0.10$) instead of 95% ($p \leq 0.05$). These experiments were also performed using a sterile needle dipped in PBS to rule out death as a result of wounding and survival curves matched those of yolk-GAL4 expressing flies (data not shown).
doi:10.1371/journal.pgen.1002618.g008

Human Condensin non-SMC subunits are capable of forming subcomplexes *in vitro* that are separate from the SMC protein-containing holocomplex [59], but currently, the extent to which dCAP-D3 relies on the other members of the Condensin II complex remains unclear. We note that fat body cells contain polytene chromatin. Condensin II subunits have been shown to play a role in the organization of polytene chromatin in *Drosophila* nurse cells [60]. Given that RB proteins physically interact with other members of the Condensin II complex [11], it is possible that RBF1 and the entire Condensin II complex, including dCAP-D3, may be especially important for the regulation of transcription on this type of chromatin template.

A potentially significant insight is that the genes that are deregulated in both *rbf1* and *dCap-D3* mutants tend to be present in clusters located within 10 kb of one another. This clustering effect seems to be a more general feature of regulation by dCAP-D3, which is enhanced by RBF1, since clustering was far more prevalent in the list of dCAP-D3 target genes than in the list of RBF1 target genes.

We chose to focus our studies on one of the most functionally related families of clustered target genes that were co-dependent on RBF1/dCAP-D3 for activation in the adult fly: the AMP family of genes. AMP loci represent 20% of the gene clusters regulated by RBF1 and dCAP-D3 in adults. ChIP analysis of one such region, a cluster of AMP genes at the *diptericin* locus, showed this locus to be directly regulated by RBF1 and dCAP-D3 in the fat body and revealed a pattern of RBF1 and dCAP-D3-binding that was very different from the binding sites typically mapped at E2F targets. Unlike the promoter-proximal binding sites typically mapped at E2F-regulated promoters, RBF1 and dCAP-D3 bound to two distant regions, one upstream of the promoter and one downstream of the *diptericin B* translation termination codon, a pattern that is suggestive of an insulator function. We hypothesize that RBF1 and dCAP-D3 act to keep the region surrounding AMP loci insulated from chromatin modifiers and accessible to transcription factors needed for basal levels of transcription. The modEncode database shows binding sites for multiple insulator proteins, as well as GATA factor binding sites, at these regions. GATA has been previously implicated in transcriptional regulation of AMPs in the fly [61], and future studies of dCAP-D3 binding partners in *Drosophila* fat body tissue may uncover other essential activators. Additionally, the chromatin regulating com-

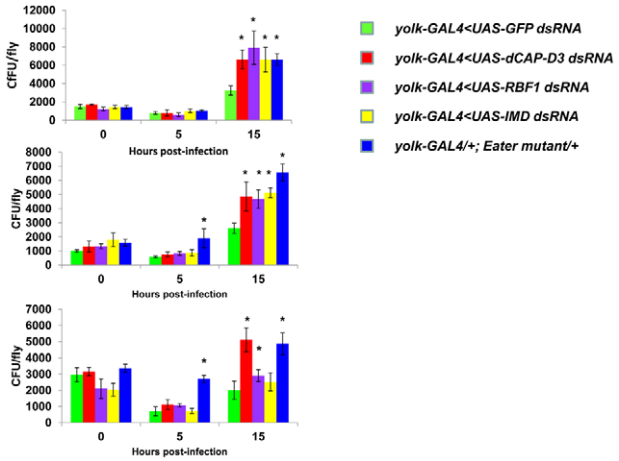

Figure 9. RBF1 and dCAP-D3 are necessary for the ability to clear bacteria *in vivo*. Adult female flies expressing RBF1 (purple) or dCAP-D3 (red) dsRNAs under the control of *yolk-GAL4* were infected with the Gram positive bacterium, *Staphylococcus aureus*. Flies expressing GFP dsRNAs under the control of *yolk-GAL4* (green) were used as "wild-type" controls. Eater mutants which are defective in phagocytosis (blue) or flies expressing IMD dsRNAs which are compromised in a major innate immune signaling pathway (yellow) were used as positive controls. Results demonstrate that at 15 hours following infection, flies expressing reduced levels of dCAP-D3 or RBF1 in the fat body cells exhibit increased numbers of bacteria in comparison to wild type controls. Three independent experiments are shown and results for each experiment are the average of three sets of three infected adults, per genotype, per timepoint. Asterisks emphasize statistical significance ($p \leq 0.05$) as determined by a students paired t-test.
doi:10.1371/journal.pgen.1002618.g009

plex, Cohesin, which exhibits an almost identical structure to Condensin [62–64], has been shown to promote looping of chromatin and to bind proteins with insulator functions [65,66]. Therefore, it remains a possibility that Condensin II, dCAP-D3 may actually possess insulator function, itself. We would like to propose that dCAP-D3 may be functioning as an insulator protein, both insulating regions of DNA containing clusters of genes from the spread of histone marks and possibly looping these regions away from the rest of the body of chromatin. This would serve to keep the region in a "poised state" available for transcription factor binding following exposure to stimuli that would induce activation. In the case of AMP genes, which are made constituitively in specific organs at low levels [37,67,68], dCAP-D3 would bind to regions flanking a cluster, and loop the cluster away from the body of chromatin. Upon systemic infection, these clusters would be more easily accessible to transcription factors like NF-κB. If dCAP-D3 is involved in looping of AMP clusters, then it may also regulate interchromosomal looping which could bring AMP clusters on different chromosomes closer together in 3D space, allowing for a faster and more coordinated activation of all AMPs.

AMP expression is essential for the ability of the fly to recover from bacterial infection. Experiments with bacterial pathogens show that RBF1 and dCAP-D3 are both necessary for induction and maintenance of the AMP gene, *drosomycin* following infection, but only dCAP-D3 is necessary for the induction of the *diptericin* AMP gene. Similarly, survival curves indicate, that while dCAP-D3 deficient flies die more quickly in response to both Gram positive and Gram negative bacterial infection, RBF1 deficient flies only die faster in response to Gram positive bacterial infection. The differences seen between RBF1 and dCAP-D3 deficient flies in diptericin induction cannot be attributed to functional compensation by the other *Drosophila* RB protein family member, RBF2, since results show that loss of RBF2 or both RBF2 and RBF1 do not decrease AMP levels following infection. Since results demonstrate that RBF1 binds most strongly to an AMP cluster prior to infection and regulates basal levels of almost all AMPs tested, we hypothesize that RBF1 (and possibly RBF2) may be more important for cooperating with dCAP-D3 to regulate basal levels of AMPs. Reports have shown that basal expression levels of various AMPs are regulated in a gene-, sex-, and tissue-specific manner, and it is thought that constituitive AMP expression may help to maintain a proper balance of microbial flora and/or help to prevent the onset of infections [37,68,69]. In support of this idea, one study in *Drosophila* which characterized loss of function mutants for a gene called *caspar*, showed that *caspar* mutants increased constituitive transcript levels of diptericin but not transcript levels following infection. This correlated with increased resistance to septic infection with Gram negative bacteria [70], proving that changes in basal levels of AMPs do have significant effects on the survival of infected flies. Additionally, disruption of Caudal expression, a protein which suppresses NF-κB mediated AMP expression following exposure to commensal bacteria, causes severe defects in the mutualistic interaction between gut and commensal bacteria [71]. It is therefore possible that RBF1 and dCAP-D3 may help to maintain the balance of microbial flora in specific organs of the adult fly and/or be involved in a surveillance-type mechanism to prevent the start of infection. RBF1 deficient flies also exhibit defects in *Drosomycin* induction following Gram positive bacterial infection. Mutation to Drosophila GNBP-1, an immune recognition protein required to activate the Toll pathway in response to infection with Gram positive bacteria has been show to result in decreased *Drosomycin* induction and decreased survival rates, without affecting expression of *Diptericin* [72,73]. Therefore, it is possible that inefficient levels of *Drosomycin*, a major downstream effector of the Toll receptor pathway, combined with decreased basal transcription levels of a majority of the other AMPs, would cause RBF1 deficient flies to die faster following infection with Gram positive *S. aureus* but not Gram negative *P. aeruginosa*.

Some dCAP-D3 remains localized to DNA in RBF1 deficient flies [11] and it is also possible that other proteins may help to promote the localization of dCAP-D3 to AMP gene clusters following infection. Given that dCAP-D3 regulates many AMPs including some that do not also depend on RBF1 for activation, and given that dCAP-D3 binding to an AMP locus increases with time after infection whereas RBF1 binding is at its highest levels at the start of infection, it may not be too surprising that dCAP-D3 showed a more pronounced biological role in pathogen assays involving two different species of bacteria.

Remarkably, and perhaps unexpectedly, the levels of both RBF1 and dCAP-D3 impact the basal levels of human AMP transcripts, as well. This indicates that the mechanism of RBF1/dCAP-D3 regulation may not be unique to *Drosophila*. It is striking that many of the human AMP genes (namely, the defensins) are clustered together in a region that spans approximately 1 Mb of DNA. It seems telling that both the clustering of these genes, and a dependence on pRB and CAP-D3, is apparently conserved from flies to humans. The fact that dCAP-D3 and RBF1 dependent activation of *Drosomycin* was necessary for resistance to Gram positive bacterial infection in flies suggests the same could also be true for the human orthologs in human cells. Human AMPs expressed by epithelial cells, phagocytes and neutrophils are an important component of the human innate immune system.

Human AMPs are often downregulated by various microbial pathogenicity mechanisms upon infection [58,74–76]. They have also been reported to play roles in the suppression of various diseases and maladies including cancer and Inflammatory Bowel Disease [77]. We note that the chronic or acute loss of Rb expression from MEFs resulted in an unexplained decrease in the expression of a large number of genes that are involved in the innate immune system [78]. In humans, the bacterium, *Shigella flexneri* was recently shown to down regulate the host innate immune response by specifically binding to the LXCXE cleft of pRB, the same site that we had previously shown to be necessary for CAP-D3 binding [11,79]. An improved understanding of how RB and CAP-D3 regulate AMPs in human cells may provide insight into how these proteins are able to regulate clusters of genes, and may also open up new avenues for therapeutic targeting of infection and disease. Further studies of in differentiated human cells may identify additional sets of genes that are regulated by pRB and CAP-D3.

Materials and Methods

Fly strains

W^{1118} flies were used as "wild type" controls for microarray experiments. Unless otherwise noted, the genotype of RBF mutants was a transheterozygous combination of $rbf1^{\Delta 14}/rbf1^{120a}$ which was obtained by mating $rbf1^{\Delta 14}/FM7$, *GFP* virgins to $rbf1^{120a}/FM7$, *GFP* males at 18°C. Similarly, the genotype of CAP-D3 mutants was a transheterozygous combination of $dCAP\text{-}D3^{\Delta 25}/dCAP\text{-}D3^{c07081}$ which was obtained by mating $dCAP\text{-}D3^{\Delta 25}/CyO$, *GFP* virgins to $dCAP\text{-}D3^{c07081}/CyO$, *GFP* males at 23°C. *yolk-GAL4/FM7c* flies were a kind gift of M. Birnbaum and the timing of expression driven by *yolk-GAL4* has been previously characterized in [40]. The RBF1, dCAP-D3, RBF2, and IMD dsRNA expressing strains were obtained from the VDRC and their transformant IDs were 10696, 29657, 100635, and 101834 respectively. UASt-FLAG-HA tagged strains were created by first amplifying the ORF from either the CAP-D3 RE18364 cDNA clone (DGRC) or the RBF1 LD02906 cDNA clone (DGRC) using Pfx polymerase (Invitrogen). The pENTR/D-TOPO Cloning Kit (Invitrogen) was used to clone the ORF into a Gateway entry vector as described in the manufacturer's protocol and at http://www.ciwemb.edu/labs/murphy/Gateway%20vectors.html. The LR Clonase kit (Invitrogen) was then used to recombine the ORF into the pUASt-FHW vector (DGRC) described in detail at the website mentioned above. pUASt-FLAG-HA-RBF1 and pUASt-FLAG-HA-dCAP-D3 vectors were then injected into embryos to create transgenic fly lines expressing the tagged proteins. Mutant flies used as positive controls in infection experiments included the Imd^1 strain which was a generous gift from L. Stuart and the *Eater* mutant strain [51]. All flies were maintained at 25°C and placed in vials containing standard dextrose medium.

Cell culture and RNAi

hTERT-RPE-1 cells were grown in Dulbecco'sModified Essential Medium (DMEM) supplemented with 10% fetal bovine serum (FBS) and 1% penicillin/streptomycin. RNAimax (Invitrogen) was used, according to manufacturer's protocol, to transfect non-targeting, RB, and CAP-D3 specific siRNAs (described in [12]) at final concentrations of 100 nM. Total RNA was harvested 48 hours post transfection and reverse transcribed into cDNA, as described below.

qRT–PCR

TRIzol (Invitrogen) was used to harvest total RNA from whole flies/specific tissues according to the manufacturer's protocol. After RNA was purified using the Qiagen RNAeasy kit, the Taqman Reverse Transcription kit (Applied Biosystems) was used to reverse transcribe 1.5 µg of RNA into cDNA. qRT-PCR was performed using the Roche Lightcycler 480 to amplify 15 µL reactions containing .5 µL of cDNA, .5 µL of a 10 µM primer mix and 7.5 µL of SYBR Green Master Mix (Roche). All qRT-PCR experiments were performed using three groups of 5 flies per genotype and three independent experiments were performed. Primer sequences are as follows: Rbf1qPCR F1-CTGCAGGGCTACGAGACGTAC, Rbf1qPCR R1 GTGTGCTGGTTCTTCGGCAGG, Rbf2qPCR R1-CTCCCAGTGCTTCTAGCACGC, Rbf2qPCR F1-CGTGAACGCCTTAGAGGTGCC, dCAP-D3 qPCR F3-CGTGCTGTTGCTTTACTTCGGCC, dCAP-D3 qPCR R3- GGCGCATGATGAAGAGCATATCCTG, AttAqPCR F1-GTGGTCCAGTCACAACTGGCG, AttAqPCR R1- CTTGGCATCCAGATTGTGTCTGCC, DroqPCR F1-CACCATCGTTTTCCTGCTGCTTGC, DroqPCR R1-GGTGATCCTCGATGGCCAGTG, AttBqPCR F1- CTCAAAGCGGTCCAGTCACAACTG, AttBqPCR R1- GAATAAATTGGCATGGGCCTCCTGC, Dro4qPCR F1- GTTTGCTCTCCTCGCTGTGGTG, Dro4qPCR R1-GCCCAGCAAGGACCACTGAATC, Dro3qPCR F1- GGCCAACACTGTTTTGGCACGTG, Dro3qPCR R1- GTCCCTCCTCAATGCAGAGACG, Dro2qPCR F1- GTTGTCCTGGCCGCCAATATGG, Dro2qPCR R1- GGACTGCAGTGGCCACTGATATG, DptBqPCR F1- GGACTGGCTTGTGCCTTCTCG, DptBqPCR R1- CAGGGGCACATCAAAATTGGGAGC, DrsqPCR F1-GTACTTGTTCGCCCTCTTCGCTG, DrsqPCR R1- CAGGTCTCGTTGTCCCAGACG, DptqPCR F1- GCTTATCCGATGCCCGACGAC, DptqPCR R1-GTGACCCTGGACTGCAAAGCC, DefqPCR F1- CAAACGCAGACGGCCTTGTCG, DefqPCR R1- AAGCGAGCCACATGCGACCTAC, Dro5qPCR F1- CAAGTTCCTGTACCTCTTCCTGGC, Dro5qPCR R1- CAGGGTCCTCCGTATCTTCCAG, Dro6qPCR F1-CTTCGCACCAGCATTGCAGCC, Dro6qPCR R1-GAAGGTACAGACCTCCCTGTGC, Dro7qPCR F1- GGCTGCAGTGTCCACTGGTTC, Dro7qPCR R1- CACATGCCGACTGCCTTTCCG, MtkqPCR F1- GATTTTTCTGGCCCTGCTGGGTG, MtkqPCR R1- GGTTGGTTAGGATTGAAGGGCGAC, rp49qPCR F1- TACAGGCCCAAGATCGTGAAG, rp49qPCR R1- GACGCACTCTGTTGTCGATACC, CecCqPCR F1-CAATCGGAAGCCGGTTGGCTG, CecqPCR R1-GCGCAATTCCCAGTCCTTGAATGG, AndqPCR F1- CATTTTGGCCATCAGCGTGGGTC, AndqPCR R1- GGGCTTAGCAAAGCCAATTCCCAC, AttCqPCR F1- GTACTTGGCTCCCTTGCGGTG, AttCqPCR R1- CTTAGGTCCAATCGGGCATCGG, AttDqPCR F1- CCAAGGGAGTTTATGGAGCGGTC, AttDqPCR R1- GCTCTGGAAGAGATTGGCTTGGG, CecA1qPCR F1- CAATCGGAAGCTGGGTGGCTG, CecA1qPCR R1- GGCGGCTTGTTGAGCGATTCC, CecA2qPCR F1- GGACAATCGGAAGCTGGTTGGC, CecA2qPCR R1- GGCCTGTTGAGCGATTCCCAG, CecBqPCR F1- GATTCCGAGGACCTGGATTGAGG, CecBqPCR R1-GGCCATCAGCCTGGGAAACTC, tub84BqPCR F1- GGCAAGGAGATCGTCGATCTGG, tub84BqPCR R1- GACGCTCCATCAGCAGCGAG, hCAP-D3qPCR F1- TCCGGAAGCAGGCCCTCCAG, hCAP-D3qPCR R1- GGACCTGGCTGTCGTCCCCA, hRBqPCR F1- AGCTGTGGGACAGGGTTGTGTC, hRBqPCR R1- CAACCTCAAGAGCGCACGCC, eaterqPCR F1: CTCGTATCGGCTCAGATCTGCAC, eaterqPCR R1: CATCTGAGTGCGGAGCTCCTTAC, IMDqPCR F1- CGAATCCACTGGAGCAACAGCTG, IMDqPCR R1-GTTTCCACGCACTTGGGCGAG, hGAPDHqPCR F1- AGCCTCCCGCTTCGCTCTCT, hGAPDHqPCR R1- CCAGGCGCCCAATACGACCA, orc1qPCR F1- CATCATCCTCAAA-

CACGCGCTGC, orc1qPCR R1- CCCTCGACGAGGCGTAAAAGC, cg5250qPCR F1- GACATTGCCGGAGGTGAAGAGC, cg5250qPCR R1- CTATTCGACTATGTGGTGGGCCTG, dupqPCR F1- GGGTGGCGGTATTTTTGTGGGAG, dupqPCR R1- CAACAGGAAACTCCGCGACGC, mus209qPCR F1- CTTGTCGAAGCCATCGGAACGC, mus209qPCR R1- GGGTCAAGCCACCATCCTGAAG, dnkqPCR F1- CCGCCCCAACCAACAAGAAGC, dnkqPCR R1- CCTCCAGCGTATTGTACATGCCC, RnrSqPCR F1- GAAGAAGGCAAGCACGTGCGAG, RnrSqPCR R1- CCAGTACCACGACATCTGGCAG, dnapoldeltaqPCR F1- CCATCGCCCATTAGCAGAGTCTG, dnapoldeltaqPCR R1- GGAACCTCCAATGGACATGCCAAG, mcm7qPCR F1- CATTGAGCACCGCCTGATGATGG, mcm7qPCR R1- GAGTGCGCCTTCTCTGTGGAC, mcm3qPCR F1- CGAGGTGATGGAACAGGGTCG, mcm3qPCR R1- GAAAGCAGCGAATCCTGCAGTCC, mcm2qPCR F1- GAGATCCCGCAGGACTTGTTGC, mcm2qPCR R1- CAAAAGACTCCTGTCGCAGCTGG, mcm5qPCR F1- CTGGTCTCACGGCTTCGGTTATG, mcm5qPCR R1- GCCACACGATCATCCTCTCGC, dnapolalpha50qPCR F1- CCTTCTACCGTTGGCTATCGTATGG, dnapolalpha50qPCR R1- CAGCTTGGGTATCAAAGCAGAGG, DEFA-1qPCR F1- TGCCCTCTCTGGTCACCCTGC, DEFA-1qPCR R1- GCCTGGAGTGGCTCAGCCTG, DEFB-3qPCR F1- GCGTGGGGTGAAGCCTAGCA, DEFB-3qPCR R1- AGCTGAGCACAGCACACCGG.

Generation of anti–dCAP-D3 antibody

The rabbit anti–dCAP-D3 YZ834 antibody was generated by Yenzyme Corporation. The antibody was purified using the BIO-RAD Affi-Gel 10 Gel according to manufacturer's protocol.

Immunofluorescence analysis of cryosections

Adult female flies were cryosectioned (10 μm) and stained as previously described [80]. Primary antibodies included RBF1 (DX2), dCAP-D3 (YZ384), and anti-GFP (Jackson Immunoresearch). Images were obtained using a Zeiss LSM510 Confocal microscope.

Preprocessing of array data

Nimblegen microarray data were pretreated according to the manufacturer's recommendation and replicate probes were averaged. Affymetrix microarray data was downloaded from array express as raw .CEL files and normalized by robust multi array averaging (RMA)[RMS] before further analysis [81]. The entire set of microarray data can be found in Table S1.

Hypothesis testing

Differentially expressed genes were identified using a linear model with a moderated T-test [82]. P values were corrected for multiple testing by calculating false discovery rates using the method of Benjamini and Hochberg [83]. Genes with a false discovery rate (FDR)<0.15 and a log2 fold change >0.1 were taken as significant. Gene ontology (GO) annotations were downloaded from FLYBASE [84], and gene ontology terms overrepresented on the lists of differentially expressed genes were identified using a hypergeometric test. P-values from the hypergeometric test were corrected for multiple testing using the same method as for the individual genes and GO-categories with FDR<0.05 were taken as significant.

Gene clustering analysis

Chromosomal positions of transcription start and stop sites for all genes on the chip were taken from FLYBASE. Genes were counted as clustered if they overlapped, or if the genes lay within 10 000 base pairs of each other. Overall chromosomal clustering for a list of genes was quantified as the number of genes that co-localize according to this criterion. Significance of co-localization was evaluated by comparing to lists of randomly selected genes from the same chip.

Infection of flies with pathogenic bacteria

S. aureus and *P. aeruginosa* bacteria were gifts from L. Stuart. *S. aureus* was grown in a shaking incubator at 37°C, in DIFCO Columbia broth (BD Biosciences) supplemented with 2% NaCl and *P. aeruginosa* was grown in a shaking incubator at 37°C in DIFCO Luria broth (BD Biosciences). Bacteria were inoculated in 10 mL cultures grown overnight. 10^{-4} bacterial cells were then inoculated into a new 10 mL culture and this was grown to an $OD_{600\ nm}$ of 0.5. These cultures were then centrifuged at 3000 rpm in a 1.5 mL eppendorf tube for 5 minutes at 4°C and subsequently washed twice with PBS. After a third centrifugation, PBS wash was removed from the pellet and 25 μL of new PBS was used to resuspend the pellet. Infections were performed as previously described [85]. Specifically, a .25 mm diameter straight stainless steel needle and pin vise (Ted Pella Inc, Redding, CA) were used to infect adult flies. The needle was dipped into the resuspended bacterial pellet and used to prick the thorax of a CO_2-anesthetized adult fly in a region just underneath where the wing connects to the thorax. Flies were then separated from the needle using a brush and put into fresh vials containing standard dextrose medium with no more than 10 flies per vial.

Chromatin immunoprecipitation

40 flies per IP were used in all ChIP experiments. Flies were homogenized with a KONTES pellet pestle grinder (Kimble Chase) in 1 mL of buffer A (60 mM KCl, 15 mM NaCl, 4 mM MgCl2, 15 mM HEPES pH 7.6, .5% Triton X-100, .5 mM DTT, EDTA-free protease inhibitors cocktail (Roche)) containing 1.8% formaldehyde. Homogenized flies were incubated at RT for 15 minutes, at which point glycine was added to a concentration of 225 mM. 2–4 mLs of homogenized flies were transferred to 15 mL conical tubes and centrifuged at 4°C for 5 min at 4000 g. Supernatant was discarded and pellets were washed with 3 mL of buffer A. Tubes were centrifuged as described above, supernatant was discarded, and pellets were washed with 3 mL of buffer B (140 mM NaCl, 15 mM HEPES pH 7.6, 1 mM EDTA, .5 mM EGTA, 1% Triton, .5 mM DTT, .1% sodium deoxycholate, EDTA free protease inhibitors cocktail). Tubes were centrifuged as described above, supernatant was discarded, and 500 μL of buffer B+1% SDS per IP was added to each tube. Tubes were rotated at 4°C for 20 min. Samples were then sonicated using the Branson sonifier at a setting of 3, with 8 sonication intervals of 20 seconds interspersed by 10 second breaks. Tubes were centrifuged at 4°C for 5 min at 2000 RPM and 500 μL supernatant was used for each IP. 50 μL of Dynal Protein A beads (Invitrogen) per IP were prepared according to the manufacturer's recommendations. Beads were incubated with anti-FLAG M2 antibody (Sigma) or dCAP-D3 antibody (YZ384) for 2 hours at RT with rotation. Beads were washed according to manufacturer's protocol and added to the diluted chromatin samples which were then incubated at 4°C overnight, with rotation. Samples were centrifuged at 3000 RPM, 4°C for 1 min and washed three times with buffer B+.05% SDS and once with TE. Bound protein was eluted by adding 125 μL of Buffer C (1%SDS, .2% NaCl, TE) to the beads for 30 min at 65°C. Samples were again centrifuged and eluates were harvested and incubated for 4 hours at 65°C to reverse crosslinks. Samples were digested with Proteinase K and RNase A (Sigma), phenol-chloroform

extracted, and ethanol precipitated. DNA pellets were dissolved in 105 µL of ddH2O and .5 µL was used per qRT-PCR reaction.

Survival curves

Flies were collected approximately 5–8 days after eclosure and were infected as described above. Following infection, each group of flies was placed in a new vial of food and monitored for the number of surviving flies at each timepoint. Three experiments were performed, with each experiment including 3 groups of 10 flies per genotype per timepoint. Survival statistics were calculated using a cox proportional hazard model, and hazard ratios with a two sided p-value less than 0.05 were taken as significant.

Bacterial clearance assays

Flies were anestitized by CO2 inhalation and infected as described above. Following infection, flies were dipped in 95% Ethanol, air dried, and placed into 1.5 mL Eppendorf tubes containing 500 µL of PBS. Flies were homogenized with a Kontes battery powered homogenizer and plastic pestle (USA scientific). The tubes were centrifuged for 2 min at 3000 rpm. Various dilutions were plated onto Columbia CNA with 5% Sheep's Blood Agar (Becton Dickinson and Company). This type of agar contains antibiotics to inhibit growth of organisms other than *Staphylococcus aureus*.

Supporting Information

Figure S1 dCAP-D3 and RBF1 mutants expressing a transheterozygous combination of alleles retain approximately 15% of wild type protein expression. qRT-PCR (A) and Immunoblots (B) for *rbf1* transcript levels/protein levels and *dCap-D3* transcript levels/protein in wild type (w^{1118}) and dCAP-D3 transheterozygous mutant ($dCAP\text{-}D3^{c07081/\Delta 25}$) or RBF1 transheterozygous mutant ($rbf1^{120a/\Delta 14}$) female flies indicates that mutants retain 10–15% of wild-type protein expression levels. Transcript levels were normalized to *tubulin 84B* mRNA levels and α-tubulin was used as a loading control in B.
(TIF)

Figure S2 RBF1 regulates E2F targets in specific tissues of the adult fly. Ovaries were dissected from female adult flies and cDNA was made from either carcass or ovaries. Top table: qRT-PCR analyses performed on cDNA from ovaries shows that decreased RBF1 expression results in the upregulation of a few E2F targets while decreased dCAP-D3 expression largely has no effect. Bottom table: qRT-PCR analyses performed on cDNA from carcass without ovaries shows that decreased RBF1 expression in the carcass does result in upregulation of many E2F targets, however, dCAP-D3 does not share regulation of these genes with RBF1. Transcript levels were normalized to *tubulin 84B* mRNA levels. All results were significant with p-values≤0.05.
(TIF)

Figure S3 RBF1 and dCAP-D3 antibodies are specific. Immunostaining for dCAP-D3 (A) and RBF1 (B) in cryosections of abdomens of adult female flies expressing dCAP-D3 (A) or RBF1 (B) dsRNA in combination with GFP protein in fat body cells shows the antibodies recognize protein where dsRNAs are not expressed. Flies used in A were of the genotype *yolk-GAL4, UAS-GFP/+;+;UAS-dCAP-D3 dsRNA*, and flies used in B were of the genotype *yolk-GAL4, UAS-GFP/+;+;UAS-RBF1 dsRNA*.
(TIF)

Figure S4 qRT–PCR analysis of genes adjacent to the *diptericin* locus. qRT–PCR analysis of cDNA from 1) flies expressing driver alone (*yolk-GAL4/+;+;+*), 2) flies expressing *rbf1 dsRNA (yolk-GAL4;+;UAS-rbf1 dsRNA)* in the fat body cells and 3) flies expressing *dCAP-D3 dsRNA (yolk-GAL4;+;UAS-dCAP-D3 dsRNA)* in the fat body cells demonstrates that *CG43070* is also activated by RBF1 and dCAP-D3.
(TIF)

Figure S5 Endogenous dCAP-D3 binds to *CG5250* in a similar pattern as FLAG-HA-dCAP-D3. A) qRT-PCR was performed on cDNA generated from whole female flies (1) expressing yolk-GAL4 driver alone (*yolk-GAL4/+; +;+*) or (2) exhibiting acute, fat body specific knockdown of dCAP-D3 (*yolk-GAL4/+; +/UAS-dCAP-D3 dsRNA/+*). Transcript levels for genes surrounding *CG5250* indicate that *CG5250* is the only gene in the locus that is significantly regulated by dCAP-D3. B) Graphic representation of the *CG5250* locus on which ChIP for dCAP-D3 in both the whole adult and the adult fat body was performed. Relative positions of primer sets used are listed under the diagram of the locus. *CG5250* is highlighted in red since it is repressed by dCAP-D3 in the whole adult fly. C) Chromatin immunoprecipitation for FLAG protein in female adult flies expressing FLAG-HA-dCAP-D3 in the fat body (*yolk-GAL4/+; +; UAS-FLAG-HA-dCap-D3/+*) shows that the *CG5250* locus is a direct target of dCAP-D3. ChIP signal corresponding to FLAG-HA-dCAP-D3 binding in the absence of *Staphylococcus aureus* infection is colored in burgundy. ChIP signal corresponding to FLAG-HA-dCAP-D3 binding two and four hours after *S. aureus* infection is colored in blue and yellow, respectively. D) ChIP for endogenous dCAP-D3 in whole adult flies at the *CG5250* locus demonstrates the dCAP-D3 binding pattern is identical to the pattern exhibited specifically in the fat body.
(TIF)

Figure S6 Confirmation of rbf1 and rbf2 transcript knockdown in flies expressing RBF2 or RBF1 and RBF2 dsRNAs. qRT-PCR was performed on cDNAs from flies deficient for RBF2 alone or deficient for a combination of both RBF1 and RBF2.
(TIF)

Figure S7 RBF2 does not regulate AMP induction following bacterial infection. Adult female flies expressing RBF2 (turquoise) or a combination of RBF1 and RBF2 (black) dsRNAs under the control of *yolk-GAL4* were infected with the Gram positive bacteria, *Staphylococcus aureus*. A) qRT-PCR analyses for transcript levels of the *Drosomycin* AMP gene in these flies show that control flies expressing GFP dsRNAs under the control of *yolk-GAL4* (green) undergo a large induction of AMPs at 8–24 hours post-infection. Flies expressing RBF2 dsRNA or a combination of RBF1 and RBF2 dsRNAs show no significant, repeated changes in transcript levels upon comparison to control flies. B) qRT-PCR analyses for transcript levels of the *Diptericin* AMP gene in these flies show that control flies expressing GFP dsRNAs under the control of *yolk-GAL4* (green) undergo a large induction of AMPs at 8–24 hours post-infection. Flies expressing RBF2 dsRNA or a combination of RBF1 and RBF2 dsRNAs exhibit a significant decrease in basal transcript levels in the majority of experiments, but do not exhibit significant changes in transcript levels following infection. Three independent experiments are shown and results for each experiment are the average of three sets of five infected adults. The inset boxes in the upper right corner of each graph are a larger representation of the 0 hour timepoint and therefore depict basal transcription levels. Asterisks emphasize statistical significance (p≤0.05) as determined by a students paired t-test.
(TIF)

Figure S8 RBF2 deficiency in the fat body does not significantly affect survival following bacterial infection. Adult female flies expressing RBF2 (turquoise) dsRNAs or a combination of RBF1 and RBF2 dsRNAs (black) under the control of *yolk-GAL4* were infected with the Gram positive bacterium, *Staphylococcus aureus* (A) or

the Gram negative bacterium, *Pseudomonas aeruginosa* (B). Flies expressing GFP dsRNAs under the control of *yolk-GAL4* (green) were used as "wild-type" controls. Eater mutants which are defective in phagocytosis (blue) or flies expressing IMD dsRNAs which are compromised in the Gram negative arm of the innate immune signaling pathway (yellow) were used as positive controls. Results demonstrate that flies expressing reduced levels of RBF2 or reduced levels of both RBF1 and RBF2 in the fat body cells do not significantly and repeatedly affect survival times in response to either type of infection upon comparison to wild type controls. Three independent experiments are depicted with results of each experiment shown as the average of three sets of 10 infected adults per genotype. Results are presented as cox regression models with statistical significance ($p \leq 0.05$) represented as shaded areas above and below the curves. These experiments were also performed using a sterile needle dipped in PBS to rule out death as a result of wounding and survival curves matched those of yolk-GAL4 expressing flies (data not shown).
(TIF)

Figure S9 Regulation of AMP genes by RB and CAP-D3 is conserved in human cells. A) RPE-1 cells were transfected with (1) non-targeting Control siRNA, (2) pRB siRNA or (3)CAP-D3 siRNAs. qRT-PCR analyses were performed on cDNAs generated from cellular RNA collected 48 hours post transfection and results show that RB and CAP-D3 are significantly decreased. B) qRT-PCR for AMPs in cells described in A shows that pRB or dCAP-D3 deficiency results in significant decreases in basal levels of two human AMP genes.
(TIF)

Table S1 Microarray data from multiple samples of wild type cDNA, dCAP-D3 mutant cDNA, and RBF1 mutant cDNA. Experiments were performed using Nimblegen 385 k whole genome arrays. A detailed description of the information found in each column is provided to the right of the table.
(XLS)

Table S2 Analysis of clustering frequencies among dCAP-D3 and/or RBF1 regulated target genes. A detailed description of the information found in each column is provided to the right of the table. Numbers within individual columns are arbitrary and designate genes present within the same cluster; they do not indicate any information about the strength of their misregulation in mutant flies.
(XLS)

Table S3 List of significant Gene Ontology categories represented by the total number of shared RBF1/dCAP-D3 target genes in the adult fly. Column C lists the Gene Ontology (GO) term. Column D lists the term name associated with the GO category. Column E lists the total number of significant genes found in this GO category. Column F lists the total number of genes found in this GO category. Column G lists the P values associated with the GO category. Column H lists the actual Flybase Gene Numbers associated with the microarray genes found in the GO category.
(XLS)

Table S4 dCAP-D3/RBF1 do not regulate the majority of genes previously reported to be involved in phagocytosis. Microarray data from dCAP-D3 mutant adult flies vs. wild type flies (Table S1) was analyzed for changes to transcript levels of 19 genes previously reported to be involved in phagocytosis (Column A). Only two genes were shown to be misregulated in the mutant flies (Columns B and C).
(XLS)

Table S5 dCAP-D3/RBF1 do not regulate the majority of genes previously reported to be involved in coagulation and melanization. Microarray data from dCAP-D3 mutant adult flies vs. wild type flies (Table S1) was analyzed for changes to transcript levels of 18 genes previously reported to be involved in coagulation and melanization (Column A). Only one gene was shown to be misregulated in the mutant flies (Columns B and C).
(XLS)

Acknowledgments

We thank Morris Birnbaum, Lynda Stuart, Christine Kocks, and Neal Silverman for reagents used in this paper. We thank Spiros Artavanis-Tsakonas and the Harvard/Exelixis Collection for the use of multiple *Drosophila* stocks. We thank Andrea Livey in the Pathology Core at the M.G.H. Cancer Center for cryosectioning of flies. We would also like to thank Nicholas Paquette, Lynda Stuart, and the members of the Dyson lab for advice and technical assistance.

Author Contributions

Conceived and designed the experiments: MSL JAW EA NJD. Performed the experiments: MSL JAW. Analyzed the data: MSL EA NJD. Contributed reagents/materials/analysis tools: N-SM MMSH AG SR. Wrote the paper: MSL NJD.

References

1. Hanahan D, Weinberg RA (2000) The hallmarks of cancer. Cell 100: 57–70.
2. Sherr CJ, McCormick F (2002) The RB and p53 pathways in cancer. Cancer Cell 2: 103–112.
3. Trimarchi JM, Lees JA (2002) Sibling rivalry in the E2F family. Nat Rev Mol Cell Biol 3: 11–20.
4. Thomas DM, Carty SA, Piscopo DM, Lee JS, Wang WF, et al. (2001) The retinoblastoma protein acts as a transcriptional coactivator required for osteogenic differentiation. Mol Cell 8: 303–316.
5. Schneider J, Gu W, Zhu L, Mahdavi V, Nadal-Ginard B (1994) Reversal of terminal differentiation mediated by p107 in Rb-/- muscle cells 10.1126/science.8197461. Science 264: 1467–1471.
6. Novitch B, Mulligan G, Jacks T, Lassar A (1996) Skeletal muscle cells lacking the retinoblastoma protein display defects in muscle gene expression and accumulate in S and G2 phases of the cell cycle 10.1083/jcb.135.2.441. J Cell Biol 135: 441–456.
7. Zacksenhaus E, Jiang Z, Chung D, Marth JD, Phillips RA, et al. (1996) pRb controls proliferation, differentiation, and death of skeletal muscle cells and other lineages during embryogenesis. Genes Dev 10: 3051–3064.
8. Nicolay BN, Bayarmagnai B, Moon NS, Benevolenskaya EV, Frolov MV (2010) Combined inactivation of pRB and hippo pathways induces dedifferentiation in the Drosophila retina. PLoS Genet 6: e1000918. doi:10.1371/journal.pgen.1000918.
9. Longworth MS, Dyson NJ (2010) pRb, a local chromatin organizer with global possibilities. Chromosoma 119: 1–11.
10. Isaac CE, Francis SM, Martens AL, Julian LM, Seifried LA, et al. (2006) The retinoblastoma protein regulates pericentric heterochromatin. Mol Cell Biol 26: 3659–3671.
11. Longworth MS, Herr A, Ji JY, Dyson NJ (2008) RBF1 promotes chromatin condensation through a conserved interaction with the Condensin II protein dCAP-D3. Genes Dev 22: 1011–1024.
12. Manning AL, Longworth MS, Dyson NJ (2010) Loss of pRB causes centromere dysfunction and chromosomal instability. Genes Dev 24: 1364–1376.
13. Gerlich D, Hirota T, Koch B, Peters JM, Ellenberg J (2006) Condensin I stabilizes chromosomes mechanically through a dynamic interaction in live cells. Curr Biol 16: 333–344.
14. Ono T, Losada A, Hirano M, Myers MP, Neuwald AF, et al. (2003) Differential contributions of condensin I and condensin II to mitotic chromosome architecture in vertebrate cells. Cell 115: 109–121.
15. Steffensen S, Coelho PA, Cobbe N, Vass S, Costa M, et al. (2001) A role for Drosophila SMC4 in the resolution of sister chromatids in mitosis. Curr Biol 11: 295–307.
16. Hirota T, Gerlich D, Koch B, Ellenberg J, Peters JM (2004) Distinct functions of condensin I and II in mitotic chromosome assembly. J Cell Sci 117: 6435–6445.
17. Bazett-Jones DP, Kimura K, Hirano T (2002) Efficient supercoiling of DNA by a single condensin complex as revealed by electron spectroscopic imaging. Mol Cell 9: 1183–1190.
18. Strick TR, Kawaguchi T, Hirano T (2004) Real-time detection of single-molecule DNA compaction by condensin I. Curr Biol 14: 874–880.

19. Ono T, Fang Y, Spector DL, Hirano T (2004) Spatial and temporal regulation of Condensins I and II in mitotic chromosome assembly in human cells. Mol Biol Cell 15: 3296–3308.
20. Kimura K, Cuvier O, Hirano T (2001) Chromosome condensation by a human condensin complex in Xenopus egg extracts. J Biol Chem 276: 5417–5420.
21. Gosling KM, Makaroff LE, Theodoratos A, Kim YH, Whittle B, et al. (2007) A mutation in a chromosome condensin II subunit, kleisin beta, specifically disrupts T cell development. Proc Natl Acad Sci U S A 104: 12445–12450.
22. Xu Y, Leung CG, Lee DC, Kennedy BK, Crispino JD (2006) MTB, the murine homolog of condensin II subunit CAP-G2, represses transcription and promotes erythroid cell differentiation. Leukemia 20: 1261–1269.
23. Cobbe N, Savvidou E, Heck MM (2006) Diverse mitotic and interphase functions of condensins in Drosophila. Genetics 172: 991–1008.
24. Dej KJ, Ahn C, Orr-Weaver TL (2004) Mutations in the Drosophila condensin subunit dCAP-G: defining the role of condensin for chromosome condensation in mitosis and gene expression in interphase. Genetics 168: 895–906.
25. Lemaitre B, Hoffmann J (2007) The host defense of Drosophila melanogaster. Annu Rev Immunol 25: 697–743.
26. Dimova DK, Stevaux O, Frolov MV, Dyson NJ (2003) Cell cycle-dependent and cell cycle-independent control of transcription by the Drosophila E2F/RB pathway. Genes Dev 17: 2308–2320.
27. Kwon SY, Xiao H, Glover BP, Tjian R, Wu C, et al. (2008) The nucleosome remodeling factor (NURF) regulates genes involved in Drosophila innate immunity. Dev Biol 316: 538–547.
28. Meister M (2004) Blood cells of Drosophila: cell lineages and role in host defence. Curr Opin Immunol 16: 10–15.
29. Kurucz E, Markus R, Zsamboki J, Folkl-Medzihradszky K, Darula Z, et al. (2007) Nimrod, a putative phagocytosis receptor with EGF repeats in Drosophila plasmatocytes. Curr Biol 17: 649–654.
30. Lebestky T, Chang T, Hartenstein V, Banerjee U (2000) Specification of Drosophila hematopoietic lineage by conserved transcription factors. Science 288: 146–149.
31. Alfonso TB, Jones BW (2002) gcm2 promotes glial cell differentiation and is required with glial cells missing for macrophage development in Drosophila. Dev Biol 248: 369–383.
32. Lanot R, Zachary D, Holder F, Meister M (2001) Postembryonic hematopoiesis in Drosophila. Dev Biol 230: 243–257.
33. Elrod-Erickson M, Mishra S, Schneider D (2000) Interactions between the cellular and humoral immune responses in Drosophila. Curr Biol 10: 781–784.
34. Nappi AJ, Ottaviani E (2000) Cytotoxicity and cytotoxic molecules in invertebrates. Bioessays 22: 469–480.
35. Irving P, Ubeda JM, Doucet D, Troxler L, Lagueux M, et al. (2005) New insights into Drosophila larval haemocyte functions through genome-wide analysis. Cell Microbiol 7: 335–350.
36. Wertheim B, Kraaijeveld AR, Schuster E, Blanc E, Hopkins M, et al. (2005) Genome-wide gene expression in response to parasitoid attack in Drosophila. Genome Biol 6: R94.
37. Uvell H, Engstrom Y (2007) A multilayered defense against infection: combinatorial control of insect immune genes. Trends Genet 23: 342–349.
38. Brennan CA, Anderson KV (2004) Drosophila: the genetics of innate immune recognition and response. Annu Rev Immunol 22: 457–483.
39. Imler JL, Bulet P (2005) Antimicrobial peptides in Drosophila: structures, activities and gene regulation. Chem Immunol Allergy 86: 1–21.
40. DiAngelo JR, Birnbaum MJ (2009) Regulation of fat cell mass by insulin in Drosophila melanogaster. Mol Cell Biol 29: 6341–6352.
41. Aggarwal K, Silverman N (2008) Positive and negative regulation of the Drosophila immune response. BMB Rep 41: 267–277.
42. Ferrandon D, Imler JL, Hetru C, Hoffmann JA (2007) The Drosophila systemic immune response: sensing and signalling during bacterial and fungal infections. Nat Rev Immunol 7: 862–874.
43. Senger K, Harris K, Levine M (2006) GATA factors participate in tissue-specific immune responses in Drosophila larvae. Proc Natl Acad Sci U S A 103: 15957–15962.
44. Tanji T, Yun EY, Ip YT (2010) Heterodimers of NF-kappaB transcription factors DIF and Relish regulate antimicrobial peptide genes in Drosophila. Proc Natl Acad Sci U S A 107: 14715–14720.
45. Meister M, Braun A, Kappler C, Reichhart JM, Hoffmann JA (1994) Insect immunity. A transgenic analysis in Drosophila defines several functional domains in the diptericin promoter. Embo J 13: 5958–5966.
46. Georgel P, Meister M, Kappler C, Lemaitre B, Reichhart JM, et al. (1993) Insect immunity: the diptericin promoter contains multiple functional regulatory sequences homologous to mammalian acute-phase response elements. Biochem Biophys Res Commun 197: 508–517.
47. Kappler C, Meister M, Lagueux M, Gateff E, Hoffmann JA, et al. (1993) Insect immunity. Two 17 bp repeats nesting a kappa B-related sequence confer inducibility to the diptericin gene and bind a polypeptide in bacteria-challenged Drosophila. Embo J 12: 1561–1568.
48. Valanne S, Myllymaki H, Kallio J, Schmid MR, Kleino A, et al. (2010) Genome-wide RNA interference in Drosophila cells identifies G protein-coupled receptor kinase 2 as a conserved regulator of NF-kappaB signaling. J Immunol 184: 6188–6198.
49. Meng X, Khanuja BS, Ip YT (1999) Toll receptor-mediated Drosophila immune response requires Dif, an NF-kappaB factor. Genes Dev 13: 792–797.
50. Kaneko T, Silverman N (2005) Bacterial recognition and signalling by the Drosophila IMD pathway. Cell Microbiol 7: 461–469.
51. Kocks C, Cho JH, Nehme N, Ulvila J, Pearson AM, et al. (2005) Eater, a transmembrane protein mediating phagocytosis of bacterial pathogens in Drosophila. Cell 123: 335–346.
52. Ayres JS, Freitag N, Schneider DS (2008) Identification of Drosophila mutants altering defense of and endurance to Listeria monocytogenes infection. Genetics 178: 1807–1815.
53. Ayres JS, Schneider DS (2008) A signaling protease required for melanization in Drosophila affects resistance and tolerance of infections. PLoS Biol 6: e305. doi:10.1371/journal.pbio.0060305.
54. Dionne MS, Pham LN, Shirasu-Hiza M, Schneider DS (2006) Akt and FOXO dysregulation contribute to infection-induced wasting in Drosophila. Curr Biol 16: 1977–1985.
55. Schneider DS, Ayres JS (2008) Two ways to survive infection: what resistance and tolerance can teach us about treating infectious diseases. Nat Rev Immunol 8: 889–895.
56. Korenjak M, Taylor-Harding B, Binne UK, Satterlee JS, Stevaux O, et al. (2004) Native E2F/RBF complexes contain Myb-interacting proteins and repress transcription of developmentally controlled E2F target genes. Cell 119: 181–193.
57. Lewis PW, Beall EL, Fleischer TC, Georlette D, Link AJ, et al. (2004) Identification of a Drosophila Myb-E2F2/RBF transcriptional repressor complex. Genes Dev 18: 2929–2940.
58. Diamond G, Beckloff N, Weinberg A, Kisich KO (2009) The roles of antimicrobial peptides in innate host defense. Curr Pharm Des 15: 2377–2392.
59. Kimura K, Hirano T (2000) Dual roles of the 11S regulatory subcomplex in condensin functions. Proc Natl Acad Sci U S A 97: 11972–11977.
60. Hartl TA, Smith HF, Bosco G (2008) Chromosome alignment and transvection are antagonized by condensin II. Science 322: 1384–1387.
61. Petersen UM, Kadalayil L, Rehorn KP, Hoshizaki DK, Reuter R, et al. (1999) Serpent regulates Drosophila immunity genes in the larval fat body through an essential GATA motif. Embo J 18: 4013–4022.
62. Hirano T (2006) At the heart of the chromosome: SMC proteins in action. Nat Rev Mol Cell Biol 7: 311–322.
63. Nasmyth K, Haering CH (2005) The structure and function of SMC and kleisin complexes. Annu Rev Biochem 74: 595–648.
64. Hirano T (2005) SMC proteins and chromosome mechanics: from bacteria to humans. Philos Trans R Soc Lond B Biol Sci 360: 507–514.
65. Nativio R, Wendt KS, Ito Y, Huddleston JE, Uribe-Lewis S, et al. (2009) Cohesin is required for higher-order chromatin conformation at the imprinted IGF2-H19 locus. PLoS Genet 5: e1000739. doi:10.1371/journal.pgen.1000739.
66. Wendt KS, Yoshida K, Itoh T, Bando M, Koch B, et al. (2008) Cohesin mediates transcriptional insulation by CCCTC-binding factor. Nature 451: 796–801.
67. Ferrandon D, Jung AC, Criqui M, Lemaitre B, Uttenweiler-Joseph S, et al. (1998) A drosomycin-GFP reporter transgene reveals a local immune response in Drosophila that is not dependent on the Toll pathway. Embo J 17: 1217–1227.
68. Ryu JH, Nam KB, Oh CT, Nam HJ, Kim SH, et al. (2004) The homeobox gene Caudal regulates constitutive local expression of antimicrobial peptide genes in Drosophila epithelia. Mol Cell Biol 24: 172–185.
69. Tzou P, Ohresser S, Ferrandon D, Capovilla M, Reichhart JM, et al. (2000) Tissue-specific inducible expression of antimicrobial peptide genes in Drosophila surface epithelia. Immunity 13: 737–748.
70. Kim M, Lee JH, Lee SY, Kim E, Chung J (2006) Caspar, a suppressor of antibacterial immunity in Drosophila. Proc Natl Acad Sci U S A 103: 16358–16363.
71. Ryu JH, Kim SH, Lee HY, Bai JY, Nam YD, et al. (2008) Innate immune homeostasis by the homeobox gene caudal and commensal-gut mutualism in Drosophila. Science 319: 777–782.
72. Gobert V, Gottar M, Matskevich AA, Rutschmann S, Royet J, et al. (2003) Dual activation of the Drosophila toll pathway by two pattern recognition receptors. Science 302: 2126–2130.
73. Pili-Floury S, Leulier F, Takahashi K, Saigo K, Samain E, et al. (2004) In vivo RNA interference analysis reveals an unexpected role for GNBP1 in the defense against Gram-positive bacterial infection in Drosophila adults. J Biol Chem 279: 12848–12853.
74. Bergman P, Johansson L, Asp V, Plant L, Gudmundsson GH, et al. (2005) Neisseria gonorrhoeae downregulates expression of the human antimicrobial peptide LL-37. Cell Microbiol 7: 1009–1017.
75. Chakraborty K, Ghosh S, Koley H, Mukhopadhyay AK, Ramamurthy T, et al. (2008) Bacterial exotoxins downregulate cathelicidin (hCAP-18/LL-37) and human beta-defensin 1 (HBD-1) expression in the intestinal epithelial cells. Cell Microbiol 10: 2520–2537.
76. Sperandio B, Regnault B, Guo J, Zhang Z, Stanley SL, Jr., et al. (2008) Virulent Shigella flexneri subverts the host innate immune response through manipulation of antimicrobial peptide gene expression. J Exp Med 205: 1121–1132.
77. Wehkamp J, Salzman NH, Porter E, Nuding S, Weichenthal M, et al. (2005) Reduced Paneth cell alpha-defensins in ileal Crohn's disease. Proc Natl Acad Sci U S A 102: 18129–18134.
78. Markey MP, Bergseid J, Bosco EE, Stengel K, Xu H, et al. (2007) Loss of the retinoblastoma tumor suppressor: differential action on transcriptional programs related to cell cycle control and immune function. Oncogene 26: 6307–6318.

79. Zurawski DV, Mumy KL, Faherty CS, McCormick BA, Maurelli AT (2009) Shigella flexneri type III secretion system effectors OspB and OspF target the nucleus to downregulate the host inflammatory response via interactions with retinoblastoma protein. Mol Microbiol 71: 350–368.
80. Tsichritzis T, Gaentzsch PC, Kosmidis S, Brown AE, Skoulakis EM, et al. (2007) A Drosophila ortholog of the human cylindromatosis tumor suppressor gene regulates triglyceride content and antibacterial defense. Development 134: 2605–2614.
81. Bolstad BM, Irizarry RA, Astrand M, Speed TP (2003) A comparison of normalization methods for high density oligonucleotide array data based on variance and bias. Bioinformatics 19: 185–193.
82. Smyth GK (2004) Linear models and empirical bayes methods for assessing differential expression in microarray experiments. Stat Appl Genet Mol Biol 3: Article3.
83. Benjamini Y, Hochberg Y (1995) Controlling the false discovery rate: a practical and powerful approach to multiple testing. Journal of the Royal Statistical Society Series 57: 289–300.
84. Tweedie S, Ashburner M, Falls K, Leyland P, McQuilton P, et al. (2009) FlyBase: enhancing Drosophila Gene Ontology annotations. Nucleic Acids Res 37: D555–559.
85. Romeo Y, Lemaitre B (2008) Drosophila immunity: methods for monitoring the activity of Toll and Imd signaling pathways. Methods Mol Biol 415: 379–394.

Human Molecular Genetics, 2012, Vol. 21, No. 24 ***5239–5245***
doi:10.1093/hmg/dds370
Advance Access published on September 4, 2012

Expression of *SMARCB1 (INI1)* mutations in familial schwannomatosis

Miriam J. Smith[1,†], James A. Walker[1,2,3], Yiping Shen[3], Anat Stemmer-Rachamimov[4], James F. Gusella[3] and Scott R. Plotkin[1,5,*]

[1]Department of Neurology, [2]Massachusetts General Hospital Center for Cancer Research, [3]Center for Human Genetic Research, [4]Division of Neuropathology, [5]Pappas Center for Neuro-oncology, Massachusetts General Hospital, Boston, MA 02114, USA

Received June 21, 2012; Revised August 10, 2012; Accepted August 28, 2012

Genetic changes in the *SMARCB1* tumor suppressor gene have recently been reported in tumors and blood from families with schwannomatosis. Exon scanning of all nine *SMARCB1* exons in genomic DNA from our cohort of families meeting the criteria for 'definite' or 'presumptive' schwannomatosis previously revealed constitutional alterations in 13 of 19 families (68%). Screening of four new familial schwannomatosis probands identified one additional constitutional alteration. We confirmed the presence of mRNA transcripts for two missense alterations, four mutations of conserved splice motifs and two additional mutations, in less conserved sequences, which also affect splicing. Furthermore, we found that transcripts for a rare 3′-untranslated region (c.*82C > T) alteration shared by four unrelated families did not produce splice variants but did show unequal allelic expression, suggesting that the alteration is either causative itself or linked to an unidentified causative mutation. Overexpression studies in cells lacking SMARCB1 suggest that mutant SMARCB1 proteins, like wild-type SMARCB1 protein, retain the ability to suppress cyclin D1 activity. These data, together with the expression of SMARCB1 protein in a proportion of cells from schwannomatosis-related schwannomas, suggest that these tumors develop through a mechanism that is distinct from that of rhabdoid tumors in which SMARCB1 protein is completely absent in tumor cells.

INTRODUCTION

Schwannomatosis (MIM#162091) is a third major form of neurofibromatosis, that is clinically and genetically distinct from NF1 (MIM#162200) and NF2 (MIM#101000) (1). The most common clinical symptom of schwannomatosis is intractable pain, although the mechanism by which this occurs is not well understood. Tumors from familial schwannomatosis patients frequently harbor somatic truncating mutations at the *NF2* (MIM#607379) gene on the long arm of chromosome 22 and loss of the wild-type *NF2* allele. However, they do not carry germline *NF2* mutations (2). Recently, a number of constitutional alterations have been reported in familial and some sporadic schwannomatosis patients in the *SMARCB1* (MIM#601607) gene (3–6), which is situated 5.8 Mb proximal to *NF2*.

Loss of *SMARCB1* has been linked previously to development of rhabdoid tumors (RTPS1; MIM#609322) (7). Rhabdoid tumors are highly malignant, appear in the first few years after birth, and are almost always lethal. Several RTPS1 families have been described (8) to include family members who are constitutional carriers of a *SMARCB1* mutation, but who never develop schwannomas. Recently, a multigenerational family was described with multiple members affected by either malignant rhabdoid tumors or by schwannomatosis, all of whom share a common germline *SMARCB1* exon 6 duplication mutation (9). A second family affected by RTPS1 and schwannoma has also been described with a c.472C > T *SMARCB1* mutation (10).

The existence of adult mutation carriers in RTPS1 families has led to the hypothesis that the risk of rhabdoid tumor development from these mutations is time dependent (6,11), in

*To whom correspondence should be addressed at: Massachusetts General Hospital, 55 Fruit St, Yawkey 9E, Boston, MA 02114, USA. Tel: +1 6177263650; Fax: +1 6176432591; Email: splotkin@partners.org
†Present address: St Mary's Hospital, University of Manchester, Manchester, M13 9WL, UK.

which case the development of schwannomas later in life becomes feasible. However, the majority of RTPS1 and schwannomatosis families remain distinct, making it more likely that the type or location of the mutation determines the resulting disease status.

Almost all of the constitutional *SMARCB1* alterations found in familial schwannomatosis patients are predicted to be non-truncating. In contrast, the mutations found in RTPS1 are mainly truncating mutations and large deletions, which lead to a complete loss of SMARCB1 protein. This difference in mutation type may underlie the difference in phenotype presented by these two conditions.

To address this issue, we have carried out analysis of *SMARCB1* transcripts from 14 schwannomatosis families, shown to harbor constitutional alterations (6), in order to verify expression of the non-truncated products predicted from each mutation.

RESULTS

Immunohistochemistry of schwannomas reveals mosaic pattern of SMARCB1 expression

Immunostaining for schwannomas from families 1, 5 and 10 which harbor the c.*82C > T mutation and family 11 harboring the c.364G > T mutation have been published previously (12) and show a mosaic pattern of staining for SMARCB1 protein, consistent with loss of expression in a subset of tumor cells. Tumor sections from families 9 and 19 were subsequently analyzed by immunostaining for SMARCB1 and also revealed a mosaic pattern of mixed positive and negative nuclei in all four schwannomas from a member of family 19 (c.795 + 1G > T) and a single schwannoma from family 9 (c.158G > T). Representative staining is shown for a tumor from family 19 in Figure 1. No tumors were available for testing from other families in this study.

cDNA analysis of familial schwannomatosis samples

To confirm the predicted effects of constitutional mutations identified previously (6), we analyzed cDNA derived from mRNA of lymphoblastoid cell lines carrying each of the 10 germline alterations found in 14 families. The results are summarized in Table 1. Representative chromatograms of the sequencing results for each of the seven mutant transcripts predicted to produce a viable protein and the three predicted to undergo nonsense-mediated decay are shown in Figure 2A–J.

Missense mutations

Each of the missense alterations, c.41C > A (p.Pro14His) and c.158G > T (p. Arg53Leu), found in family 4, and families 9 and PA-3, respectively, was detected in the cDNA transcript generated from its corresponding lymphoblast cell line (Fig. 2A and B), indicating that the mutant allele for both of these alterations is expressed at the mRNA level.

Splicing alterations

Four mutations were detected in conserved splice sites in four kindreds. An intron 3 mutation (c.362 + 1G > A) amplified a faint band containing a splice variant that results in an in-frame deletion of the last 45 bp of exon 3 (Fig. 2C). An exon 4 alteration, c.364G > T, caused skipping of exon 4, without changing the reading frame (Fig. 2D). Another mutation at the ultimate base of exon 4, c.500G > A, produced altered splicing that resulted in the in-frame loss of the last 111 bp of the exon (c.390_500del, Fig. 2E). The intron 6 change, c.795 + 1G > T produced two alternative splice variants. The first involved the in-frame inclusion of the first 45 bp of intron 6 (Fig. 2F) while the second, which was much less abundant, involved skipping of exon 6, with the resulting frame-shift predicted to lead to a premature stop codon and mRNA decay (Fig. 2G).

Sequence analysis of lymphocyte DNA from family 23 [family 07-367 in Eaton *et al*., (10)] identified the nonsense mutation c.472C > T in exon 4. We isolated three alternately spliced cDNA amplicons derived from the corresponding lymphoblast cell line RNA for this family. First, amplification of exons 3–6 detected two different deletions: complete exon 4 loss (c.363_500del) and partial exon 4 deletion (c.390_500del). Amplicons for exons 5–9 then detected a deletion of the whole of exon 7 (Fig. 1H). The exon 4 changes in the transcript were the same as those found in other families and have the potential to produce non-truncated protein. However, the presence of the exon 7 deletion would lead to a premature stop codon and destabilize these mutant transcripts; therefore, they are predicted to undergo nonsense-mediated decay.

Two additional potential splice site alterations were identified further from the consensus splice sequence the intron 4 change, c.500 + 5G > T, and the intron 5 change, c.629-5T > G. Interestingly, the former leads to the same splicing alteration as the c.500G > A mutation, five bases away (Fig. 2E). The intron 5 alteration, c.629-5T > G, in family P/Qu, seems to disrupt the exon 6 splice acceptor sequence, leading to the insertion of 145 bp of the 3′ end of intron 5 (Fig. 2I), using a cryptic splice acceptor, ag/TTT. This alteration results in a premature stop codon within the intronic sequence and is predicted to lead to mRNA decay.

Variants of uncertain significance

Four unrelated families contained the same alteration, c.*82C > T, within their 3′UTR (Fig. 2J). This alteration was not found in an unaffected panel of 100 alleles and is not recorded in the dbSNP database (6,13). None of the four families produced splice variants in the cDNA analysis screen, but the alteration was observed in the transcript.

Allelic expression analysis of the c.*82C > T alteration

Allelic expression analysis has previously been used to quantify under- or overexpression of mutant *NF2* transcripts from NF2 patient-derived lymphoblast cell RNAs (14). We used this technique to measure expression levels of the c.*82C > T alteration.

The full-length *SMARCB1* transcripts were amplified, sequenced and the level of expression of the mutant 'T' allele in cDNA was calculated, relative to the genomic sequence, using the Mutation Surveyor DNA analysis program (SoftGenetics, State College, PA, USA). The results revealed unequal allelic expression, with a decreased expression of

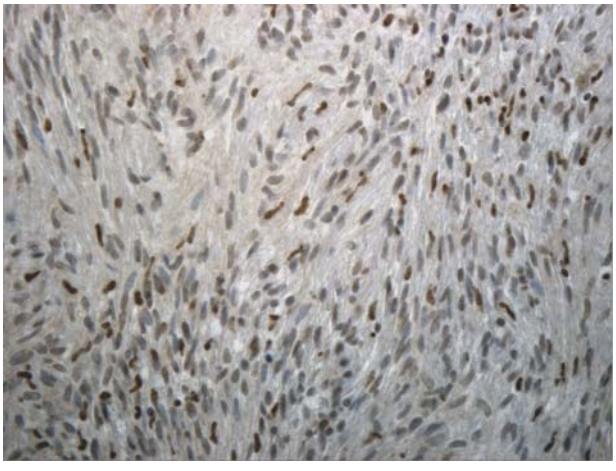

Figure 1. Immunostaining for SMARCB1 shows a mosaic pattern of SMARCB1 expression in a schwannoma from family 19 with a mixture of positive (brown) and negative (blue) nuclei in cells.

Table 1. Germline mutations found in familial schwannomatosis kindreds and the effects observed in mRNA (family 23 has both schwannomatosis and RTPS1)

Family ID	Exon	Germline mutation	Mutant amplicons identified
4	1	c.41C > A	r.41C > A
9	2	c.158G > T	r.158G > U
PA-1	2	c.158G > T	r.158G > U
E	3	c.362 + 1G > A	r.318_362del
11	4	c.364G > T	r.363_500del
23	4	c.472C > T	r.363_500del, r.390_500del, r.796_986del
PA-3	4	c.500G > A	r.390_500del
V	4	c.500 + 5G > T	r.390_500del
P/Qu	6	c.629-5T > G	r.500ins501-145_501-1
19	6	c.795 + 1G > T	r.795_796ins795 + 1_795 + 45ins, r.628_795del
1	9	c.*82C > T	r.*82C > U
3	9	c.*82C > T	r.*82C > U
5	9	c.*82C > T	r.*82C > U
10	9	c.*82C > T	r.*82C > U

the mutant allele by ~27% compared with the wild-type. To ensure that differences in expression for the c.*82C > T change were not due to differential expression in lymphoblastoid cells, two known SNPs (rs34399789 and rs2229354), identified on an unaffected allele in two families, were tested for unequal expression in unaffected family members. These polymorphisms both showed equal expression in full-length *SMARCB1* cDNA. The results suggest that the c.*82C > T alteration is associated with reduced expression and is either causative or linked to a causative mutation.

The *SMARCB1* mutant 3′UTR alters mRNA stability

To substantiate the effect of the mutant *SMARCB1* 3′UTR on RNA expression levels, we transfected HEK293T cells with a pGL3-promoter luciferase vector containing a wild-type *SMARCB1* 3′UTR, or a c.*82C > T mutant 3′UTR. Forty-eight hours after transfection, the level of luciferase expression was significantly reduced under the regulation of the c.*82C > T mutant 3′UTR compared with the wild-type 3′UTR (Fig. 3A). To distinguish between the possibilities of the c.*82C > T mutation affecting either translational efficiency or stability of the mRNA, we performed qRT–PCR on RNA extracted from HEK293T cells transfected with luciferase constructs bearing the wild-type or the c.*82C > T 3′UTRs, at 48 and 96 h post-transfection. At 48 and 96 h, the c.*82C > T mutant mRNA levels were reduced by ~20 and ~45%, respectively, compared with the wild-type (Fig. 3B). Together, these results suggest that the c.*82C > T mutant 3′UTR leads to a reduced expression of the *SMARCB1* transcript, possibly by destabilizing the mRNA.

Cyclin D1 reporter activity is appropriately suppressed by mutant SMARCB1

To begin to elucidate the mechanism by which mutations in *SMARCB1* affect its normal function in cells, we created expression constructs for three of the mutant *SMARCB1* transcripts found in our cohort, predicted to result in altered protein sequence. The exon 1 missense, c.41C > A, and exon 2 missense, c.158G > T, mutations were created by site-directed mutagenesis. The splice mutant lacking exon 4 was isolated from full-length cDNA derived from mRNA from a lymphoblastoid cell line with the c.364G > T mutation. These expression constructs were used to determine whether mutant SMARCB1 proteins are able to suppress elevated cyclin D1 expression, as has been shown previously for wild-type SMARCB1 (15). A luciferase reporter construct containing the cyclin D1 promoter region −1745 to +35 was used to transfect MON cells, which lack endogenous SMARCB1 and have elevated levels of cyclin D1 (15). This construct was co-transfected with either a wild-type SMARCB1 construct or a mutant transcript construct. When wild-type SMARCB1 was reintroduced into MON cells, luciferase expression was suppressed by ~60% (Fig. 4) similar to previous reports (15). Similarly, when MON cells were transfected with mutant *SMARCB1* constructs, luciferase expression was suppressed by 53% (exon 1 missense), 74% (exon 2 missense) or 65% (exon 4 deletion). The results show that these schwannomatosis-related mutant SMARCB1 proteins retain the ability to repress cyclin D1 transcription.

DISCUSSION

Exon scanning analysis of *SMARCB1* in our cohort of familial schwannomatosis patients has now identified a total of 14/23 (61%) probands with a germline point mutation. The majority of these mutations are predicted to be non-truncating. This contrasts with the mutational spectrum of RTPS1 in which mutations are predicted to be truncating (7,16). We analyzed cDNA from this select group of familial schwannomatosis patients to confirm the predicted effects of constitutional mutations identified during initial *SMARCB1* exon scanning and found that almost all of the constitutional alterations in the *SMARCB1* gene produced a mutant transcript that is likely to produce a non-truncated protein.

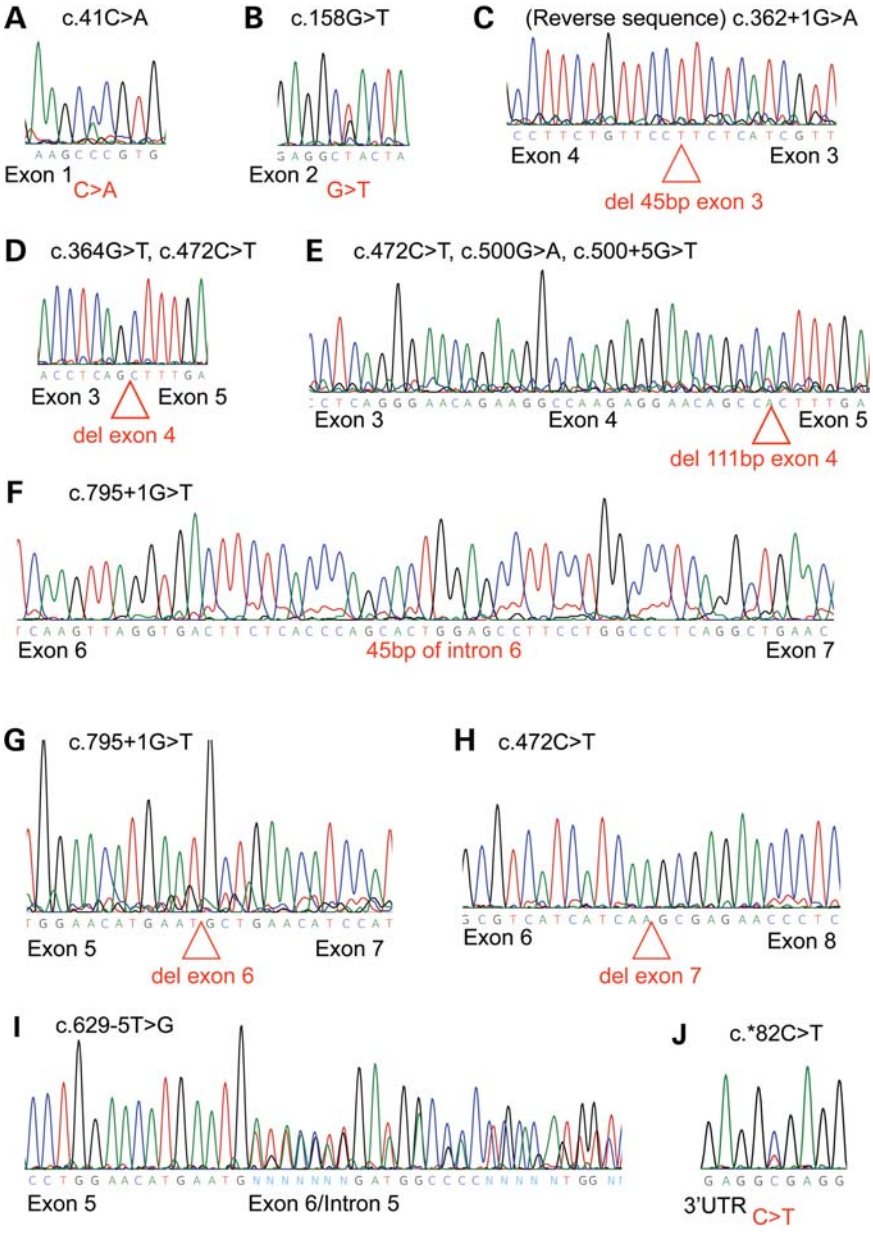

Figure 2. Chromatograms showing *SMARCB1* mutant transcripts identified in the study. (**A**) Exon 1 missense mutation; (**B**) exon 2 missense mutation found in families 9 and PA1; (**C**) exon 3 splice mutation that removes the first 45 bp of exon 3; (**D**) in-frame deletion of the entire exon 4 sequence found in families 11 and 23;(**E**) exon 4 splice mutation leading to the deletion of the last 111 bp of exon 4 in families PA-3, V and 23; (**F**) exon 6 splice mutation causing inclusion of the first 45 bp of intron 6; (**G**) family 19 transcript deleting exon 6, predicted to cause nonsense-mediated decay; (**H**) family 23 deletion of exon 7, predicted to cause nonsense-mediated decay; (**I**) family P/Qu mutant transcript including 145 bp of intron 5, predicted to cause nonsense-mediated decay; (**J**) 3′UTR change found in families 1, 3, 5 and 10.

Families P/Qu and 23 both produced mutant transcripts that are likely to be degraded by nonsense-mediated decay. Family 23 has a family history of both schwannomatosis and RTPS1 and, in addition to the truncating mutation, also has a somatic deletion of the wild-type *SMARCB1* allele in a tumor (10). The c.472C > T nonsense mutation is known to predispose to RTPS1, but it is unclear why some members of the same family developed schwannomas rather than rhabdoid tumors. It is possible that a modifier gene is involved. It is also unclear how the mutation, which occurs in exon 4, causes a deletion of exon 7. It is possible that a second, unidentified, mutation exists within intron 6, leading to skipping of exon 7.

The only mutant transcript detected in family P/Qu contained an insertion of the last 145 bp of intron 5, which leads to a stop codon 26 codons into the insertion. This is predicted to lead to mRNA decay and no expression of the mutant copy of *SMARCB1*. This family did not show loss of heterozygosity (LOH) by microsatellite marker analysis at the *SMARCB1* locus, suggesting that the wild-type copy of *SMARCB1* is still present in tumors, although it remains

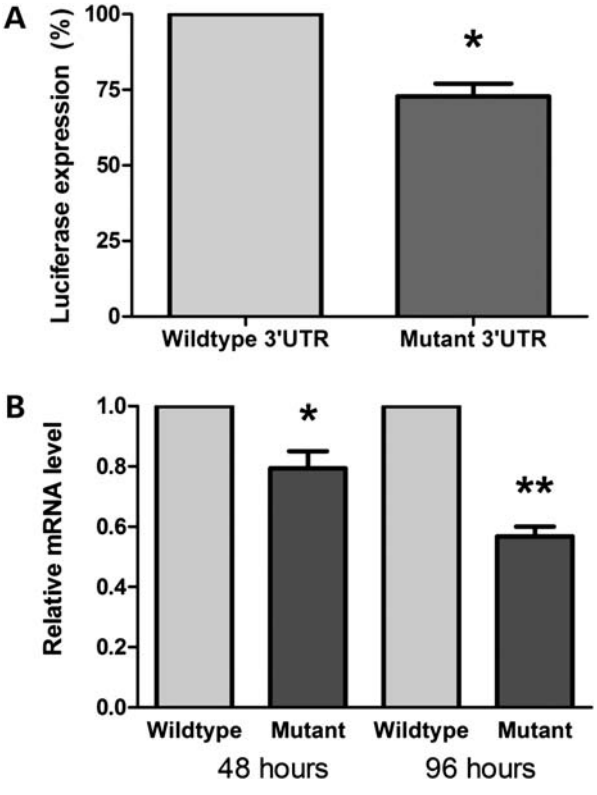

Figure 3. The *SMARCB1* mutant 3′UTR alters mRNA stability. Relative mRNA expression levels of wild-type and mutant *SMARCB1* 3′untranslated regions in HEK293T cells. (**A**) Luciferase levels indicate the relative expression under the control of wild-type and c.*82C > T mutated *SMARCB1* 3′UTRs, normalized to transfection efficiency by GFP fluorescence $^{*}P < 0.01$. (**B**) qRT–PCR of wild-type and mutant *SMARCB1* 3′UTR expression levels at 48 and 96 h post-transfection normalized to both GFP and GAPDH $^{*}P < 0.015$; $^{**}P < 0.001$.

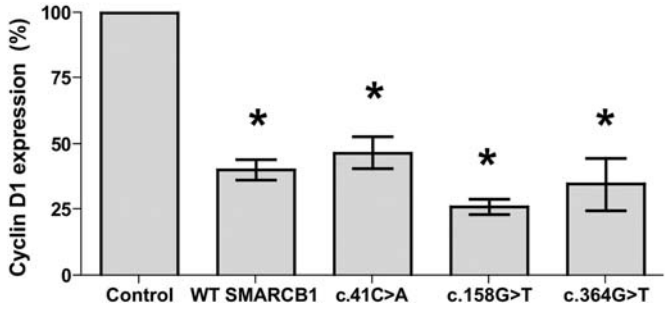

Figure 4. Cyclin D1 activity is appropriately suppressed by both wild-type and mutant SMARCB1 proteins. Introduction of both wild-type and mutant *SMARCB1* transcripts (c.41C > A missense, c.158G > T missense or c.364G > T splice mutant) into MON cells which lack endogenous SMARCB1 leads to suppression of luciferase reporter activity under the control of the cyclin D1 promoter. Normalized to transfection efficiency by GFP fluorescence $^{*}P < 0.05$.

possible that other mechanisms may affect this remaining allele. LOH was, however, seen at the *NF2* locus—downstream of *SMARCB1*—in a tumor from family P/Qu, supporting the theory that co-mutation of these two genes is involved in schwannoma formation (4–6). Unfortunately, no tumor material was available for immunohistochemical analysis.

Tumors from schwannomatosis kindreds frequently carry *SMARCB1* alterations in conjunction with loss of the wild-type allele. The combination of a constitutional *SMARCB1* mutation with a somatically acquired truncating mutation in the *NF2* gene and loss of the wild-type copies of both genes indicates cross-talk between tumorigenic pathways and a complex mechanism of schwannoma formation in this disorder. Indeed, a multi-hit hypothesis has been suggested (3–6).

The alteration, c.*82C > T, found in the 3′ UTR of four unrelated kindreds (13) in our cohort, showed no splice variants, but was detected by sequencing of the full-length transcript from lymphoblast cell lines, suggesting that the mutant mRNA is expressed. Allelic expression analysis, and qRT–PCR on cells transfected with wild-type and mutant 3′UTRs, showed unequal expression with decreased levels of the mutant allele in comparison with the wild-type. Families 3 and 5, for which tumor DNA was available, showed LOH for both the *SMARCB1* and *NF2* loci and showed somatic mutation of the remaining *NF2* allele (6). These results, together with the frequency of this alteration in unrelated families, support a pathogenic status for the c.*82C > T mutation and implicate it in the occurrence of schwannomatosis disease.

SMARCB1 regulation of cyclin D1

Loss of SMARCB1 in RTPS1 leads to upregulation of cyclin D1 and progression into the cell cycle. A cyclin D1 repression assay showed that schwannomatosis-related missense and splice mutants are capable of suppressing cyclin D1 activity in a similar way to that shown for the wild-type SMARCB1 protein. This finding suggests that the downstream effects of *SMARCB1* alterations are different in schwannomatosis compared with RTPS1, with cyclin D1 and related cell cycle processes being affected primarily in the RTPS1 tumors.

Immunohistochemistry for SMARCB1 revealed a mosaic pattern of mixed positive and negative nuclei in all tumor specimens. In a previous report, this finding was interpreted as loss of protein expression in a subset of tumor cells resulting in a mosaic of null and haploinsufficient cells (12). This could be as a result of transient or unstable expression. However, further work would be required to determine this. It is also unclear why the exon 2 mutation, which appears to produce a more highly expressed transcript, also leads to a mosaic pattern of protein production. It could be that the mutant DNA is transcribed normally, while the mutant mRNA is mis-folded, causing a reduction in translation efficiency.

This data, in conjunction with the different spectrum of mutations in comparison with that seen in RTPS1, suggests that in familial schwannomatosis kindreds, almost all constitutional alterations in the *SMARCB1* gene are capable of producing mutant, but viable transcripts, that yield SMARCB1 protein with altered levels of functionality in schwannoma tumor cells. Further work is required to determine the precise mechanism by which mutant SMARCB1 protein can promote the pathogenesis of schwannomas.

MATERIALS AND METHODS

Patient material

We studied 13 of 19 carefully characterized schwannomatosis kindreds described previously (6) and four additional familial probands. Lymphoblastoid cell lines were established from peripheral blood samples as described previously (17). High-molecular-weight DNA was extracted from peripheral blood leukocytes, cultured lymphoblasts, frozen pulverized tumor, cultured tumor and normal tissues obtained at autopsy using a PureGene DNA isolation kit (Gentra Systems, Minneapolis, MN, USA). This study was approved by the Institutional Review Board of Partners HealthCare and informed consent was obtained from the patients participating in the study. For patients who had died, an autopsy permit was used as consent.

Multiplex ligation-dependent probe amplification

Multiplex ligation-dependent probe amplification was carried out as described by Boyd *et al*. (6), using a SALSA multiplex ligation-dependent probe amplification P258 SMARCB1 kit (MRC-Holland, Amsterdam, the Netherlands). Briefly, 20–500 ng DNA were used for hybridization, ligation and amplification of the *SMARCB1* exon probes according to the manufacturer's instructions. The amplification products were analyzed using an ABI 3730 DNA Analyzer, with Biomek FX robotics and with GeneScan 500 LIZ (Applied Biosystems, Foster City, CA, USA) as the internal size standard. Relative probe signals were calculated by dividing each measured peak by the sum of all peak areas for that sample. DNA from four unaffected individuals was used for control samples.

cDNA analysis

mRNA was extracted from frozen cell pellets of established lymphoblastoid cell lines for each kindred, using the PolyA-Tract mRNA extraction kit (Promega, Madison, WI, USA). Poly(A)+ mRNA was reverse transcribed to cDNA with oligo(d)T primers, using the Superscript III cDNA first strand synthesis kit (Invitrogen, Carlesbad, CA, USA). Full-length *SMARCB1* and three overlapping fragments of the *SMARCB1* transcript were PCR amplified from the cDNAs using nested primers. For the full-length transcript, the primers 5′-CAGCCCTCCTGATCCCT-3′ and 5′-CCCAAT CTTCTGAGATGCTC-3′ were used. The reverse primer 5′-ACAAATGGAATGTGTGCCGG-3′ was used when the 3′UTR SNPs were amplified. Exons 1 through 4 were amplified with primers 5′-CAGCCCTCCTGATCCCT-3′ and 5′-TCACAGCTGGGTCATGGTC-3′, exons 3–6 were amplified by 5′-CACGGATACACGACTCTAGC-3′ and 5′-CACT CAAACTGGTCCACC-3′ and for exons 5–9, 5′-CCATG CTCCACAACCATC-3′ and 5′-CCCAATCTTCTGAGATGC TC-3′were used. PCR products were electrophoresed on 2% agarose gels, with a normal control. Aberrantly sized fragments were excised and analyzed by direct sequencing on an ABI Prism 3730 DNA analyzer.

Quantitative analysis of the c.*82C > T mutation (previously denoted c.1240C > T) was carried out using the Mutation Surveyor program v3.20 (Softgenetics LLC, State College, PA, USA) by comparison of relative levels of C and T alleles in cDNA with reference to levels in genomic DNA.

Construction of wild-type and mutant *SMARCB1* expression vectors

Mutagenic primers were designed to introduce the c.41C > A and c.158G > T point mutations identified in our cohort into the wild-type human *SMARCB1* sequence obtained from Origene (Rockville, MD, USA). Site-directed mutagenesis was carried out using the Quick-change site-directed mutagenesis kits (Stratagene, Carlesbad, CA, USA). Mutagenic primers for c.41C > A were GACCTTCGGGCAGAAG CACGTGAAGTTCCAGCTGG and CCAGCTGGAACTTCA CGTGCTTCTGCCCGAAGGTC. Mutagenic primers used for c.158G > T were CCCTCACTCTGGAGGCTACTAGCCAC TGTGGAAG and CTTCCACAGTGGCTAGTAGCCTCCA GAGTGAGGG.

The splice mutant lacking exon 4 was obtained by PCR amplification of full-length cDNA generated from mRNA of a lymphoblastoid cell line from family 11, using a forward primer containing an *Nhe*I restriction site, GCATGCTAG CATGATGATGATGGCGCTGAGC, and a reverse primer containing a *Hin*dIII restriction site, TTTAAGCTTCCA GGCCGGGGCCGTGTT. Each mutant transcript was subcloned into a pcDNA plasmid, containing a C-terminal GFP tag.

For the cyclin D1 repression experiment, the cyclin D1 promoter region −1745 to +35 was sub-cloned into the pGL3-basic plasmid, which contains a luciferase reporter gene (Promega, Madison, WI, USA).

For the 3′UTR experiment, site-directed mutagenesis was used to generate the c.*82C > T mutant, with primers TGGCAAGGACAGAGGTGAGGGGACAGCCCA and TGG GCTGTCCCCTCACCTCTGTCCTTGCCA. cDNAs representing the wild-type and c.*82C > T mutant 3′UTRs were each sub-cloned into the pGL3-promoter vector, downstream of the luciferase coding region.

Cell lines

HEK293T cells were purchased from ATCC (Manassas, VA , USA). MON tumor cells were obtained from the laboratory of Dr Olivier Delattre.

Luciferase reporter assays

For experiments investigating *SMARCB1* 3′UTR regulation, using a luciferase reporter, HEK293T cells were co-transfected with the pGL3-promoter vector construct with either a wild-type or mutant *SMARCB1* 3′UTR and an eGFP vector, using Lipofectamine transfection reagent (Invitrogen, Carlesbad, CA, USA). Cells were harvested after 48 h and luciferase activity was measured using One-glow luciferase reagent (Promega, Madison, WI, USA).

For experiments investigating the regulation of cyclin D1, the wild-type *SMARCB1* transcript and three mutant transcripts [containing the exon 1 missense mutation (c.41C > A), the exon 2 missense mutation (c.158G > T) or the deletion of exon 4], were subcloned into the pcDNA vector with a

C-terminal GFP tag. The cyclin D1 luciferase vector was transfected into MON cells which lack endogenous SMARCB1 along with each of the *SMARCB1* constructs, or an empty GFP control vector. Cells were harvested after 48 h and luciferase activity was measured using One-glow luciferase reagent (Promega, Madison, WI, USA). Luciferase levels were normalized to transfection efficiency using GFP fluorescence.

qRT–PCR analysis of luciferase-3′UTR reporters

Total RNA was extracted from transfected cells using the RNeasy kit (Qiagen, Valencia, CA, USA) and treated with DNase (Ambion, Foster City, CA, USA). First-strand cDNA synthesis was performed using random hexamers (GE Healthcare, Piscataway, NJ, USA). Subsequently, mRNA expression levels of luciferase-3′ UTR reporters were assessed using 1 μl of the appropriate cDNA for real-time qRT–PCR using FastStart Universal SyberGreen and a LightCycler 480 machine (Roche, Indianapolis, IN, USA). The forward oligonucleotide primer (5′-GGTCTTACCGGAAAACTCGAC-3′) corresponds to a sequence at the 3′ end of the luciferase cDNA; the reverse primer (5′-CTCTGTCCTTGCCAGAAGATG-3′) is within the 3′UTR of *SMARCB1*. The results were analyzed using the comparative Ct method (ΔΔCt) and normalized to GAPDH and eGFP expression levels to ensure equal loading and transfection efficiencies.

Immunohistochemistry

Formalin-fixed, paraffin-embedded tissue sections from four schwannomas resected from member of family 19 (c.795 + 1G > T) and a single schwannoma from family 9 were immunostained using a commercial SMARCB1 antibody (BD Transduction Laboratories, Franklin Lakes, NJ, USA) along with appropriate positive (normal cortex) and negative controls (RTPS1). Antigen retrieval was achieved by microwaving in a Borg Decloaker RTU for 45 min (primary antibody concentration 1:50).

ACKNOWLEDGEMENTS

We would like to thank Dr Olivier Delattre for the generous gift of MON cells and Dr Ganjam Kalpana for reagents and technical assistance with the luciferase assays. We would also like to thank Robert Maher for help with formatting of the figures.

Conflict of Interest statement. None declared.

FUNDING

This work was supported in part by NINDS grant NS24279 and by the Harvard Medical School Center for Neurofibromatosis and Allied Disorders. J.A.W. is supported by the DOD (W81XWH-09-1-0487). M.J.S. is currently supported by the Children's Tumor Foundation and the Association for International Cancer Research.

REFERENCES

1. MacCollin, M., Chiocca, E.A., Evans, D.G., Friedman, J.M., Horvitz, R., Jaramillo, D., Lev, M., Mautner, V.F., Niimura, M., Plotkin, S.R. *et al.* (2005) Diagnostic criteria for schwannomatosis. *Neurology*, **64**, 1838–1845.
2. MacCollin, M., Willett, C., Heinrich, B., Jacoby, L.B., Acierno, J.S. Jr, Perry, A. and Louis, D.N. (2003) Familial schwannomatosis: exclusion of the NF2 locus as the germline event. *Neurology*, **60**, 1968–1974.
3. Hulsebos, T.J., Plomp, A.S., Wolterman, R.A., Robanus-Maandag, E.C., Baas, F. and Wesseling, P. (2007) Germline mutation of INI1/SMARCB1 in familial schwannomatosis. *Am. J. Hum. Genet.*, **80**, 805–810.
4. Sestini, R., Bacci, C., Provenzano, A., Genuardi, M. and Papi, L. (2008) Evidence of a four-hit mechanism involving SMARCB1 and NF2 in schwannomatosis-associated schwannomas. *Hum. Mutat.*, **29**, 227–231.
5. Hadfield, K.D., Newman, W.G., Bowers, N.L., Wallace, A., Bolger, C., Colley, A., McCann, E., Trump, D., Prescott, T. and Evans, D.G. (2008) Molecular characterisation of SMARCB1 and NF2 in familial and sporadic schwannomatosis. *J. Med. Genet.*, **45**, 332–339.
6. Boyd, C., Smith, M.J., Kluwe, L., Balogh, A., Maccollin, M. and Plotkin, S.R. (2008) Alterations in the SMARCB1 (INI1) tumor suppressor gene in familial schwannomatosis. *Clin. Genet.*, **74**, 358–366.
7. Versteege, I., Sevenet, N., Lange, J., Rousseau-Merck, M.F., Ambros, P., Handgretinger, R., Aurias, A. and Delattre, O. (1998) Truncating mutations of hSNF5/INI1 in aggressive paediatric cancer. *Nature*, **394**, 203–206.
8. Sevenet, N., Sheridan, E., Amram, D., Schneider, P., Handgretinger, R. and Delattre, O. (1999) Constitutional mutations of the hSNF5/INI1 gene predispose to a variety of cancers. *Am. J. Hum. Genet.*, **65**, 1342–1348.
9. Swensen, J.J., Keyser, J., Coffin, C.M., Biegel, J.A., Viskochil, D.H. and Williams, M.S. (2009) Familial occurrence of schwannomas and malignant rhabdoid tumour associated with a duplication in SMARCB1. *J. Med. Genet.*, **46**, 68–72.
10. Eaton, K.W., Tooke, L.S., Wainwright, L.M., Judkins, A.R. and Biegel, J.A. (2011) Spectrum of SMARCB1/INI1 mutations in familial and sporadic rhabdoid tumors. *Pediatr. Blood Cancer*, **56**, 7–15.
11. Janson, K., Nedzi, L.A., David, O., Schorin, M., Walsh, J.W., Bhattacharjee, M., Pridjian, G., Tan, L., Judkins, A.R. and Biegel, J.A. (2006) Predisposition to atypical teratoid/rhabdoid tumor due to an inherited INI1 mutation. *Pediatr. Blood Cancer*, **47**, 279–284.
12. Patil, S., Perry, A., Maccollin, M., Dong, S., Betensky, R.A., Yeh, T.H., Gutmann, D.H. and Stemmer-Rachamimov, A.O. (2008) Immunohistochemical analysis supports a role for INI1/SMARCB1 in hereditary forms of schwannomas, but not in solitary, sporadic schwannomas. *Brain Pathol. (Zurich, Switzerland)*, **18**, 517–519.
13. Smith, M.J., Boyd, C.D., MacCollin, M.M. and Plotkin, S.R. (2009) Identity analysis of schwannomatosis kindreds with recurrent constitutional SMARCB1 (INI1) alterations. *Clin. Genet.*, **75**, 501–502.
14. Jacoby, L.B., MacCollin, M., Parry, D.M., Kluwe, L., Lynch, J., Jones, D. and Gusella, J.F. (1999) Allelic expression of the NF2 gene in neurofibromatosis 2 and schwannomatosis. *Neurogenetics*, **2**, 101–108.
15. Zhang, Z.K., Davies, K.P., Allen, J., Zhu, L., Pestell, R.G., Zagzag, D. and Kalpana, G.V. (2002) Cell cycle arrest and repression of cyclin D1 transcription by INI1/hSNF5. *Mol. Cell. Biol.*, **22**, 5975–5988.
16. Biegel, J.A., Zhou, J.Y., Rorke, L.B., Stenstrom, C., Wainwright, L.M. and Fogelgren, B. (1999) Germ-line and acquired mutations of INI1 in atypical teratoid and rhabdoid tumors. *Cancer Res.*, **59**, 74–79.
17. Anderson, M.A. and Gusella, J.F. (1984) Use of cyclosporin A in establishing Epstein-Barr virus-transformed human lymphoblastoid cell lines. *In Vitro*, **20**, 856–858.